

**Interaction between
hemodynamics and morphology
in normal and abnormal
cardiac development**

Cover: © 1996, by E.H. Kees, Leiden, The Netherlands

© 1996 by M.L.A. Broekhuizen

All rights reserved. No part of this book may be reproduced or transmitted, in any form or by any means, without written permission from the author.

ISBN 90-9009873-9

The hemodynamic part of this research was carried out at the Department of Obstetrics and Gynecology of the Academic Hospital Rotterdam, Erasmus University Rotterdam. The morphologic evaluation was carried out at the Department of Anatomy and Embryology of the Leiden University.

The research presented in this thesis was supported by a grant (Jubileumsubsidie) of the Netherlands Heart Foundation in collaboration with the Netherlands Organization for Scientific Research, Grant 900-516-096.

Financial support by the Netherlands Heart Foundation for the publication of this thesis is gratefully acknowledged.

Printed by Ponsen & Looijen BV Wageningen

INTERACTION BETWEEN HEMODYNAMICS AND MORPHOLOGY
IN NORMAL AND ABNORMAL CARDIAC DEVELOPMENT

Interactie van haemodynamiek en morfologie in normale en abnormale hartontwikkeling

Proefschrift

ter verkrijging van de graad van doctor
aan de Erasmus Universiteit Rotterdam
op gezag van de Rector Magnificus
Prof. Dr P. W. C. Akkermans M. A.
en volgens besluit van het College voor Promoties
de openbare verdediging zal plaatsvinden op

woensdag 23 oktober 1996 om 15.45 uur

door

MONIQUE LOUISE ALEXANDRA BROEKHUIZEN
geboren te Haarlem

Promotiecommissie

Promotor: Prof. Jhr. Dr. J. W. Wladimiroff
Promotor: Prof. Dr. A. C. Gittenberger-de Groot

Overige leden: Prof. Dr. J. C. Molenaar
Prof. Dr. J. Baan
Prof. Dr. J. R. G. Kuipers

Co-promotor: Dr. R. E. Poelmann

Brains first, and then, hard work
(Eeyore)

To Marion and Brigitte
To Evert

Contents

Chapter	1	General Introduction	1
	1.1	Introductory remarks	
	1.2	The chick embryo	
	1.3	Definition of objectives	
	1.4	References	
Chapter	2	Intervention models and analyzing techniques	9
	2.1	Introductory remarks	
	2.2	Induction of cardiac anomalies with all-trans retinoic acid in the chick embryo <i>(published in Cardiology in the Young 1992; 2:311-317 and adapted for this thesis)</i>	
	2.3	Abnormal cardiac development due to ligation of the vitelline vein. The venous clip model	
	2.4	Analyzing techniques	
	2.5	References	
Chapter	3	Hemodynamic evaluation of normal chick embryos	51
	3.1	Introductory remarks	
	3.2	Hemodynamic parameters of stage 20 to stage 35 chick embryo <i>(published in Pediatric Research 1993; 34:44-46)</i>	
	3.3	References	
Chapter	4	Hemodynamic evaluation of the preinnervated chick embryonic heart, the retinoic acid model	63
	4.1	Introductory remarks	
	4.2	Hemodynamic parameters of the stage 24 chick embryo	
	4.3	Pressure-volume relationship of the stage 21 and stage 24 chick embryo	
	4.4	References	

Chapter	5	Hemodynamic evaluation of the stage 34 chick embryo the retinoic acid model	81
	5.1	Introductory remarks	
	5.2	Hemodynamic changes in stage 34 chick embryos after treatment with all-trans retinoic acid <i>(published in Pediatric Research 1995; 38:342-348, and adapted for this thesis)</i>	
	5.3	References	
Chapter	6	Altered parasympathetic innervation after retinoic acid treatment	103
	6.1	Introductory remarks	
	6.2	Impaired neural crest derived parasympathetic innervation of embryonic chick hearts in the presence of altered hemodynamics after treatment with all-trans retinoic acid <i>(submitted)</i>	
	6.3	References	
Chapter	7	Hemodynamic evaluation of chick embryos after venous clip	127
	7.1	Introductory remarks	
	7.2	Altered hemodynamics in chick embryos after clipping the vitelline vein.	
	7.3	References	
Chapter	8	Summary and General Discussion	151
Samenvatting en algemene discussie			159
Curriculum vitae			165
List of publications			167
Dankwoord			173

CHAPTER 1

GENERAL INTRODUCTION

1.1 Introductory remarks

Heart development is undeniably a biomechanical process that obeys the laws of physics. Energy is required for each step, from uncoiling and transcription of DNA to every beat of the embryonic heart. The cardiovascular system is not built from a ready made design, but rather moulds from a muscle-wrapped tube into a complex four-chambered heart. This developmental process is directed by morpho-regulatory genes, guided by feedback mechanisms that control growth, and integrated through biological mechanisms that interact with gene products. The coordination of gene expression and gene spin-off generate a sarcomere, a myocyte, the myocardium, the cardiac loop and ultimately the four-chambered heart: the crux of normal development.

In The Netherlands approximately 1500 infants with a cardiac anomaly are born each year. Disordered developmental mechanisms are likely responsible for the pathogenesis of a large proportion of cardiac defects. Some heart defects are primary malformations, basic developmental errors which occur during the early stages of cardiovascular morphogenesis, while others are defects caused by environmental influences encountered during intra-uterine life (Spranger et al. 1982). These influences include specific cardiac teratogens like retinoic acid, alterations in intracardiac blood flow, and vascular and myocardial injury from infectious or toxic agents. Congenital heart disease still accounts for the largest component of infant mortality. In spite of excellent surgery there is a lingering morbidity, and mortality that limits life expectancy of many children with congenital heart disease. Insight into mechanisms which relate structure and function during cardiovascular development may help define etiologies of congenital heart disease.

A program grant supported by the Netherlands Heart Foundation and the Netherlands Organization for Scientific Research allowed intensive investigation of the interaction of hemodynamics and morphogenesis in normal and abnormal heart development. The chick embryo, that shares the morphologic characteristics of the human embryo during early heart development, was chosen as the animal model. The chick embryo allows both hemodynamic evaluation of blood flow and pressure by micro-Doppler and servo-null pressure techniques as well as manipulation by teratogens such as all-trans retinoic acid, and mechanical manipulation through alteration of blood flow. In this thesis hemodynamics and morphology of normal and abnormal cardiac development are studied according to two types of intervention techniques, i.e. the retinoic acid model and the venous clip model. The latter model was devised by the research team of the Department of Anatomy and Embryology, Leiden University. This thesis is part of our long-term aim to pertain a better understanding into mechanisms which relate form and function during cardiovascular development.

1.2 The chick embryo

By the time the hen lays her egg, the arrangement of structures corresponds with eggs which "have been boiled" (Patten 1952). If opened, a circular whitish area will be seen on top of the yolk. In fertilized eggs this area is more pronounced due to aggregation of cells and is known as the blastoderm. Two types of yolk can be differentiated, "white yolk and yellow yolk" (Patten 1952). The outer lining of the yolk is formed by the vitelline membrane. There are two layers of shell membrane which are in contact everywhere except at the blunt end of the egg where the inner and outer membranes are separated to form an air chamber underneath the egg shell. The egg shell is composed mainly of calcareous salts and is porous. The latter allows exchange of gases with the outside air by means of vascular membranes that are in connection with the embryo (Patten 1952). After the egg has been laid, development ceases unless the temperature is kept up to the temperature of the mother. However, moderate cooling of the egg does not result in the death of the embryo. Development may be resumed by the hen or after artificial incubation even after the egg has been kept at room temperature for many days.

The incubation period of the chick embryo is 21 days. It is divided into 46 stages based on external landmarks, including somite number, limb size, and cardiac morphology. The characterization of the developmental stages of the chick embryo is known as the Hamburger and Hamilton (HH) staging system (Hamburger and Hamilton 1951). In 1992 and in 1994 a supplement to the Hamburger and Hamilton staging system was described by Sanes (1992) and Murray and Wilson (1994). During the different phases of development, different characters become prominent. The HH staging system is used by investigators worldwide.

The primary experimental model for the investigation of cardiac morphogenesis has been the chick embryo. Cardiovascular functional maturation is under investigation in human embryonic, fetal, and neonatal studies, and in both in-vivo and in-vitro studies in chick embryo, dog, mouse, rabbit, rat, and lamb models (Keller 1993). At similar stages of development, avian and mammalian embryonic physiology is comparable (Nakazawa et al. 1988).

In this thesis fertile white Leghorn chick eggs were incubated at 38°C and staged according to Hamburger and Hamilton (1951). At stage 15 (24-27 somites and 50-55 hrs of incubation), embryos were subjected to treatment with all-trans retinoic acid. At this stage the heart is merely a beating muscle-wrapped tube. The ventricular loop of the heart is rightward and ventral to the atrioventricular canal. The prospective limb-areas do not protrude yet, and are therefore, not demarcated (Figure 1a). At stage 17 (29-32 somites and 52-64 hours of incubation) venous clip experiments were performed. The heart is looped at this stage. The limb buds are distinct swellings of approximately the same size. All flexures are more accentuated than in stage 15 (Figure 1b).

Physiologic measurements were performed at stage 24 (day 4 of incubation) and stage 34 (day 8 of incubation). At stage 24 the two atria can be distinguished. The interventricular groove indicates the beginning of the separation of the ventricle into right and left ventricle. The wing and leg-buds are distinctly longer than wide (Figure 1*c*). At stage 34 a four-chambered heart is established. By then the limbs have grown considerably (Figure 1*d*).

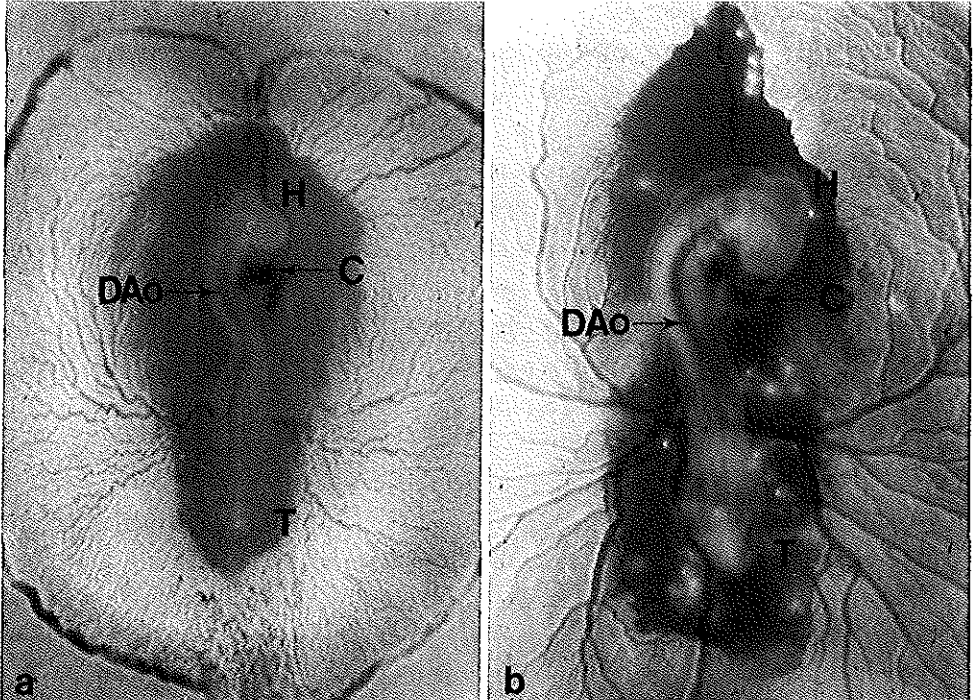


Figure 1. a. Stage 15 embryo. (H: head; C: cardia; DAo: dorsal aorta; T: tail)
b. Stage 17 embryo. (H: head; C: cardia; DAo: dorsal aorta; T: tail)

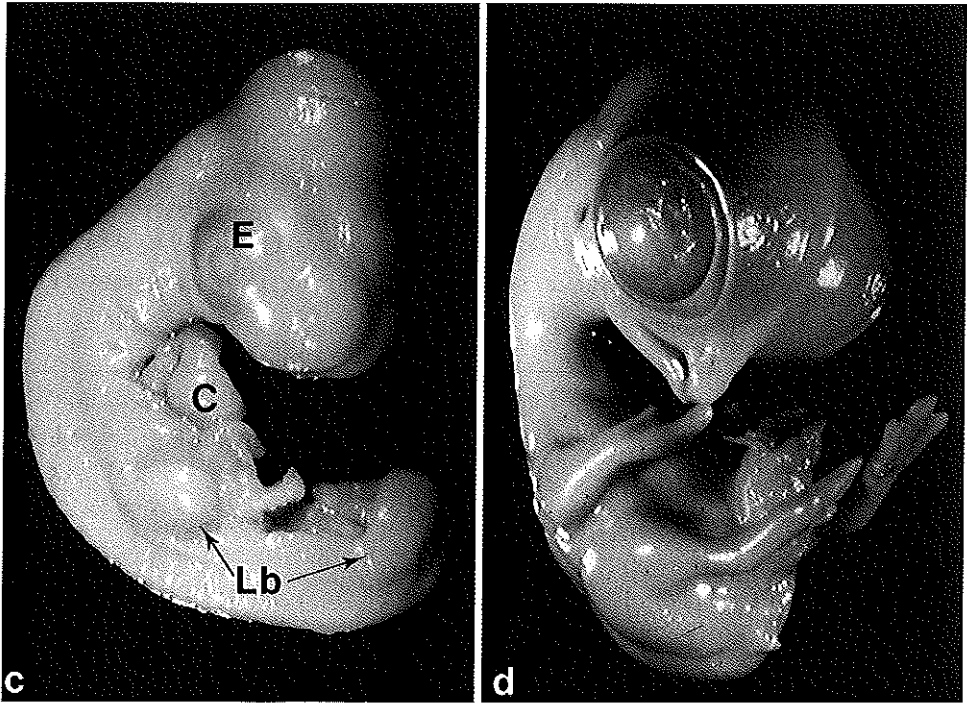


Figure 1. c. Stage 24 embryo. (E: eye; C: cardia; Lb: limb-buds)
d. Stage 34 embryo.

1.3 Definition of objectives

In order to study hemodynamics in abnormal heart development, the first objective was to develop intervention models in which cardiac anomalies could be induced. Following an introduction two models are presented: the retinoic acid model (*chapter 2.2*), and the venous clip model (*chapter 2.3*).

For further studies on hemodynamics associated with abnormal heart development, the second objective was to obtain insight into data on normal flow velocity parameters from stage 20 up to stage 35 (*chapter 3*).

The third objective was to determine the hemodynamic profile of chick embryos, before development of the autonomic nervous system of the heart, after retinoic acid treatment (*chapter 4.2*). The fourth objective was to pursue in this stage the feasibility of the pressure-volume loop recording relative to the retinoic acid model (*chapter 4.3*).

The fifth objective was to investigate whether a difference in hemodynamics exists between embryos with a normally developing heart and embryos with a developing congenital heart malformation after all-trans retinoic acid treatment (*chapter 5*).

The sixth objective was to determine the degree of altered contractility after retinoic acid treatment, through investigation of myocardial innervation. To obtain insight in the innervation of the hearts, immunohistochemical techniques were applied. Data are discussed in *chapter 6*.

The seventh and last objective was to establish whether a difference in hemodynamics exists between embryos with a normally developing heart and embryos with a developing congenital heart malformation after venous clip. Results are presented in *chapter 7*.

1.4 References

- Hamburger V, Hamilton HL (1951) A series of normal stages in the development of the chick embryo. *J Morph* 88:49-92.
- Keller BB, Clark EB (1993) Cardiovascular structural and functional maturation. *Curr Opin Cardiol* 8:98-107.
- Murray BM, Wilson DJ (1994) A scanning electron microscopic study of the normal development of the chick wing from stages 19 to 36. *Anat Embryol* 189:147-155.
- Nakazawa M, Miyagawa S, Ohno T, Miura S, Takao A (1988) Developmental hemodynamic changes in rat embryos at 11 to 15 days of gestation: normal data of blood pressure and the effect of caffeine compared to data from chick embryo. *Pediatr Res* 23:200-205.
- Patten BM (1952) Early embryology of the chick. Maple Press Company, York, PA.
- Sanes JR (1992) On the republication of the Hamburger-Hamilton stage series. *Dev Dyn* 195:229-230.
- Spranger J, Benirschke K, Hall JG, Lenz W, Lowry RB, Opitz JM, Pinsky L, Schwarzacher HG, Smith DW (1982) Errors of morphogenesis: concepts and terms. *J Peds* 100:160-165.

CHAPTER 2

**INTERVENTION MODELS
AND
ANALYZING TECHNIQUES**

2.1 Introductory remarks

To obtain insight into hemodynamics of abnormal heart development, two intervention models were developed to induce cardiac defects: the retinoic acid model, and the venous clip model.

The retinoic acid model (Chapter 2.2)

All-trans retinoic acid has an essential role in normal development but in excess leads to malformations. Congenital malformations have been described after therapeutic use of retinoids and retinol derivatives, for acne and psoriasis during the first trimester of gestation (Lammer et al. 1985). These malformations comprise cardiovascular and facial defects. Cardiovascular anomalies in rat and chick embryos following retinoic acid treatment include outflow tract septation defects (Taylor 1981; Pexieder et al. 1992; Bouman et al. 1995; Broekhuizen et al. 1992, 1995). Experiments with receptors and related substances of retinoic acid show that this substance is active in neural crest cell differentiation (Chambon 1993). In chapter 2.2 the retinoic acid model in the chick embryo is presented. In an addendum to chapter 2.2 additional data on the morphology of the retinoic acid model are presented. The study was performed in collaboration with Hannie Bouman of the Department of Anatomy and Embryology of Leiden University.

The venous clip model (Chapter 2.3)

Another model was developed in which solely a mechanical interference leads to comparable cardiovascular anomalies within the same spectrum as after retinoic acid induction: the venous clip model. This model was devised in the Department of Anatomy and Embryology of Leiden University and developed by Bianca Hogers. The blood flow pattern in normal heart development was studied (Hogers et al. 1995) followed by a study on the effect of venous clip interventions (Hogers et al. submitted). A consistent but continuously changing pattern during development implicates the importance of intracardiac blood flow on heart development.

Chapter 2.4 describes the techniques that were used to obtain insight into the cardiovascular function of chick embryos that were subjected either to retinoic acid or venous clip. Assessment of hemodynamic parameters was acquired through simultaneous measurement of blood flow velocities, with a 20 MHz directional pulsed Doppler velocity meter, and blood pressures with a servo-null system. Analysis of the hemodynamic parameters will be discussed.

2.2 Induction of cardiac anomalies with all-trans retinoic acid in the chick embryo

*Monique L. A. Broekhuizen¹, Juriy W. Wladimiroff¹, Dick Tibboel², Robert E. Poelmann³,
Arnold C. Wenink³ and Adriana C. Gittenberger-de Groot³*

From the Department of Obstetrics and Gynecology¹, Department of Pediatric Surgery², Sophia's Children's Hospital, Erasmus University of Rotterdam, and the Department of Anatomy and Embryology³, Leiden University, Leiden, The Netherlands

Summary

To study the interaction between hemodynamics and morphology in abnormal development of the heart, it is essential to have an animal model with specific and reproducible cardiac malformations. A standardized method was developed for inducing such an anomaly in the chick embryo. For this purpose, all-trans retinoic acid, dissolved in 2% dimethylsulphoxide, was applied on the vitelline membrane of the embryo in concentrations of 1.0 µg or 0.3 µg. A total of 207 embryos, staged according to Hamburger and Hamilton, were treated at stages 10 (33 hours of incubation) and 15 (50-55 hours of incubation). Three control groups consisted of embryos solely treated with dimethylsulphoxide, sham-operated chicks, and untreated embryos, respectively. The embryos were sacrificed on the 9th, 10th and 11th days of incubation and hearts were examined by microdissection. Additional histologic studies were undertaken in 110 cases. Embryos treated with retinoic acid at both stages of development showed a high percentage of lesions falling within the general spectrum of double outlet right ventricle. The abnormality varied from merely a rightward shift of the aorta to cases with an additional subaortic ventricular septal defect, which, in combination with the rightward positioned aorta, was classified as a double outlet right ventricle. Histologic examination showed the presence of muscular tissue between the leaflets of the aortic and mitral valves. No other types of cardiac malformations were seen. Our results, with respect to timing, resemble data from studies made of hearts after surgical ablation of neural crest at comparable stages. Both method and timing of treatment with retinoic acid are important factors for the induction of specific and reproducible cardiac anomalies. This chick model allows for further detailed study of development of double outlet right ventricle, as well as the assessment of early detectable hemodynamic changes.

Introduction

Classically, the understanding of the development of the heart and great vessels is based on collections of normal embryos and, incidentally, abnormal hearts from infants who died before or following surgery. Based on data from these abnormal hearts, and from available normal embryonic and fetal hearts, theories were developed to explain pathogenesis of cardiac lesions. Although these studies have direct relevance for clinical management, the etiology of congenital cardiac anomalies, with particular emphasis on the interaction between hemodynamics and morphology, cannot be extracted from these observations.

It is obvious that flow, blood pressure and heart rate have implications for the intricate relationship of form and function (Clark et al. 1983). Micro-Doppler and micro-pressure studies in normal chick embryos have provided valuable information on this relationship (Hu and Clark 1989). Morphologically abnormal hearts from embryonic chicks are necessary to obtain a comparable insight into the hemodynamics in abnormal cardiac development. Spontaneous anomalies, however, do not provide the necessary reproducible sequence of stages for these hemodynamic studies. It was necessary, therefore, to develop a standardized method for inducing specific and reproducible cardiac anomalies in the chick embryo.

A number of investigators have tried to induce congenital anomalies of the heart either by mechanical interference with blood flow (Rychter 1962; Colvee and Hurlle 1983), or by application of known teratogens at different stages of development (Pexieder 1986; Loeber et al. 1988).

Our standardized method for inducing specific and reproducible cardiac anomalies used a relatively easy and non-traumatic approach, namely applying all-trans retinoic acid on the vitelline membrane of the chick embryo in early stages of development. All-trans retinoic acid is a well-known teratogen for this purpose (Jelínek and Kistler 1981; Chytil 1984; Lammer et al. 1985; Rosa et al. 1986; Yasuda et al. 1986; Kawashima et al 1987; Hart et al 1990). The resulting cardiac malformations resemble closely those described after ablation of the neural crest (Le Douarin 1982; Kirby and Stewart 1983; Kirby 1987; Nishibitake et al. 1987; Kirby 1988; Kirby and Waldo 1990).

In this investigation, we have endeavoured to demonstrate whether administration of a single dose of all-trans retinoic acid in various developmental stages does result in reproducible cardiovascular anomalies and, if so, what is the nature of these anomalies.

Materials and Methods

Fertilized white Leghorn chick eggs were incubated (blunt end up) at 38°C and staged according to Hamburger and Hamilton (Hamburger and Hamilton 1951). The material was subdivided into groups of embryos treated with a solution of all-trans retinoic acid and dimethylsulphoxide, embryos treated with dimethylsulphoxide, sham-operated embryos, control embryos (Table 1).

Each embryo, with the exception of the controls, was exposed by creating a window in the shell followed by removal of the overlying membranes. A solution containing retinoic acid or solely the solvent dimethylsulphoxide was then deposited on the vitelline membrane of the embryo using a Hamilton syringe.

In a pilot study retinoic acid was dissolved in 10% dimethylsulphoxide using concentrations of 1.0 µgr, 0.3 µgr and 0.1 µgr, respectively. The embryos were treated at three stages, namely stage 10 (33 hours of incubation), 15 (50-55 hours of incubation) and 20 (72 hours of incubation), respectively. Since no cardiac anomalies could be established following treatment at stage 20, further experiments were performed only at stage 10 and stage 15. The high mortality rate produced in the pilot study by the use of 10% dimethylsulphoxide solution led to a choice of the lowest concentration possible in which retinoic acid would still dissolve, this being a 2% solution (Table 1). The solution with a concentration of 0.1 µgr retinoic acid also failed to produce abnormalities, so was not used further.

Table 1. Total number of chick embryos used in this study.

Medium	Treated at stage		Examined at stage		
	10	15	35	36	37
1.0 µg RA in 2% DMSO	40		40		
		40	40		
0.3 µg RA in 2% DMSO	40		15	15	17
		47	40		
DMSO	40		40		
		40	40		
Sham	20		20		
		20	20		
Control	40		40		

RA: retinoic acid; DMSO: dimethylsulphoxide.

Following administration of the solution, the window was sealed with tape and the egg reincubated. Embryos were examined at stage 35 through 37 (between day 9 and 11 of incubation). The hearts were fixed in a dilated state with 4% neutral buffered formalin for one week, after which they were examined under a dissecting microscope. The base of the heart was studied in order to establish the relationship between aorta and pulmonary trunk. Subsequently, thin transverse sections (approximately 1 mm thick) of the heart were made, using a razor blade, to examine the morphology of the outflow tracts and the integrity of the ventricular septum. To verify the results of dissection, 110 specimens were serially sectioned at 5 μm thickness, stained with hematoxylin and eosin, and examined microscopically (Table 3).

To exclude a possible delay in closure of the interventricular communication of the embryonic heart, a process which is normally completed by stage 34 (day 8, Sissman 1970), 47 additional embryos were treated with a solution of 1.0 μgr at stage 15 and examined at stage 35 (15 embryos), stage 36 (15 embryos) and stage 37 (17 embryos) (Table 1). The initial screening of the hearts was performed by one investigator. All abnormal hearts, and one-tenth of hearts judged to be normal, were reviewed by an independent investigator.

Results

The pulmonary orifice is usually positioned in front of and to the left of the aortic orifice. The ascending aorta is very short, the aortic arch and the right and left brachiocephalic artery originating directly distal to the aortic orifice (Figure 1*a*).

Treated chick hearts showed normal, as well as abnormal, positions of the arterial trunks. The minimal abnormality noted in the position of the great vessels was characterized by a shift of the aorta to the right (Figure 1*b*). This anomaly was seen in 25 of 40 hearts of embryos treated with a 1.0 μgr solution at stage 10, and in 23 of 40 at stage 15 (Table 2). The embryos treated at these stages with a concentration of 0.3 μgr retinoic acid showed 21 of 40 and 22 of 40 hearts, respectively, with this abnormal position of the arterial trunks (Table 2).

After external examination, internal inspection was performed of sections obtained using the razor blade (Figure 1*c*). In a number of the cases having an abnormal position of the arterial trunks, we could then distinguish a ventricular septal defect in subaortic position which, in combination with the rightward shift of the aorta, produced the ventriculoarterial connection of double outlet right ventricle. The presence or absence of fibrous continuity between the leaflets of the mitral and aortic valves in these hearts could only be determined following histological investigation (Figure 1*d*).

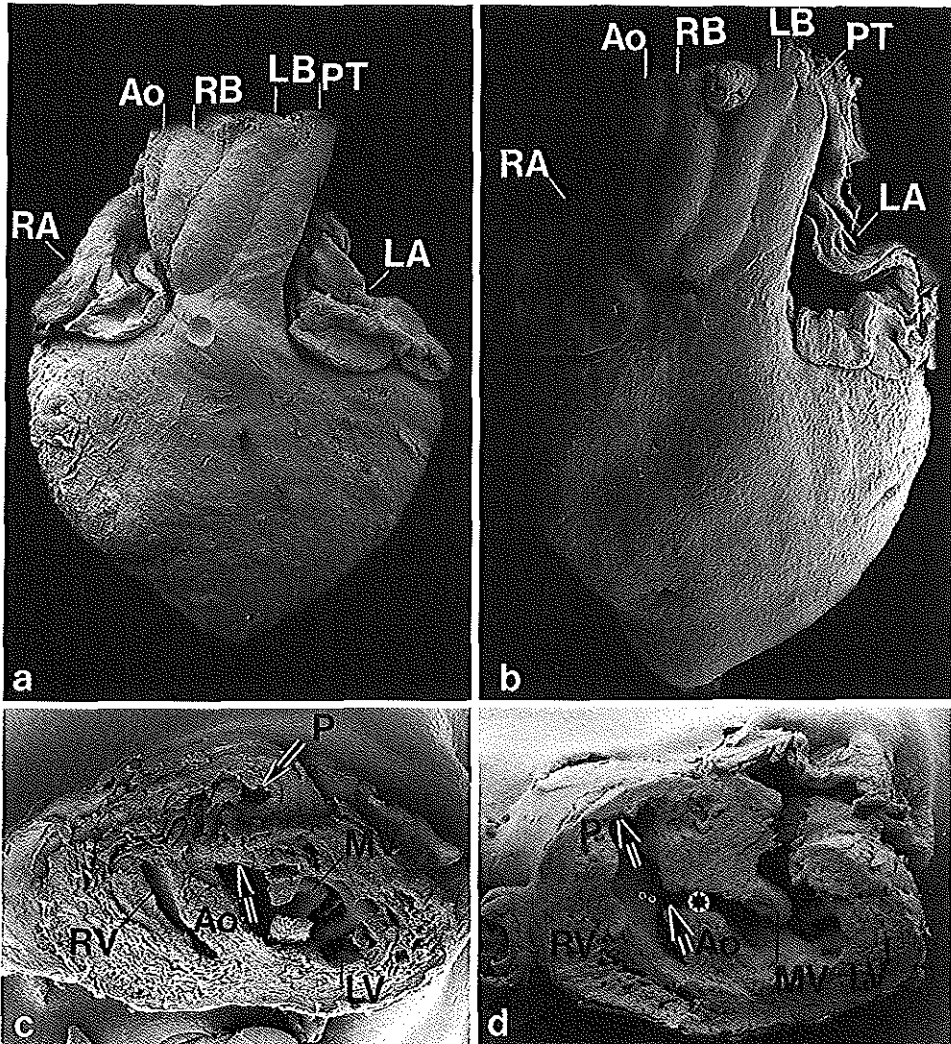


Figure 1. a. Anterior view of a normal heart of a nine day embryo. The great vessels are in normal position as viewed by scanning electron microscopy, (30 X) b. Anterior view of an abnormal heart of a day nine embryo after treatment with all-trans retinoic acid. The aorta and brachiocephalic arteries are displaced to the right, (30 X). c. Transverse section at the level of the outflow tract of a normal nine day embryonic heart, (50 X). d. Transverse section of a heart after retinoic acid. It is sectioned as in Figure 1c at outflow tract level, showing a ventricular septal defect (*). The arrows point towards the pulmonary (P) and aortic (Ao) orifices that are separated by the outlet septum (·). The aortic orifice is in direct continuity with the right ventricle (RV). (RA: right atrium; Ao: aorta; RB: right brachiocephalic artery; LB: left brachiocephalic artery; PT: pulmonary trunk; P: pulmonary orifice; MV: mitral valve; LA: left atrium)

The incidence of double outlet right ventricle in the embryos treated with all-trans retinoic acid at stage 10 and stage 15 are shown in Figure 2, *a-d* and Table 2, along with findings from the normal cases and frequency of deaths. One embryo displayed a heart with a normal position of the arterial trunks in combination with a muscular ventricular septal defect (Figure 2c), a feature which had escaped detection following external examination.

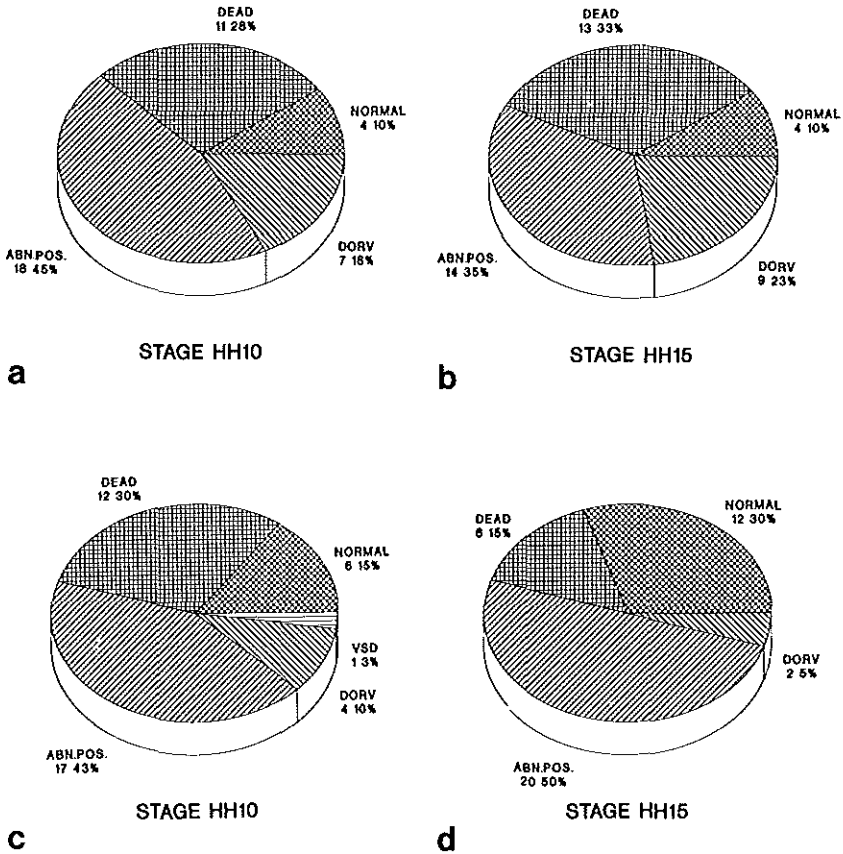


Figure 2. Diagrams showing the results after treatment with 1.0 µgr and 0.3 µgr retinoic acid at stage 10 (a,c) and stage 15 (b,d) of development.

Table 2. Gross morphological assessment of hearts from treated embryos with an abnormal position of the arterial trunks.

	n	Examined at		
		Day 9 stage 35	Day 10 stage 36	Day 11 stage 37
		APOS/DORV	APOS/DORV	APOS/DORV
1.0 µg RA in 2% DMSO				
stage 10	25	18 / 7		
stage 15	23	14 / 9		
	37	6 / 4	11 / 2	10 / 4
0.3 µg RA in 2% DMSO				
stage 10	21	17 / 4		
stage 15	22	20 / 2		

APOS: abnormal position of the great vessels; *DORV:* double outlet right ventricle; *n*= number of embryos; *RA:* retinoic acid.

In hearts of embryos which were not treated with retinoic acid an abnormal position of the arterial trunks was never observed (Table 2). A common arterial trunk, giving rise to both the systemic and pulmonary circulation, was found in two hearts (one from stage 10 and the other from stage 15) treated solely with dimethylsulphoxide. Of the embryos, 17 and 11 treated in this fashion died after treatment at stage 10 and stage 15, respectively (Figure 3*a,b*).

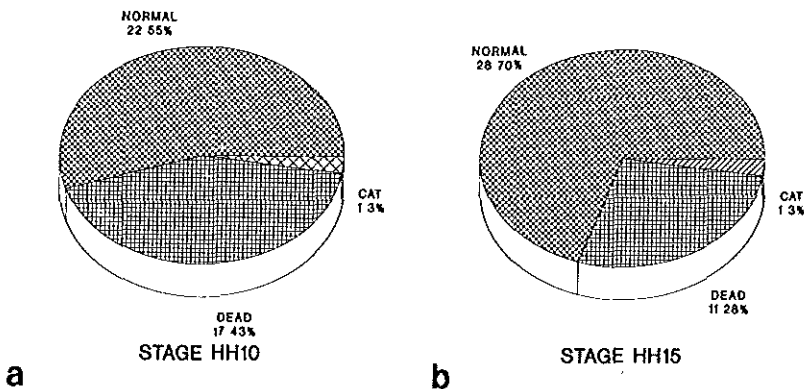


Figure 3. Diagrams showing the results after treatment with dimethylsulphoxide in stage 10 (a) and stage 15 (b) of development.

One muscular ventricular septal defect in combination with a normal position of the arterial trunks was found in the sham group, while nine embryos died (Figure 4a). No cardiac anomalies were seen in the control group in which three embryos died (Figure 4b).

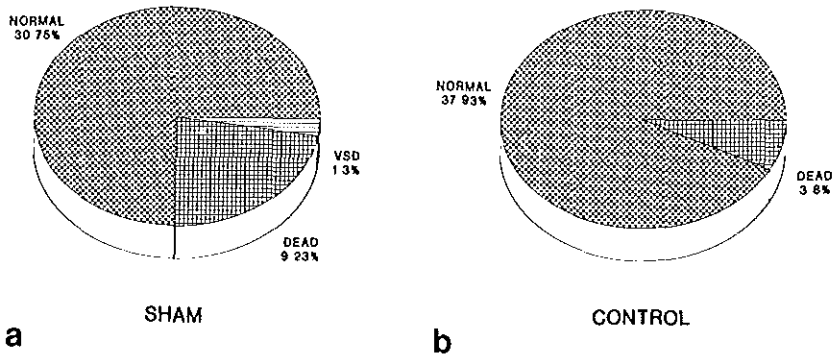


Figure 4. Diagrams showing the results obtained in the sham (a) and control (b) groups.

The results of the histologic investigation of selected specimens are given in Table 3. The macroscopic diagnosis of normal hearts was confirmed at microscopy (Figure 5a). This was also the case for hearts diagnosed as having double outlet right ventricle (Figure 5b), and common arterial trunk, and for the ventricular septal defect in the sham-operated embryo. In the 56 embryos with the diagnosis of solely a rightward displacement of the aortic orifice, an additional 10 were shown to have a small subaortic ventricular septal defect at a level that was missed following sectioning with the razor blade (Table 3). This increases the total incidence of diagnosed double outlet right ventricle. The histological study showed that sparse muscular tissue was present between the leaflets of the aortic and mitral valves, which was not the case in the normal hearts studied. Histology also showed that the defect was located in subvalvar position, and demonstrated partial non-fusion of the outflow tract ridges.

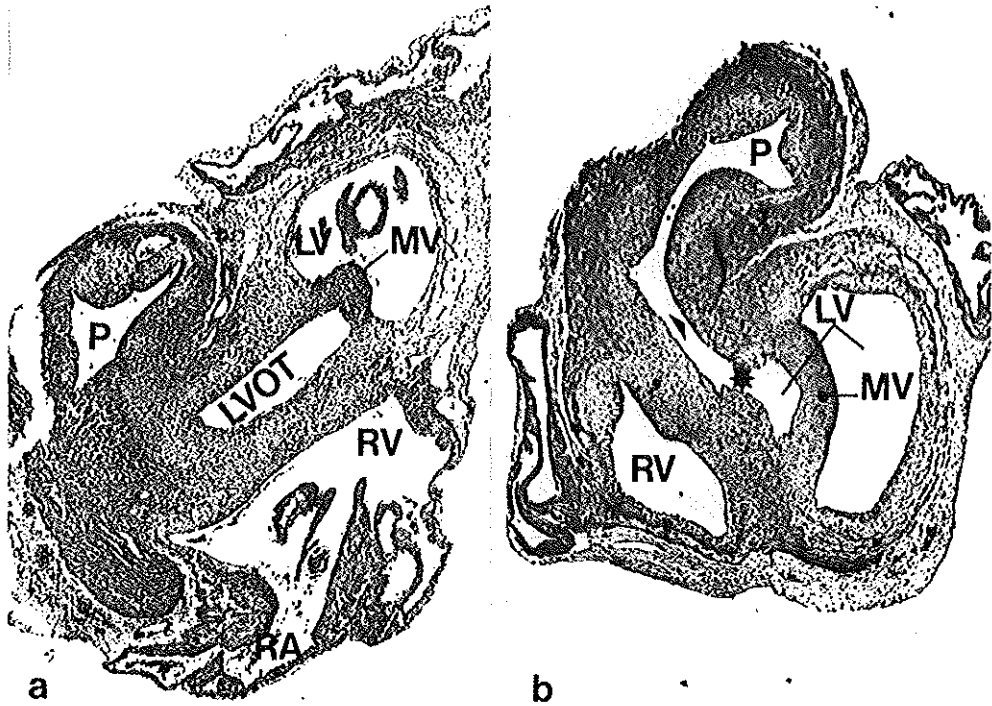


Figure 5. a. Transverse light microscopic section through the outflow tract of a normal heart (RV: right ventricle; P: pulmonary orifice; LV: left ventricle; MV: mitral valve; LVOT: left ventricular outflow tract). b. Transverse section through the outflow tract of a heart with double outlet right ventricle. Both the pulmonary (P) and the aortic orifice are situated above the right ventricle (RV), (compare with Figure 1d). The pulmonary orifice (P) below the outlet septum is in continuity (·) with the outflow tract to the aorta (arrowhead). The ventricular septal defect () is interposed between the outflow to the aorta and the left ventricle (LV). (MV: mitral valve)*

Table 3. Results of histological survey of selected specimens. The diagnosis before and after serial sectioning is displayed.

Group	Treated at stage 10				Treated at stage 15			
	Assessed at stage 35				Assessed at stage 35			
	Serial Sectioning		Serial Sectioning		Serial Sectioning		Serial Sectioning	
	Before	After		Before	After		Before	After
1.0 µg RA in 2% DMSO	APOS	14	DORV	4	APOS	14	DORV	2
	DORV	5	DORV	5	DORV	4	DORV	4
	Normal	1	Normal	1	Normal	2	Normal	2
0.3 µg RA in 2% DMSO	APOS	16	DORV	3	APOS	12	DORV	1
	DORV	3	DORV	3	DORV	2	DORV	2
	Normal	1	Normal	1	Normal	6	Normal	6
DMSO	Normal	4	Normal	4	Normal	4	Normal	4
	CAT	1	CAT	1	CAT	1	CAT	1
Sham	Normal	9	Normal	9				
	VSD	1	VSD	1				
Control	Normal	10	Normal	10				

APOS: abnormal position of the great vessels; DORV: double outlet right ventricle; CAT: common arterial trunk; VSD: minute ventricular septal defect.

Closure of the interventricular communication

To exclude a possible delay in closure of the normal interventricular communication of the embryonic heart, 47 embryos treated with 1.0 µgr retinoic acid at the 15th stage were examined at stage 35, day 9 (15 embryos), stage 36, day 10 (15 embryos) and stage 37, day 11 (17 embryos) (Table 1). An abnormal position of the great vessels was seen in 37 of the 47 hearts, being evenly spread over the various developmental stages (Table 2). A total of 10 hearts were diagnosed as double outlet right ventricle following sectioning with a razor blade.

Discussion

Stage of treatment

Our study shows that a specific and reproducible cardiovascular anomaly can be induced with administration of a single dose of all-trans retinoic acid in staged chick embryos. The highest percentage of anomalies was seen after treatment at Hamburger and Hamilton stage 10 and stage 15. Treatment at stage 20 did not lead to abnormal cardiac development.

These findings are at variance with data from Hart et al. (1990) and Jelínek and Kistler (1981). These workers described a variety of defects found as a result of treatment with retinoic acid at later stages of development. Hart et al. (1990) injected the retinoic acid into the yolk sac at stage 12 through 29 (day 2 to day 6), Jelínek and Kistler (1981) injected it subgerminally or into the amniotic cavity at stage 12 to 24 (day 2 to day 4). Both sets of authors reported a high mortality in embryos treated at stage 12 as a result of the cytotoxicity of retinoic acid, a mortality which decreased with the advancing stage of treatment. This phenomenon was not seen in our experiments, in which the solution of retinoic acid was not directly injected into the yolk sac or amniotic cavity, but was allowed to diffuse through the various membranes to reach the embryo.

Mechanism of induction of cardiac anomalies

It has been suggested that 13-cis retinoic acid induces abnormalities in the chick embryo by its effect on cells from the neural crest (Hassel et al. 1977). Hart et al. (1990) stated that the induced cardiac malformations could not result from a direct interference with migration of these cells since this process is completed by the end of the third day (stage 20). The effect they observed was maximal at the fourth to the sixth day. Instead, they postulated that the effect was mediated through an interference with mesenchymal differentiation of a subpopulation of cells from the neural crest. The effect can be direct, through cytotoxicity (Jelínek and Kistler 1981), or indirect, as a result of alterations in region-specific signals necessary for homing of cells from the neural crest or for their differentiation.

If timing of administration is important, our results correlate more closely with those described after surgical ablation of the neural crest during stage 8 through 11 (Kirby 1987; Kirby and Waldo 1990). Here, too, most cardiac anomalies were found after interference at relatively young stages. Moreover, no cardiac malformations were seen when ablation was performed after the 11th stage. The slight difference in stages of treatment to obtain comparable results between our studies can be explained by the span of time needed for retinoic acid, which was placed on the vitelline membrane, to reach the migrating cells from the neural crest.

Our data suggest a direct effect of retinoic acid on the migrating population of cells, as has also been indicated from other studies (Maden et al. 1991; Ruberte et al. 1991). Further research is necessary to elucidate the exact mechanism underlying the effect of retinoic acid on the embryo at the cellular level in which both timing and technique of administration are taken into account.

Variations in cardiac anomalies

The cardiac malformations reported in animal models of teratogenesis produced by retinoic acid (Jelínek and Kistler 1981; Taylor 1981; Yasuda et al. 1986; Hart et al. 1990), and following exposure of pregnant women to Accutane (de La Cruz et al. 1984; Lammer et al. 1985), show a large variety of abnormalities: common arterial trunk, complete transposition, ventricular septal defects, and double outlet right ventricle. In the present study, however, early and single administration of retinoic acid induced a specific spectrum of double outlet right ventricle. The extreme form consists of double outlet right ventricle with subaortic ventricular septal defect detectable at microdissection. Additional histological studies increased the observed incidence of this form of double outlet right ventricle. It was also shown that lesion resulted from abnormalities located at subvalvar level, with a nonfusion of the outlet ridges. At this stage of developmental differentiation, muscle tissue was still present between the leaflets of the aortic and mitral valves, being suggestive of a type of double outlet right ventricle with aortic-mitral valvar discontinuity. The minor manifestation of the malformation was expressed by an abnormal position of the arterial trunks, dominated by a rightward displacement of the aorta without an underlying ventricular septal defect. The possibility of delayed ventricular septation was excluded following the observation of identical malformations in embryos which were allowed to survive until stage 37 (day 11).

A more extensive study will be conducted on the mechanism underlying the development of this type of double outlet right ventricle. This model in the chick embryo allows for evaluation of cellular biological aspects of the influence of retinoic acid on cardiac morphogenesis as well as the assessment of the hemodynamic parameters involved. The paper of Vuillemin et al. (1991), describing the pathogenesis of double outlet right ventricle in the trisomic mouse, very rightly states "that the same final phenotype can be reached by quite different pathogenetic pathways". Combination of the various data are essential for our extrapolation of the results towards the cardiac abnormalities as seen in the human.

ADDENDUM TO CHAPTER 2.2

The additional data that are presented in this addendum are based on a collaborative study on the morphology of double outlet right ventricle after treatment with all-trans retinoic acid (Bouman et al. 1995). Macroscopic and histologic examinations were supported through graphic reconstruction techniques to obtain a three-dimensional image of the hearts including the internal structure. In particular the location and level of the ventricular septal defect was examined and its relation to the aortic, pulmonary, and atrioventricular orifices.

Graphic reconstructions revealed that normal hearts of embryos of the three control groups had a long subaortic outflow tract with a more or less vertical course (Figure 6a). The contour of the apex, which is mainly formed by the left ventricle, is pointed. The boundary between the left and the right ventricles, i.e. the location of the septum, is recognizable by a groove in the apex. In this stage the ventricular septum is complete. It gradually passes to the right and crosses behind the right ventricular outflow tract. The tricuspid orifice is positioned to the right of the aortic orifice (Figure 6a).

Hearts of retinoic acid treated embryos showed an abnormal horizontal course of the outflow tract. The horizontal course was also seen in hearts diagnosed as double outlet right ventricle (Figure 6b), instead of vertical as seen in normal hearts of embryos of the three control groups (Figure 6a). The ventricular septal defect was located in a subaortic position in this horizontal part. The defect was surrounded by cushion tissue.

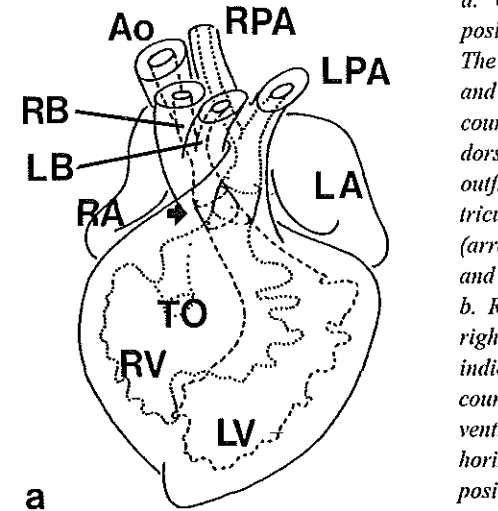
An extreme form of double outlet right ventricle is illustrated in Figure 6c. The ventricular septal defect was located subaortically in the horizontal part of the left ventricular outflow tract. The caudal part of the defect extended into the inflow tract of the right ventricle. The ventricular septal defect was bordered by cushion tissue cranially and dorsally. The ventral border of the ventricular septal defect, i.e. the outlet septum, and the caudal border of the ventricular septal defect, i.e. the main part of the interventricular septum, consisted of myocardium. The abnormal location of the tricuspid orifice was noteworthy (Figure 6c). In these cases the tricuspid orifice was located posterior to the horizontal part of the outflow tract and to the left of the aortic orifice. The location of the ventricular septal defect and its large size, with extension into the inflow tract of the right ventricle, in combination with the abnormal position of the tricuspid orifice caused the tricuspid orifice to be located above both the right and the left ventricle. As a consequence, the blood flow was divided between the left ventricle, by crossing the horizontal part of the subaortic outflow tract, and the right ventricle via the ventricular septal defect.

Figure 6. Graphic reconstructions of chick hearts at stage 34 of development. Frontal views.

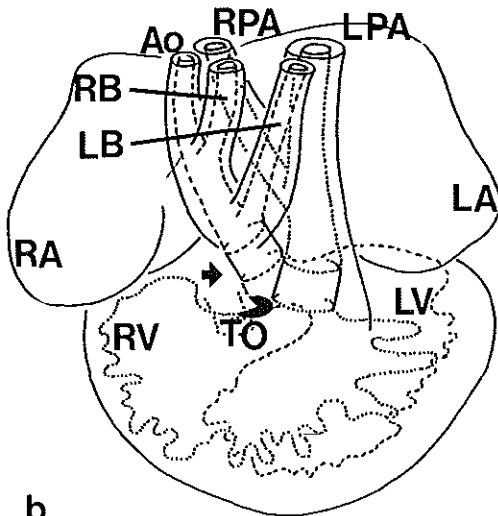
a. Untreated normal chick heart. The arterial pole is positioned between the left and right atrium (LA and RA). The broken line outlines the left ventricular cavity (LV) and its outflow tract, that has a more or less vertical course and passes the right ventricular outflow tract dorsally. The lumen of the right ventricle (RV) and its outflow tract are outlined by a dotted line. Note that the tricuspid orifice (TO) is to the right of the aortic orifice (arrow). (Ao: aorta; PT: pulmonary trunk; RB, LB: right and left brachiocephalic artery)

b. Retinoic acid treated chick heart with a double outlet right ventricle. The left ventricular outflow tract, that is indicated by a broken line, has a horizontal part in its course, before it abruptly bends cranial. The subaortic ventricular septal defect (black area) is located in that horizontal part. The tricuspid orifice (TO) is normally positioned to the right of the aortic orifice (arrow). (Ao: aorta; PT: pulmonary trunk; RB, LB: right and left brachiocephalic artery)

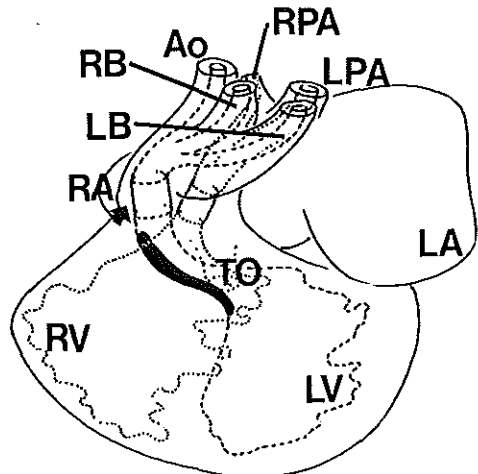
c. Retinoic acid treated chick heart with an extreme form of double outlet right ventricle and a straddling tricuspid orifice. The arterial pole is situated more above the right ventricle (RV) and both atria (RA and LA) are located more above the left ventricle (LV). The branches of the aortic arch turn to the left before they continue their course cranial. The large ventricular septal defect (black area), situated subaortically in the horizontal part of the left ventricular outflow tract extends into the inflow tract of the right ventricle. Note that the tricuspid orifice (TO) is positioned to the left of the aortic orifice (arrow). (Ao: aorta; PT: pulmonary trunk; RB, LB: right and left brachiocephalic artery)



a



b



c

Selected specimen were processed for scanning electron microscopy. Hearts were perfusion fixed in half strength Karnovsky's fixative (Karnovsky 1965) for at least 1 hr. They were then rinsed in 0.1 M sodium-cacodylate buffer (pH 7.2) and postfixed for 2 hrs at 4°C in 1% OsO₄ in the same buffer, followed by dehydration in graded ethanol. The preparations were critical point dried over CO₂ by conventional methods, sputter-coated with gold for 3 min (Balzers MED 010) and studied in the scanning electron microscope (Philips SEM 525M) and photographed).

As shown earlier in normal hearts the pulmonary orifice is positioned in front of and to the left of the aortic orifice (Figure 7*a,b*).

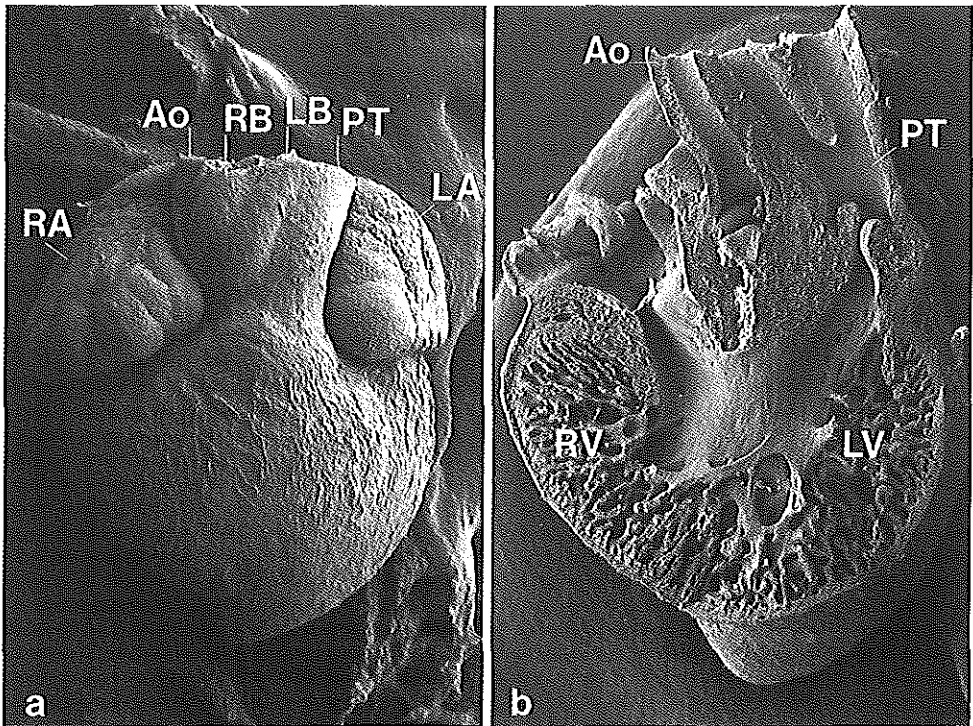


Figure 7. *a.* Scanning electron micrograph of a normal heart of a stage 34 control embryo. The great vessels are in normal position. Anterior view. (RA: right atrium; Ao: aorta; RB: right brachiocephalic artery; LB: left brachiocephalic artery; PT: pulmonary trunk; LA: left atrium) *b.* Scanning electron micrograph of a normal heart of a stage 34 control embryo. Right oblique frontal view of the right ventricle (RV) including the arterial pole. (Ao: aorta; PT: pulmonary trunk)

In a embryo with double outlet right ventricle the arterial pole was situated more above the right ventricle and positioned to the right in relation to the atrial septum (Figure 7c,d). The left and right atria were situated more above the left ventricle as compared to normal. Besides, the ascending aorta was dextroposed in relation to the pulmonary artery. The apexes of these hearts were mostly round instead of pointed, no interventricular groove being recognizable.

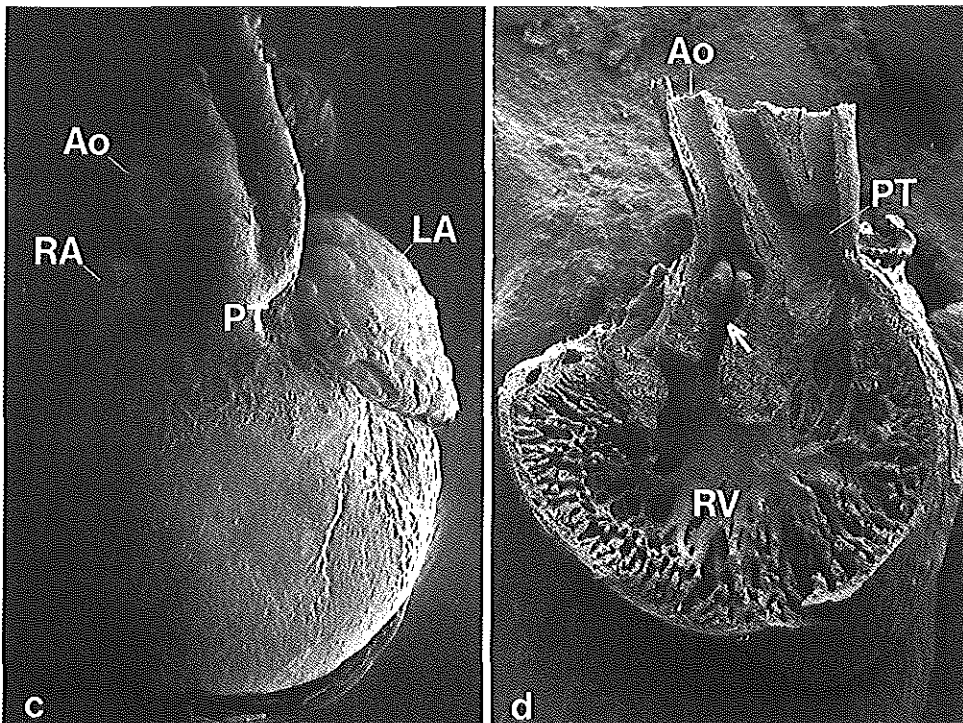


Figure 7. c. Scanning electron micrograph of an abnormal heart of a stage 34 embryo after treatment with all-trans retinoic acid. The aorta and brachiocephalic arteries are displaced to the right. Anterior view. (RA: right atrium; Ao: uorta; RB: right brachiocephalic artery; LB: left brachiocephalic artery; PT: pulmonary trunk; LA: left atrium) d. Scanning electron micrograph of a heart diagnosed as double outlet right ventricle of a stage 34 retinoic acid treated embryo. Right oblique frontal view of the right ventricle (RV) including the arterial pole. The ventricular septal defect is indicated by an arrow. (Ao: aorta; PT: pulmonary trunk)

Discussion

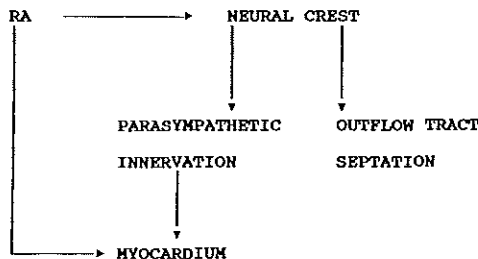
Based on data from the study of Bouman et al. (1995), it is proposed that a disturbance in the process of wedging, the second stage in the looping process, is responsible for the spectrum of double outlet right ventricle after retinoic acid treatment in the chick embryo. The first stage is the formation of the cardiac loop. Initially the early embryonic heart is a nearly straight tube, in which not yet all segments can be recognized (de la Cruz 1991). The cardiac tube curves to the right into a S-shaped structure with five segments, i.e. sinus venosus, atrium, inlet and outlet developing into the mature left and right ventricle, and truncus arteriosus (Gittenberger-de Groot et al. 1995). Chick hearts start to bend at stage 11 resulting in the S-shape at stage 17 (de la Cruz et al., 1972) and a complete cardiac loop on the fourth day of incubation (Steding and Seidl, 1980). In this stage the truncus arteriosus is positioned above the outlet segment and in front of the right side of the atrium. The atrioventricular canal connecting the atrium with the inlet segment, is positioned above this left-sided inlet segment. The inlet segment, in its turn, communicates with the right-sided outlet segment via the primary foramen. Internally there is no indication of ventricular septation.

The second stage is the process resulting in a wedged position of the arterial pole between the tricuspid and mitral orifices and a completely septated four chambered heart with connections of the aorta and pulmonary artery with the left and right outflow tracts, and the left and right atrioventricular orifices with the inflow tracts of the left and right ventricles. This process of wedging is described by Van Mierop and Gessner (1972, 1979) as a medial shift of the truncus arteriosus and a rightward shift of the atrioventricular canal, followed by septation. Lamers et al. (1992) describe the process as a remodelling process in the inner curvature of the looped heart with rightward expansion of the atrioventricular junction and a leftward migration of the subaortic part of the outflow segment. This wedging process is impaired in the spectrum of double outlet right ventricle seen after retinoic acid treatment (Bouman et al. 1995). In the most extreme form there is a limited rightward expansion of the atrioventricular canal, which results in a rightward location of the tricuspid orifice. This limited expansion in combination with an incomplete leftward migration of the aorta could be responsible for an aorta connected to the right ventricle, an incomplete interventricular septation by malalignment, and a tricuspid orifice communicating with the right ventricle via the ventricular septal defect and the subaortic outflow tract.

The cardiac malformations presently produced appear to be part of a spectrum with a normal formation of septa in both the truncus arteriosus and the atrioventricular canal. Besides, a transposition of the great arteries and the related lesion of double outlet right ventricle with subpulmonary defect, do not occur in our spectrum.

Although Anderson (1974) proposed that double outlet right ventricle in combination with a subaortic or subpulmonary defect are part of a continuous spectrum including tetralogy of Fallot, transposition of the great arteries and intermediate types, we believe that the transposition of the great arteries and double outlet right ventricle with a subpulmonary ventricular septal defect are separate entities, and may have different pathogenesis. It has been shown to be important to distinguish morphologically transposed and non-transposed double outlet right ventricle (Bartelings and Gittenberger-de Groot 1991), and epidemiology shows that non-transposed double outlet right ventricle belongs in the category of neural crest related syndromes, transposed double outlet right ventricle being usually non-syndromic (Ferencz et al. 1995). The cardiac malformations found here belong to the non-transposed category. In experimental models transposed double outlet right ventricle has been produced in the mouse, but not in the chick (Gittenberger-de Groot 1995) suggesting species specificity.

Concerning the mechanism of retinoic acid on the heart we postulate that there may be a direct and an indirect effect on the myocardium.



Cardiac looping is related to the development of myofibrils and myofibril structure (Manasek et al. 1986; Itasaki et al. 1991; Shiraishi et al. 1992). It is described that retinoic acid has multiple effects on growth and differentiation of cardiac myocytes, including an inhibition of cell proliferation, development of heart contractions, and delay in α -actin synthesis (Wiens et al. 1992). Pexieder et al. (1995) showed that all-trans retinoic acid can modify cardiac contractility. In rat fetuses treated during pregnancy with all-trans retinoic acid, a higher sensitivity toward extracellular calcium ion variations was found. This could indicate an increased permeability of the sarcolemma and/or delayed development of the sarcoplasmic reticulum (Pexieder et al. 1995). Furthermore, they reported that all-trans retinoic acid significantly decreased the total amount of protein in morphologically normal mouse hearts and hearts that showed double outlet right ventricle. In these morphologically normal and abnormal hearts, the concentration of sarcoplasmic proteins was significantly increased and that of contractile proteins decreased.

An interaction of retinoic acid and contractile proteins could cause a disturbance in the myofibrillogenesis or myofibril arrangement and result in myocardial dysfunction accompanied by abnormal cardiac looping.

The indirect effect may result from an impaired parasympathetic innervation through a disturbance of the migration of cells from the neural crest. It is described that neural crest cells contribute to the cardiac ganglia (Kirby and Stewart 1983; Kirby 1993). Parasympathetic innervation of the heart via the cardiac ganglia could be impaired after treatment with retinoic acid. The effect of all-trans retinoic acid on the neural crest may be through cytotoxicity (Jelínek and Kistler 1981) or result from alterations in region-specific signals necessary for homing of neural crest cells or for their differentiation (Hart et al. 1990). The action of retinoic acid at the cellular level can be linked to the fact that neural crest cells show particular expression of retinoic acid binding protein (CRABP) (Maden et al. 1991). Retinoic acid receptors (RARs) and CRABPs play an important role in the mechanism of gene expression (Gudas 1992; Morris-Kay 1992; Ross 1993), but their specific spatiotemporal patterns of expression, are extremely complex (Morris-Kay 1992; Ross 1993). The study of Lohnes et al. (1994) and the accompanying study of Mendelsohn et al. (1994) of RAR double mutant mouse fetuses show that RARs are involved in the ontogenesis of many organs and that the cardiac malformations in these mutant mice are comparable to those in cardiac neural crest ablated chickens (Kirby and Waldo 1990). Furthermore, in-vitro mesenchymal cell migration is inhibited by retinoids (Smith-Thomas 1987; Thorogood et al. 1982). Impaired parasympathetic innervation through a disturbance in neural crest cell migration could lead to an alteration of the tonus of the cardiac myocytes. Both direct and indirect effects on the myocardium could generate myocardial dysfunction.

2.3 Abnormal cardiac development due to ligation of the vitelline vein.

The venous clip model

devised by Bianca Hogers, Marco C. DeRuiter, Robert E. Poelmann, and Adriana C. Gittenberger-de Groot, Department of Anatomy and Embryology, Leiden University

Introduction

Embryonic blood flow is distributed between the embryonic and extraembryonic circulations in the chick embryo, and between the embryo and placenta in mammals. The distribution of blood flow through the embryonic heart has been of major interest to developmental biologists for many years (Rychter 1962; Yoshida et al. 1983). Although these studies describe experiments in which blood from the yolk sac circulation is visualized through the heart or pharyngeal arch arteries, none were performed by injection of dye into the smallest venules of particular yolk sac regions. During normal development, stage-specific intracardiac blood flow patterns are described and the localization of these various currents is determined by the origin in the six yolk sac areas (Hogers et al. 1995). It is reported that a consistent but continuously changing flow pattern during development, indicates the importance of intracardiac blood flow on heart development.

It is described by Manasek and Monroe (1972), that the first phase of heart looping appears to be independent of blood flow. This has been recently supported by studies on gene regulation of heart looping (Dickman and Smith 1996). An additional role for blood flow is indicated in the refined modeling of the endocardial cushions and ridges as has been reported by Meuer and Bauman (1988). They showed that absence of blood flow results in cardiac lumen obstruction by cardiac jelly proliferation.

The long-term effect of blood flow on cardiovascularogenesis has been universally studied through mechanical manipulation of various arterial and heart segments resulting in a variety of cardiac outflow tract malformations (Rychter 1962; Colvee and Hurlle 1983; Clark et al. 1984). Mechanical interference in the pharyngeal arch region could restrict the migration of e.g. cardiac neural crest cells. Ablation of the cardiac neural crest leads to various cardiac anomalies ranging from anomalies of the pharyngeal arch, outflow tract (common arterial trunk, double outlet right ventricle), tricuspid valve, and ventricular septal defects (Kirby and Waldo 1990). Despite the fact that these cardiac anomalies were considered to be the effect of altered blood flow, it has to be kept in mind that manipulation in the head and neck region of the embryo could interfere with normal embryonic morphogenetic processes.

To bypass intervention side effects at the arterial side of the heart, venous blood flow has been manipulated through trans-section (Rychter and Lemez 1965) or ligation (Orts Llorca et al. 1980). However, the survival rate of the embryos was very low and the survival time was rather short.

Recently an intervention model was designed in which intracardiac blood flow was changed resulting from a rerouting of venous inflow. Cardiac malformations were induced by permanent obstruction of the right lateral vitelline vein with a microclip, the venous clip model (Hogers et al. submitted) This model will allow us to evaluate biologic aspects of the influence of blood flow on cardiac morphogenesis as well as the hemodynamic parameters involved.

The venous clip model

Fertile white Leghorn chick eggs were incubated on their side at 37°C and staged according to Hamburger and Hamilton (1951). At stage 17 (70 hrs of incubation), the egg shell was cleaned with ethanol 70% and windowed. All manipulations were performed in ovo using a dissecting microscope. The egg was kept warm in isolated foil. Above the chosen clip site the vitelline membrane was removed and a small incision was made with a tungsten needle in the yolk sac membrane, adjacent to the vitelline vein. Microclips have been devised from a nickel carrier grid, otherwise used for transmission electron microscopy. A microclip was used to clip the right lateral vitelline vein. Cessation of blood flow proximal to the microclip was confirmed. After venous clip the window was sealed with tape and the egg reincubated until stage 34 (day 8), stage 37 (day 11) and stage 45 (hatching). A total of 91 embryos were successfully ligated. Sham (n=10), in which all procedures were similar except for ligation with a microclip, and normal eggs (n=10) served as controls.

The embryos including the hearts were macroscopically evaluated, prior to fixation in a mixture of 2% glacial acetic acid in 100% ethanol at 4°C. After paraffin embedding, the embryos were serially sectioned. The 5 µm sections were alternately stained with hematoxylin/eosin and a modified Van Gieson stain.

In addition some venous clip embryos were prepared for scanning electron microscopy. Half strength Karnovsky's (1965) perfusion fixed hearts were opened frontally with iridectomy scissors. They were rinsed in 0.1 M sodium-cacodylate buffer (pH 7.2) and postfixed for 2 hrs at 4°C in 1% OsO₄ in the same buffer, followed by dehydration in graded ethanol solutions. The preparations were critical point dried over CO₂ by conventional methods, sputter-coated with gold for 3 min (Balzers MED 010) and studied in the scanning electron microscope (Philips SEM 525M).

Cardiac Malformations

Venous clip lead to anomalies of the heart and pharyngeal arch arteries in 58 cases. Only the cardiovascular system was affected. The extremities, head and eyes underwent normal morphological development. Sham and control embryos were normal except for one sham embryo, that had a small ventricular septal defect.

Venous clip resulted in a spectrum of mostly outflow tract malformations, ranging from a mild form with a low subaortic ventricular septal defect with a muscular outflow tract septum to a severe form with a high ventricular septal defect directly below semilunar valve level. In the latter, orifice septation was only produced by mesenchyme. Semilunar valve abnormalities were common in both the mild and severe types of outflow tract defects. These valve abnormalities varied from an additional leaflet and fused commissures to bicuspid aortic valve leaflets and quadrid pulmonary valve leaflets. Although the intracardiac malformations mainly consisted of outflow tract defects some atrioventricular anomalies were observed (7/58), that usually occurred in combination with a ventricular septal defect (6 out of 7 cases). Due to impaired wedging of the arterial trunk between the atrioventricular orifices, the tricuspid orifice was sometimes situated dorsal in relation to the aorta instead of to the right of the aorta.

There was also a substantial number (32/58) of pharyngeal arch artery malformations, like abnormal obliteration or persistence of the fourth pharyngeal arch artery, e.g. interruption of the aorta. Within the group of 32 embryos with pharyngeal arch artery malformations, 28 cases with additional heart anomalies were observed, while there were only 4 solitary cases.

Malformed hearts often coincided with a rightward positioned aorta. A rightward positioned aorta in combination with a subaortic ventricular septal defect was defined as double outlet right ventricle. Figure 8 shows a scanning electron micrograph of the severe form of double outlet right ventricle. Absence of proper outflow septation at valvular level results in continuous semilunar valve leaflets. Both arterial orifices are above the right ventricle.

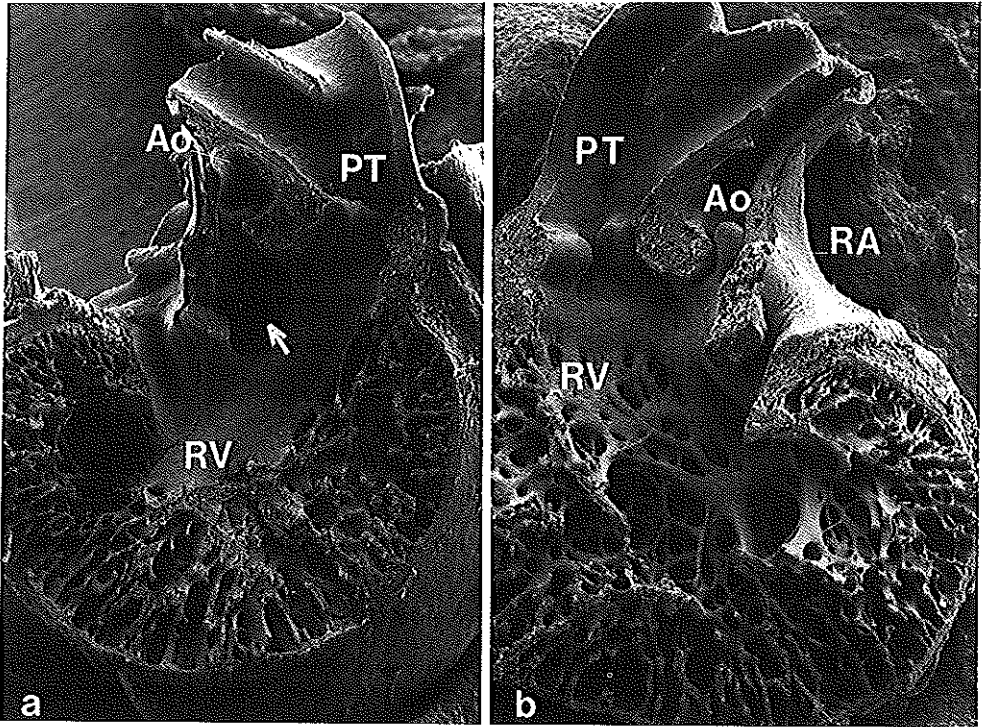


Figure 8. a. Scanning electron micrograph of a heart of a stage 34 venous clip embryo. Right oblique frontal view of the right ventricle (RV) including the arterial pole. The semilunar valves of the aorta (Ao) and pulmonary trunk (PT) are relatively small. The ventricular septal defect is indicated by an arrow. b. Scanning electron micrograph of the same stage 34 heart after venous clip as (a). The other half of the right ventricle (RV) including the arterial pole. (RA: right atrium)

Discussion

During normal development Hogers et al. (1995) described stage-specific blood flow patterns, which are considered to play an important role in heart development. In the venous clip model they were able to disturb normal flow patterns (Hogers et al. submitted). The most prominent blood flow changes were seen in the outflow tract. Permanent ligation of the right lateral vitelline vein with a microclip proved to be a good model to produce specific cardiovascular malformations, as subaortic ventricular septal defects, semilunar valve anomalies, atrioventricular valve anomalies, rightward positioned aorta, double outlet right ventricle, and pharyngeal arch artery anomalies (Hogers et al. submitted). They postulated that the observed conotruncal abnormalities are due to the changed intracardiac flow patterns because there is no direct manipulation to any part of the embryo.

The cardiac anomalies induced by venous clip are remarkably similar to malformations after cardiac neural crest ablation (Nishibitake et al. 1987; Leatherbury et al. 1993; Kirby 1993; Gittenberger-de Groot et al. 1995), excessive retinoic acid treatment (Broekhuizen et al. 1992; Bouman et al. 1995), and cervical flexure experiments (Männer et al. 1993, 1995). All present a rightward shift of the aorta, ventricular septal defects, and pharyngeal arch malformations. A number of cardiac defects obtained in all models, including the venous clip model, can be attributed to lack of proper looping particularly in later stages (Männer et al. 1993; Bouman et al. 1995; Kirby and Waldo 1995). Impaired looped hearts are characterized by an increased distance between inflow (atrioventricular canal) and outflow, a rightward position of the arterial trunk and present disturbed atrioventricular and outflow tract cushions formation. The possible causes responsible for the disturbed looping could be different for the specific models.

In conclusion, cardiac malformations induced by venous clip are similar to other models such as neural crest ablation (Nishibitake et al. 1987; Leatherbury et al. 1993; Kirby 1993; Gittenberger-de Groot et al. 1995), retinoic acid model (Broekhuizen et al. 1992), and thoracic wall closure defects (Männer et al. 1995). However, the cascade of events leading to cardiac malformations after venous clip is yet to be resolved.

2.4 Analyzing techniques

Introduction

The precise measurement of embryonic cardiovascular function has challenged investigators for more than a century (Clark 1990). The primary experimental model for the investigation of cardiac morphogenesis has been the chick embryo, and despite the small size of the embryonic chick heart, experimental methods were developed to accurately measure blood flow, blood pressure and chamber size, and to alter cardiac function or form (Clark 1989, Broekhuizen 1993, 1995). The simple fact that a stage 21 chick embryo ventricle has a pressure wave form identical to the mature left ventricle, is not only remarkable, but suggests a conservation of myocardial mechanics independent of scale. In this thesis, the study of embryonic cardiac hemodynamics was performed using a 20 MHz directional pulsed Doppler flow velocity meter and a servo-null pressure system.

Physics of blood flow using the Doppler effect

When an emitted sound beam is reflected from a moving target to a stationary receiver the frequency of the received echo signal is different from the frequency of the original emitted signal. Christian Johann Doppler (1803-1853), an Austrian physicist, was the first to describe this effect. The change in frequency is called the Doppler shift in frequency.

For those cases where a single transducer serves as both emitter and receiver (pulsed wave mode), or where the transmitter and receiver are located together (continuous wave mode), the equation relating the velocity of a moving reflector to the Doppler shift frequency, Δf (Hz), is:

$$V = (\Delta f * c) / (2 * \Delta f_0 * \cos\alpha)$$

where f_0 is the transmitted frequency (Hz), V is the velocity of the reflector (m/s), and α is the angle between the direction of the sound beam and the velocity vector (Franklin et al. 1961; Baker 1970). This equation is valid for both continuous and pulsed excitation of the transducer. Whereas pulsed wave mode allows depth selection, in continuous wave mode it is possible to register high velocities.

When pulsed excitation is used, short bursts of sound are directed into a blood vessel where they are reflected by the blood cells. The reflected sound is Doppler-shifted according to the equation above, returning to the transducer after a delay which is determined both by the speed of sound in medium, and the distance between transducer and the blood cells.

The time required for the burst of sound to travel to a reflector and back is given by the echo ranging equation: $t=2*d/c$, where t is the time delay (s), d is the distance between the transducer and the reflector (m) and c is the speed of sound in the medium (m/s).

The reflected sound, which is received by the transducer and converted back to an electrical signal, is sampled for the duration of a range gate pulse which occurs a brief instant later than the transmitted burst. The sampled value is held until the next sampling pulse, when a new value is acquired. The resulting signal represents the average or the summation of the Doppler frequency shifts associated with each reflector within a small volume within the vessel, known as the sample volume. Within the pulsed Doppler instrument the sampled echo signal is amplified and compared in phase and frequency with a reference signal from the master oscillator operating at the ultrasonic carrier frequency, Δf_0 .

Doppler velocity meter

For measurement of blood flow velocities in the chick embryo model a 20 MHz directional pulsed Doppler velocity meter (model 545C-4 by Bioengineering, University of Iowa) was used (Harley and Cole 1974; Marcus et al. 1981). Using such a high frequency has the advantage of producing stronger acoustic reflections from blood cells.

The accuracy of this equipment was tested against a calibrated velocity. Anticoagulated pig blood was pumped at constant pressures to obtain constant flows. The blood was led through a 3 mm diameter channel, which was drilled into a perspex block. At an angle of 45° to the first channel an additional channel was made in which the 750 micron Doppler probe was placed. At the outflow side of the first channel a stretch of polyvinylchloride tubing (internal diameter 3 mm, length 100 cm) was connected and marked. Only after a constant flow was acquired a stopwatch was started at the first marking point $x=0$ cm and stopped when blood reached $x=100$ cm. The calibrated blood velocity was calculated from the time elapsed in crossing this trajectory of 100 cm. The time-average of the Doppler velocity V (mm/s) was determined by recording a voltage E supplied by the Doppler velocity meter, using the equation $V = 78.25 * E / \cos 45^\circ$. The relationship between Doppler velocity and calibrated velocity was determined from regression analysis. Figure 9a depicts the relationship between Doppler velocity and calibrated velocity ($y = 1.18x - 3.24$, $r^2 = 0.99$, $SEE = 1.38$ mm/s).

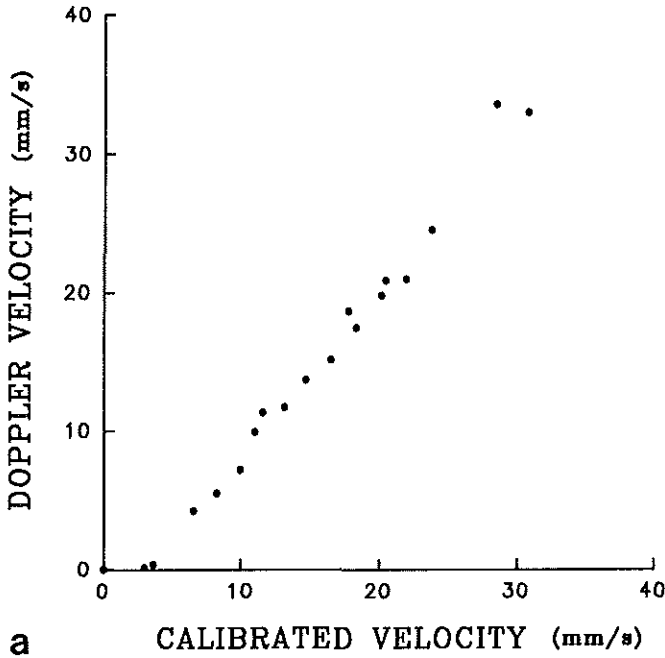
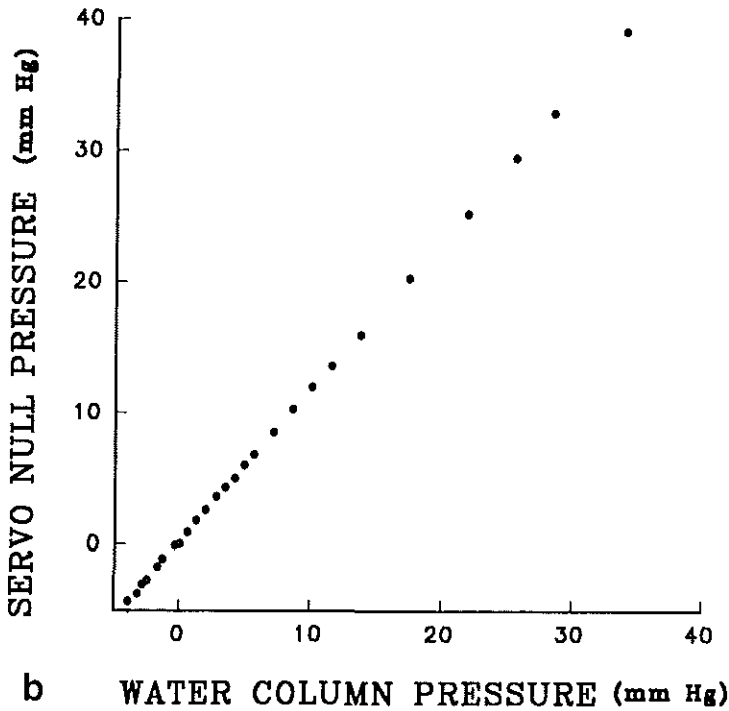


Figure 9.
a. Relationship between in-vitro Doppler velocity and calibrated velocity from 0 to 35 mm/s.



b. Relationship between servo-null pressure and water column pressure from -5 to 40 mmHg.

Using a micromanipulator and projector jig it was possible to position the Doppler probe consisting of a 750 micron piezoelectric crystal at a 45° angle to the dorsal aorta at the level of the sinus venosus (Figure 10*a,b*). A 45° angle was chosen for consistency in the velocity calculations.

The internal diameter of the dorsal aorta was measured at the same level with a filar micrometer eyepiece which was calibrated against a 10 µm scribed glass standard. The area was calculated from the equation $area = \pi d^2/4$ where d is the aortic diameter (mm).

Servo-null pressure system

Using an additional micromanipulator blood pressure was measured in the dorsal aorta at stage 24, and in the left vitelline artery at stage 34, with a servo-null system (model 900A, World Precision Instruments, Inc., Sarasota, Florida) and a fluid filled 10 µm glass micropipette attached to a microelectrode (Figure 10*a,b*). The system includes the main electronic control unit plus the pressure controller. The latter includes an amplifier, a piezoelectric valve and a pressure transducer. The piezoelectric pressure controller regulates internal pipet pressure by dynamic control of air flow into and out of a small pressure chamber (microelectrode). A vacuum source is connected to the outlet side of the chamber while a piezoelectric valve measures the entry of pressurized air into the chamber. The residual volume of the pressure chamber includes micropipette, connecting tubing and the pressure transducer on the outlet side of the piezoelectric valve. The electronic system accurately controls and adjusts the pressure in the chamber to match pressures applied externally to the microelectrode tip. Using this servo-null mechanism blood pressures can be measured in the chick.

The servo-null pressure system was tested against a standing water column. A total of 26 measurements were performed. The relationship between the servo-null pressure system and the water column pressure was determined by regression analysis. The method was linear from -5 mmHg to 40 mmHg ($y = 1.14x + 0.25$, $r^2 = 0.99$, standard error of estimate = 0.12 mm Hg) (Figure 9*b*). Zero trans-tip pressure was obtained by immersing the tip of the micropipette in the extraembryonic fluid at the level of the measured site.

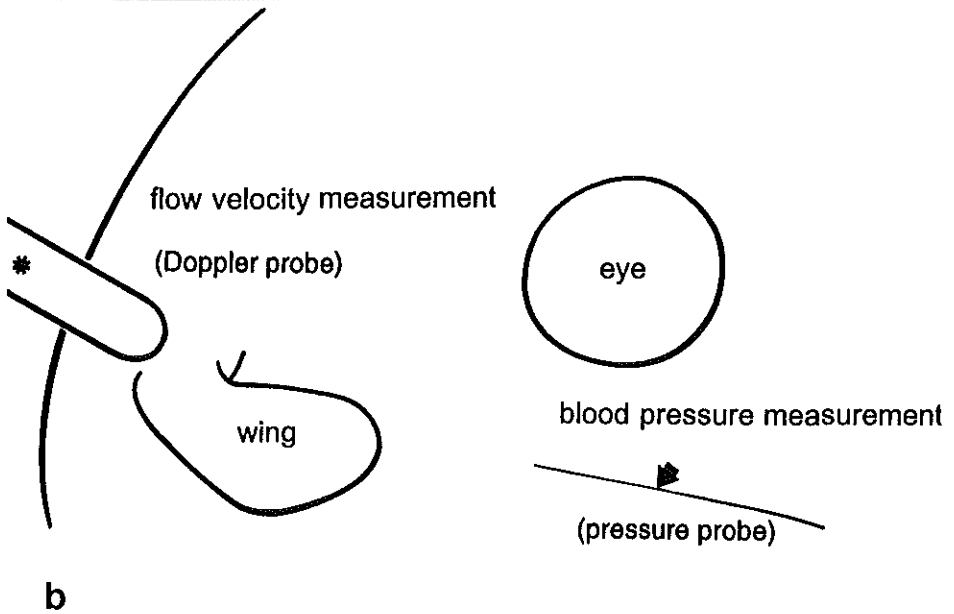
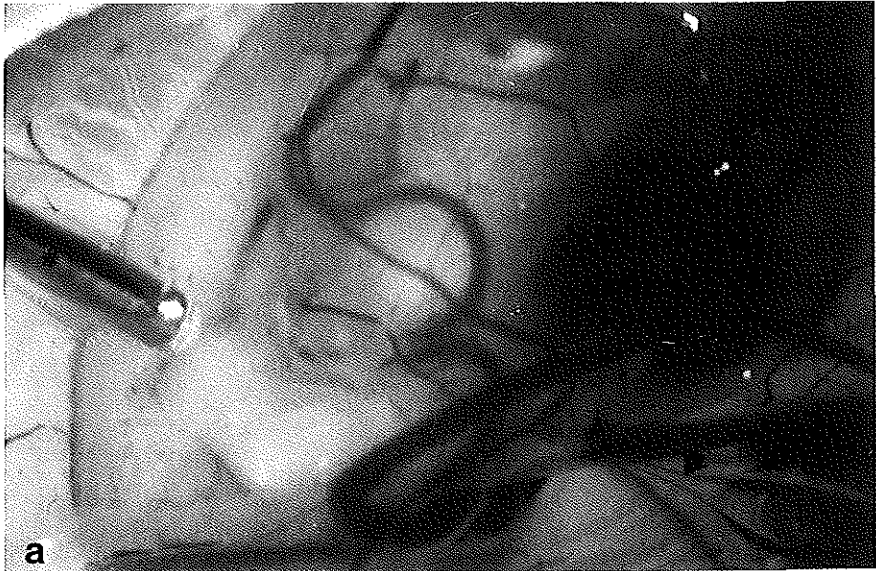


Figure 10. a,b. A stage 34 chick embryo. Dorsal aortic blood flow velocity is measured with a Doppler probe positioned at the level of the sinus venosus (). In this stage vitelline artery blood pressure is measured with a glass micropipette (arrow).*

Hemodynamic parameters

The analog wave forms were sampled at 300 Hz by a Lab Master data acquisition analog-digital board (Axon Instruments Inc.) linked to a computer. The converter offered 12 bits at an input range of -10 to 10 Volt. Data were stored in a Bernoulli disk cartridge (Iomega Corp., Roy, Utah). Peak-systolic, end-diastolic and mean blood pressures were determined. Arterial dP/dt (mmHg/s) was derived from the analog pressure signal by digital differentiation. Mean dorsal aortic blood flow (mm^3/s) was calculated as the product of the mean velocity and the area of the dorsal aorta. By measuring the cycle length between pulse waves and converting this into beats per minute (bpm), the heart rate was calculated. The peak acceleration dV/dt (mm/s^2) was derived from the dorsal aortic velocity $V(t)$ by means of digital differentiation. Figure 11 displays parameters calculated from the flow velocity wave form recording. Stroke volume (mm^3) was determined from the quotient of mean dorsal aortic blood flow and heart rate multiplied by 60. Cardiac work ($\text{mm}^3 \cdot \text{mmHg}$) is the product of stroke volume and mean arterial pressure. Vascular resistance ($\text{mmHg}/(\text{mm}^3/\text{s})$) is the quotient of mean arterial pressure and mean dorsal aortic blood flow.

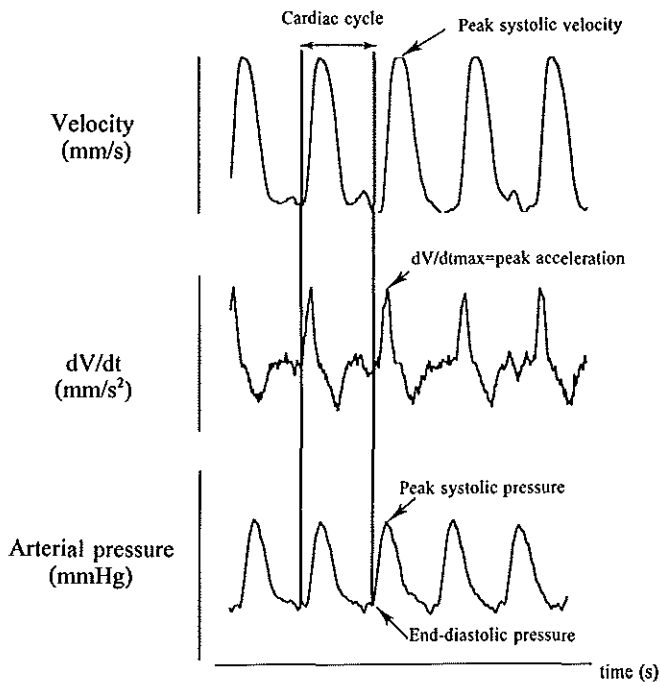


Figure 11. Parameters calculated from the flow velocity wave form.

2.5 References

- Anderson RH, Wilkinson JL, Arnold R, Becker AE, Lubkiewicz K (1974) Morphogenesis of bulboventricular malformations. II. Observations on malformed hearts. *Br Heart J* 36:948-970.
- Baker DW (1970) Pulsed ultrasonic Doppler blood-flow sensing. *IEEE Trans Sonics Ultrasonics* SU-17:170-185.
- Bartelings MM, Gittenberger-de Groot AC (1991) Morphogenetic considerations on congenital malformations of the outflow tract. Part 2: complete transposition of the great arteries and double outlet right ventricle. *Int J Cardiol* 33:5-26.
- Bouman HGA, Broekhuizen MLA, Baasten MJ, Gittenberger-de Groot AC, Wenink ACG (1995) Spectrum of looping disturbances in stage 34 chicken hearts after retinoic acid treatment. *Anat Rec* 243:101-108.
- Broekhuizen MLA, Wladimiroff JW, Tibboel D, Poelmann RE, Wenink ACG, Gittenberger-de Groot AC (1992) Induction of cardiac anomalies with all-trans retinoic acid in the chick embryo. *Cardiol Young* 2:311-317.
- Broekhuizen MLA, Mast F, Struijk PC, Van der Bie W, Mulder PGH, Gittenberger-de Groot AC, Wladimiroff JW (1993) Hemodynamic parameters of stage 20 to stage 35 chick embryo. *Pediatr Res* 34:44-46.
- Broekhuizen MLA, Bouman HGA, Mast F, Mulder PGH, Gittenberger-de Groot AC, Wladimiroff JW (1995) Hemodynamic changes in HH stage 34 chick embryos after treatment with all-trans retinoic acid. *Pediatr Res* 38:342-348.
- Chambon P (1993) The molecular and genetic dissection of the retinoid signalling pathway. *Gene* 135:223-228.
- Chytil F (1984) Retinoic acid: biochemistry, pharmacology, toxicology and therapeutic use. *Pharm Reviews* 36:935-945.
- Clark EB, Hu N, Dummett JL, Van de Kieft GK, Olson C, Tomanek R (1983) Ventricular function and morphology in chick embryo from stages 18-29. *Am J Physiol* 250:H407-H413.

Clark EB, Hu N, Rosenquist GC (1984) Effect of conotruncal constriction on aortic-mitral valve continuity in the stage 18, 21 and 24 chick embryo. *Am J Cardiol* 53:324-327.

Clark EB (1990) Hemodynamic control of the embryonic circulation. In: Clark EB, Takao A (eds) *Developmental Cardiology: Morphogenesis and Function*. Futura Publishing Company, Mount Kisco, New York, pp 291-303.

Clark EB and Takao A (1990) Overview: A focus for research in cardiovascular development. In: Clark EB, Takao A (eds) *Developmental Cardiology: Morphogenesis and Function*. Futura Publishing Company, Mount Kisco, New York, pp 3-12.

Clark EB, Markwald RR, Takao A (eds) *Developmental mechanisms of heart disease*. Futura Publishing Company, Armark, New York, pp 639-653.

Colvee E, Hurle JM (1983) Malformations of the semilunar valves produced in chick embryos by mechanical interference with cardiogenesis. *Anat Embryol* 168:59-61.

de la Cruz MV, Muñoz-Armaz S, Muñoz-Casellanos L (1972) *Development of the chick heart*. The Johns Hopkins University Press, Baltimore and London.

de la Cruz MV, Sun E, Vangvanichyakorn K, Desposito F (1984) Multiple congenital malformations associated with maternal isotretinoin therapy. *Pediatrics* 74:428-430.

de la Cruz MV, Sanchez Gomez C, Cayre R (1991) The developmental components of the ventricles: Their significance in congenital cardiac malformations. *Cardiol Young* 1:123-128.

Dickman ED, Smith SM (1996) Selective regulation of cardiomyocyte gene expression and cardiac morphogenesis by retinoic acid. *Dev Dyn* 206:39-481.

Ferencz Ch, Brenner J, Loffredo C, Kappetein AP, Wilson PD (1995) Transposition of great arteries: etiologic distinctions of outflow tract defects in a case-control study of risk factors. In: Clark EB, Markwald RR, Takao A (eds) *Developmental mechanisms of heart disease*. Futura Publishing Company, Armark, New York, pp 639-653.

Franklin DL, Schlegal W, Rushmer RF (1961) Blood flow measured by Doppler frequency shift of backscattered ultrasound. *Science* 134: 154.

Gittenberger-de Groot AC, Bartelings MM, Poelmann RE (1995) Normal and abnormal morphogenesis of the outflow tract. In: Clark EB, Markwald RR, Takao A (eds) *Developmental mechanisms of heart disease*. Futura Publishing Company, Armark, New York, pp 249-253.

Gudas LJ (1992) Retinoids, retinoid-responsive genes, cell differentiation, and cancer. *Cell Growth & Differentiation* 3:655-662.

Hamburger V, Hamilton HL (1951) A series of normal stages in the development of the chick embryo. *J Morph* 88:49-92.

Hart RC, McCue PA, Ragland WL, Winn KJ, Unger ER (1990) Avian model for 13-cis-retinoic acid embryopathy: demonstration of neural crest related defects. *Teratology* 41:463-472.

Hartley CJ, Cole JS (1974) An ultrasonic pulsed Doppler system for measuring blood flow in small vessels. *J Appl Physiol* 37:626-629.

Hassel JR, Greenberg JH, Johnston MC (1977) Inhibition of cranial neural crest cell development by vitamin A in the cultured chick embryo. *J Embryol Exp Morphol* 39:267-271.

Hogers B, DeRuiter MC, Baasten AMJ, Gittenberger-de Groot AC, Poelmann RE (1995) Intracardiac blood flow patterns related to the yolk sac circulation of the chick embryo. *Circ Res* 76:871-877.

Hu N, Clark EB (1989) Hemodynamics of stage 12 to stage 29 chick embryos. *Circ Res* 65:1665-1670.

Itasaki N, Nakamura A, Sumida H, Yasuda M (1991) Actin bundles on the right side in the caudal part of the heart tube play a role in dextro-looping in the embryonic heart. *Anat Embryol* 183:29-39.

Jellinek R, Kistler A (1981) Effect of retinoic acid upon the chick embryonic morphogenetic systems. I. The embryotoxicity dose range. *Teratology* 23:191-195.

Karnovsky MJ (1965) A formaldehyde-glutaraldehyde fixative of high osmolarity for use in electron microscopy. *J Cell Biol* 27:137A.

Kawashima H, Ohno I, Ueno Y, Nakaya S, Kato E, Taniguchi N (1987) Syndrome of microtia and aortic arch anomalies resembling isotretinoin embryopathy. *J Ped* vol 111(5):738-740.

Kirby ML, Stewart D (1983) Neural crest origin of cardiac ganglion cells in the chick embryo: identification and extirpation. *Dev Biol* 97:433- 443.

Kirby ML (1987) Cardiac morphogenesis-recent research advances. *Ped Res* 21:219-224.

Kirby ML (1988) Nodose placode provides ectomesenchyme to the developing chick heart in the absence of the cardiac neural crest. *Cell Tissue Res* 252:17-22.

Kirby ML, Waldo L (1990) Role of neural crest in congenital heart disease. *Circulation* 82:332-340.

Kirby ML (1993) Cellular and molecular contributions of the cardiac neural crest to cardiovascular development. *Trends Cardiovasc Med* 3:18-23.

Kirby ML, Waldo KL (1995) Neural crest and cardiovascular patterning. *Circ Res* 77:211-215.

Lamers WH, Wessels A, Verbeek FJ, Moorman AFM, Virágh S, Wenink ACG, Gittenberger-de Groot AC, Anderson RH (1992) New findings concerning ventricular septation in the human heart. *Circulation* 86:1194-1205.

Lammer EJ, Chen DT, Hoa RM, Agnish WD, Benke PJ, Curry CJ, Fernhoff PM, Grix AW, Lott IT, Richard JM, Sun SC (1985) Retinoic acid embryopathy. *N Engl J Med* 313:837-841.

Leatherbury L, Connuck DM, Kirby ML (1993) Neural crest ablation versus sham surgical effects in a chick embryo model of defective cardiovascular development. *Pediatr Res* 33:628-631.

Leatherbury L, Waldo K (1995) Visual understanding of cardiac development: the neural crest's contribution. *Cell Mol Biol Res* 41:279-291.

Le Douarin NM (1982) The neural crest. Cambridge University press.

Loeber CP, Hendrix MJC, Pinos de SD, Golberg SJ (1988) Trichlorethylene: A cardiac teratogen in developing chick embryos. *Ped Res* 24:740-743.

Lohnes D, Mark M, Mendelsohn C, Dollé P, Dierich A, Gorry P, Gansmuller A, Chambon P (1994) Function of the retinoic acid receptors (RARs) during development. I. Craniofacial and skeletal abnormalities in RAR double mutants. *Development* 120:2713-2748.

Maden M, Hunt P, Eriksson U, Kuroiwa A, Krumlauf R, Summerbell D (1991) Retinoic acid-binding protein, rhombomeres and the neural crest. *Development* 111:35-44.

Manasek FJ, Icardo J, Nakamura A, Sweeney (1986) Cardiogenesis: Developmental Mechanisms and Embryology. In: HA Fozzard et al. (eds) The heart and cardiovascular system. Raven Press, NY, pp 965-985.

Männer J, Seidl W, Steding G (1993) Correlation between the embryonic head flexures and cardiac development. An experimental study in chick embryos. *Anat Embryol* 188:269-285.

Männer J, Seidl W, Steding G (1995a). The role of extracardiac factors in normal and abnormal development of the chick embryo heart: cranial flexure and the ventral thoracic wall. *Anat Embryol* 191:61-72.

Männer J, Seidl W, Steding G (1995b) Embryological observations on the morphogenesis of double outlet right ventricle with subaortic ventricular septal defect and normal arrangement of the great arteries. *Thorac Cardiovasc Surgeon* 43:307-313.

Marcus M, Wright C, Doty D, Eastham C, Laughlin D, Krumm P, Fastenow C, Brody M (1981) Measurements of coronary velocity and reactive hyperemia in the coronary circulation of humans. *Circ Res* 49:877-891.

Mendelsohn C, Lohnes D, Décimo D, Lufkin T, LeMeur M, Chambon P, Mark M (1994) Function of the retinoic acid receptors (RARs) during development. II. Multiple abnormalities at various stages of organogenesis in RAR double mutants. *Development* 120:2749-2771.

Meuer HJ, Baumann R (1988) Oxygen pressure in intra- and extraembryonic blood vessels of early chick embryo. *Respir Physiol* 71:331-342.

Van Mierop LHS, Gessner IH (1972) Pathogenetic mechanisms in congenital cardiovascular malformations. *Progr Cardiovasc Dis* 15:67-85.

Van Mierop LHS (1979) Morphological development of the heart. In: Berne RM (ed) Handbook of physiology. Section 2: The cardiovascular system. Volume 1: The heart. Williams & Wilkins, Baltimore, pp 1-28.

Morriss-Kay G (1992) Retinoic acid and development. *Pathobiology* 60:264-270.

Nishibitake M, Kirby ML, van Mierop L (1987) Pathogenesis of persistent truncus arteriosus and dextroposed aorta in the chick embryo after neural crest ablation. *Circulation* 75:255-264.

Orts Llorca F, Genis-Galvez JM, Ruano-Gil D (1959) Malformations encéphaliques et microphthalmie gauche après section des vaisseaux vitellins gauches chez l'embryon de poulet. *Acta Anat* 38:1-34.

Pexieder T (1986) Teratogens. In: Pierpont ME, Moller JH, (eds). Genetics of cardiovascular disease. Martinus Nijhoff publishing.

Pexieder T, Pfizenmaier Rousseil M, Prados-Frutos JC (1992) Prenatal pathogenesis of the transposition of great arteries. In: Vogel M, Bühlmeier (eds) Transposition of the great arteries 25 years after Rashkind Balloon Septostomy. Steinkopff Verlag, Darmstadt, pp 11-27.

Pexieder T, Blanc O, Pelouch V, Ostádalová I, Milerová M, Ostádal B (1995) Late fetal development of retinoic acid induced transposition of great arteries-morphology, physiology and biochemistry. In: Clark EB, Markwald RR, Takao A (eds) Developmental Mechanisms of heart disease. Futura Publishing Company, Armark, NY, pp 297-307.

Rosa FW, Wil AL, Kelsey FO (1986) Teratogen update. Vitamin A congeners. *Teratology* 33:355-364.

Ross AC (1993) Overview of retinoid metabolism. *J Nutr* 123:346-350.

Chapter 2

Ruberte E, Dollé P, Chambon P, Morriss-Kay G (1991) Retinoic acid receptors and cellular retinoid binding proteins. II. Their differential pattern of transcription during early morphogenesis in mouse embryos. *Development* 111:45-60.

Rychter Z (1962) Experimental morphology of the aortic arches and the heart loop in the chick embryo. *Adv Morphogen* 2:333-371.

Rychter Z, Lemez L (1965) Changes in localization in aortic arches of laminar blood streams of main venous trunks to heart after exclusion of vitelline vessels on second day of incubation. *Fed Proc Transl Suppl* 24:815-820.

Sissman NJ (1970) Developmental landmarks in cardiac morphogenesis: comparative chronology. *Am J Cardiology* 25:141-148.

Shiraishi I, Takamatsu T, Minamikawa T, Fujita S (1992) 3-D observation of actin filaments during cardiac myofibrinogenesis in chick embryo using a confocal laser scanning microscope. *Anat Embryol* 185:401-408.

Smith-Thomas L, Lott I, Bronner-Fraser M (1987) Effects of isotretinoin on the behavior of neural crest cells in-vitro. *Dev Biol* 123:276-280.

Steding G, Seidl W (1980) Contribution to the development of the heart. I. Normal development. *Thorac Cardiovasc Surgeon* 28:386-409.

Taylor IM (1981) Some early effects of retinoic acid on the young hamster heart. In: Mechanisms of cardiac morphogenesis and teratogenesis. T. Pexieder, ed. Raven press, New York, Vol 5, pp. 151-161.

Thorogood P, Smith L, Nicol A, McGinty R, Garrod D (1982) Effects of vitamin A on the behavior of migratory neural crest cells in-vitro. *J Cell Sci* 57:331-350.

Vuillemin M, Pexieder T, Winking H (1991) Pathogenesis of various forms of double outlet right ventricle in mouse fetal trisomy 13. *Int J Cardiol* 281-304.

Wiens DJ, Mann TK, Feddersen DE, Rathmell WK, Franck BH (1992) Early heart development in the chick embryo: Effects of isotretinoin on cell proliferation, α -actin synthesis, and development of contractions. *Differentiation* 51:105-112.

Yasuda Y, Okamoto M, Konishi H, Matsuo T, Kihara T, Tanimura T (1986) Developmental anomalies induced by all-trans retinoic acid in fetal mice: 1. Macroscopic findings. *Teratology* 34:37-49.

Yoshida H, Manasek F, Arcilla RA (1983) Intracardiac flow patterns in early embryonic life. A reexamination. *Circ Res* 53:363-371.

CHAPTER 3

HEMODYNAMIC EVALUATION OF NORMAL CHICK EMBRYOS

3.1 Introductory remarks

In order to study hemodynamics in abnormally developing hearts of embryos treated with either all-trans retinoic acid or embryos that have been manipulated by venous clip, insight into normally functioning hearts at consecutive stages is necessary. The period of organogenesis is characterized by rapid embryo growth. Embryo weight doubles in hours while the heart grows less rapidly. At stage 18, a chick's heart accounts for 3% of the embryo mass but by hatching comprises less than 1% (Hu and Clark 1989). It is described that when expressed as a log:log relationship, heart to embryo weight is linear, similar to the relationship of heart and body weight during postnatal development and among mammals of varying body size (Rakusan 1984). The dynamic decrease in relative heart size suggests that the cardiovascular system becomes more effective with morphogenesis. Growth in response to functional demands is a fundamental characteristic of the heart. Increasing myocardial contractility is related to embryonic myocardial growth that occurs by cell proliferation or hyperplasia (Knaapen et al. 1996), and is responsive in part to environmental factors (Clark 1989, 1991). In late prenatal and postnatal development, heart growth includes both hypertrophy and hyperplasia (Fishman et al. 1978), while in the mature myocardium heart mass increases by hypertrophy alone (Zak 1984). The underlying mechanism of the events of growth from hyperplasia alone to a combination of hyperplasia and hypertrophy could be related to molecular regulation of the cell cycle (Sperelakis and Pappano 1983). Moreover, these events correlate with the appearance of functional parasympathetic and sympathetic autonomic innervation (Sperelakis and Pappano 1983).

Regulation of cardiac growth and function involves the orchestration of hemodynamic and cellular events. Recent studies imply that embryonic ventricular myocardium changes in response to cardiac hemodynamics probably as a result of myocardial and endocardial influences (Chien et al. 1993; Schneider and Parker 1993).

This chapter discusses the hemodynamic parameters of stage 20 to stage 35 embryos with normally developing hearts. For physiologic measurements a 20 MHz directional pulsed Doppler velocity meter was used. Dorsal aortic flow velocities were obtained in stage 20 to stage 35 chick embryos.

3.2 Hemodynamic parameters of stage 20 to stage 35 chick embryo

*Monique L.A. Broekhuizen,¹ Frans Mast,² Piet C. Struijk,¹ Wim van der Bie,³ Paul G.H. Mulder,⁴
Adriana C. Gittenberger-de Gooit,⁵ Juriy W. Wladimiroff,¹*

From the Department of Obstetrics and Gynecology¹, Central Research Laboratories³ and Department of Epidemiology and Biostatistics⁴, Academic Hospital Rotterdam Dijkzigt, Erasmus University, Rotterdam, Department of Thoracic Surgery², Academic Hospital Leiden, and Department of Anatomy and Embryology⁵, University of Leiden, The Netherlands

Summary

Hemodynamic parameters of the chick embryo from stage 20 (day 3 of a 21 day incubation) up to stage 35 (day 8) are described. Normal values of dorsal aortic flow velocity wave forms were measured with a 20 MHz directional pulsed Doppler velocity meter that was validated to be accurate above 5 mm/s. An analysis of variance was carried out for each of the flow velocity parameters. The correlation coefficient which represents the reproducibility was satisfactory ($r > 0.90$). There was a 17-fold rise in mean dorsal aortic blood flow (mm³/s). Heart rate doubled from 123±12 to 239±8 bpm, and stroke volume increased from 0.14±0.08 to 1.28±0.55 mm³. A stage-related rise was seen in peak systolic and mean velocities and peak acceleration. These data may serve as a basis for flow velocity wave form investigation and interpretation in developmental stages of cardiac malformations.

Introduction

High-resolution real-time ultrasound and Doppler techniques allow detailed analysis of human fetal cardiac anatomy and function during the second half of pregnancy. A reliable diagnosis of a wide range of cardiac anomalies can now be made (Kleinman et al. 1980; Allen et al. 1981; Stewart 1989), and as a result, a spectrum of cardiac pathology has emerged which appears to be different from that seen in postnatal life (Sharland et al. 1990). Moreover, Doppler studies have demonstrated abnormal flow velocity patterns in the outflow tract in the presence of atrioventricular and semilunar valve pathology (Stewart and Wladimiroff 1993).

In the developing heart, morphogenesis and hemodynamic function are closely linked. Micro-Doppler and pressure studies in chick embryos have provided valuable information on this relationship in normal heart development (Hu and Clark 1982, 1989). To study the interaction between hemodynamics and morphology in abnormal heart development, an animal model with specific and reproducible cardiac malformations is needed.

We recently developed a standardized method for inducing a spectrum of double outlet right ventricle in the stage 35 chick embryo (Broekhuizen et al. 1992). Moreover, for future studies on hemodynamics associated with abnormal heart development, normal data on flow velocity parameters from stage 20 up to stage 35 must be collected.

In this article, we report on the validity, reproducibility and normal values of dorsal aortic flow velocity wave forms in stage 20 to stage 35 chick embryos.

Materials and Methods

Fertilized white Leghorn chick eggs were incubated (blunt end up) at 38°C and staged according to Hamburger and Hamilton (1951). The material was subdivided into stages 20, 24, 27, 29, 31 and 35 (day 3 to day 8 of incubation). Stages 20 to 29 were chosen in view of earlier studies performed by Hu and Clark (1982, 1989).

For physiologic measurements, a 20 MHz directional pulsed Doppler velocity meter (model 545C-4 by Bioengineering, University of Iowa) was used (Hartley and Cole 1974; Marcus et al. 1981). The accuracy of this equipment was tested against a calibrated velocity. Anticoagulated pig blood was pumped at constant pressures to obtain constant flows. The blood was led through a 3-mm diameter channel, which was drilled into a perspex block. At an angle of 45° to the first channel an additional channel was made in which the 750- μ m Doppler probe was placed. At the outflow side of the first channel, a stretch of polyvinylchloride tubing (internal diameter 3 mm, length 100 cm) was connected and marked. Only after a constant flow was acquired a stopwatch was started at the first marking point $x = 0$ cm, and stopped when blood reached $x = 100$ cm. The calibrated blood velocity was calculated from the time elapsed in crossing this trajectory of 100 cm. The time-average of the Doppler velocity V (mm/s) was determined by recording a voltage E supplied by the Doppler velocity meter, using the equation $V = 78.25 * E / \cos 45^\circ$ (110 mm/s corresponds with 1 V). The relationship between Doppler velocity and calibrated velocity was determined from regression analysis.

Each embryo was exposed by creating a window in the shell and removing the overlying membranes. The embryo lay with its right side up and the dorsal aorta horizontal. Using a micromanipulator and projector jig, it was possible to position the Doppler probe consisting of a 750 μ m piezoelectric crystal at a 45° angle to the dorsal aorta at the level of the sinus venosus (Hu and Clark 1982, 1989). A 45° angle was chosen for consistency in the velocity calculations.

The internal diameter of the dorsal aorta was measured at the same level with a filar micrometer eyepiece that was calibrated against a 10- μ m scribed glass standard. The area was calculated from the equation $area = \pi d^2/4$ where d is the aortic diameter (mm).

Hemodynamic parameters

The analog wave forms were sampled at 300 Hz by a Lab Master data acquisition analog-digital board (Axon Instruments, Inc., Burlingame, CA) linked to a Commodore PC40 computer. The converter offered 12 bits at an input range of -10 to 10 V. Data were stored in a 5/4-inch 44 - megabyte Bernoulli disk cartridge (Iomega Corp., Roy, UT).

A total of ten embryos were studied in each stage. Only live embryos with the right side up and without any sign of bleeding were included in the final analysis. Within each embryo a 2-min wave form recording was made. Three technically high quality wave form recordings of 5 s each were selected for analysis. Each 5-s recording contained 10 to 20 wave forms depending on the stage. The mean value of a particular flow velocity parameter was first calculated for each 5-s recording and then averaged for that embryo. Finally, the mean value \pm standard deviation (SD) was calculated for all 10 embryos in each stage.

Mean dorsal aortic blood flow (Q) was calculated from $Q \text{ (mm}^3 \text{ /s)} = V * \text{area}$, where V is the mean dorsal aortic blood velocity. By measuring the cycle length between pulse waves and converting this to beats per minute (bpm), the heart rate was calculated. Stroke volume (mm^3) was determined from the quotient of mean dorsal aortic blood flow and heart rate. From the dorsal aortic dV/dt the peak acceleration (mm/s^2) was derived.

Morphologic examination

After the wave form recordings were collected all embryos were removed from the egg. The embryos were processed for histologic sectioning in a routine way by fixing in Bouin and embedding in paraffin. Thereafter, the embryos, including the hearts, were serially sectioned. The sections were 5 μm thick and stained with Mayer's hematoxylin/eosin.

Statistical analysis

The reproducibility (r) was defined according to the equation: $r = \sigma^2_B / [\sigma^2_B + (\sigma^2_W / N)]$, in which σ^2_B represents the between-embryo variance and σ^2_W the within-embryo variance of wave form parameters. These variances were estimated from an analysis of variance. The number of repeated 5-s recordings within one embryo is denoted by N, which in our study equals 3. The parameter r is the correlation coefficient between two "measurements" within one embryo, where a "measurement" is defined as the average of N repeated 5-s recordings. This clearly shows that $0 < r < 1$ and that r can be increased towards 1 by increasing the number N. The between-embryo variance σ^2_B , also includes the effect of stage.

Results

Figure 1 depicts the relationship between Doppler velocity and calibrated velocity ($y = 1.18x - 3.24$, $r^2 = 0.99$, standard error of the estimate = 1.38 mm/s).

Table 1 presents the results of the analysis of variance for each of the flow velocity parameters. The correlation coefficient that represents the reproducibility, using the average of three 5-s recordings as measurement outcome, was satisfactory.

Figure 2 gives an example of dorsal aortic flow velocity wave forms for each stage. It is clear from table 2 that an increase was observed for each flow velocity parameter and vessel area with advancing stage.

After histologic analysis all hearts were diagnosed as normal.

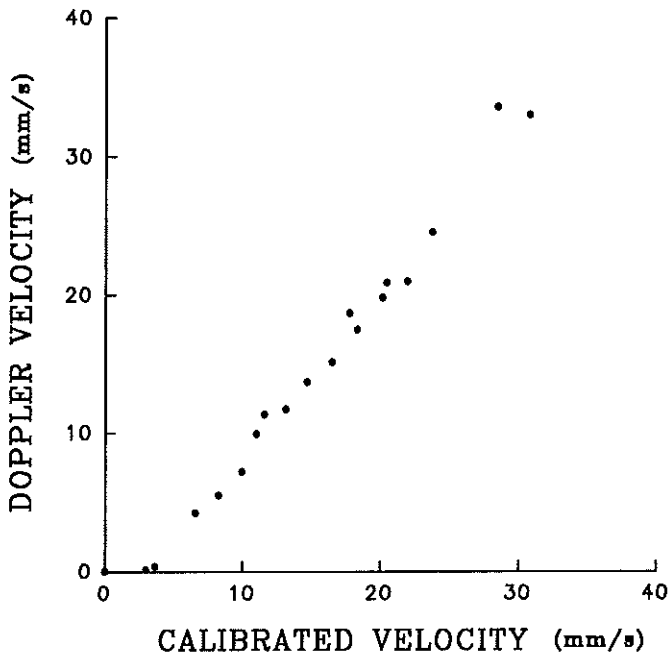


Figure 1. Doppler velocity and calibrated velocity. Relationship between in-vitro Doppler velocity and calibrated velocity from 0 to 35 mm/sec.

Table 1. Results of analysis of variance *

	σ^2_w	σ^2_B	r
Mean DAo velocity (mm/s)	2.63	32.38	0.97
Mean DAo blood flow (mm ³ /s)	0.14	2.86	0.98
Heart rate (bpm)	35.74	1754.13	0.99
Stroke Volume (mm ³)	0.02	0.44	0.98
Peak acceleration (mm/s ²)	35445	501193	0.98

* σ^2_w , variance within groups; σ^2_B , variance between groups (including stage effect);
 r = reproducibility (correlation coefficient between two "measurements", each calculated as the average of three 5-s recordings). DAo, dorsal aortic.

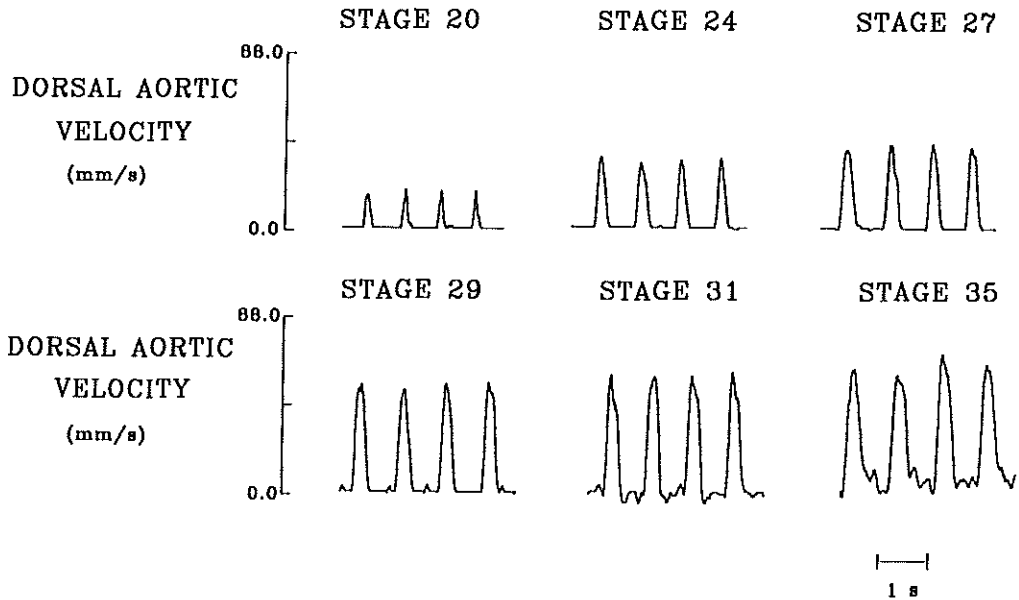


Figure 2. Analog wave forms.

Analog phasic dorsal aortic wave forms of stage 20, 24, 27, 29, 31 and 35 chick embryo.

Table 2. Dorsal aortic waveform parameters at stages 20 to 35

Hamburger-Hamilton Incubation time	Stage					
	20 (3 d)	24 (4 d)	27 (5 d)	29 (6 d)	31 (7 d)	35 (8 d)
Mean dorsal aortic velocity (mm/s)	3.9±0.8	6.1±0.9	11.4±0.7	11.9±1.2	14.1±3.5	19.9±4.4
Aortic area (mm ²)	0.07±0.02	0.14±0.02	0.15±0.01	0.17±0.01	0.21±0.02	0.25±0.02
Mean dorsal aortic blood flow (mm ³ /s)	0.3±0.1	0.9±0.1	1.8±0.2	2.0±0.2	3.0±0.8	5.1±1.3
Heart rate (bpm)	123±12	142±10	177±11	181±6	221±14	239±8
Stroke volume (mm ³)	0.14±0.08	0.35±0.08	0.59±0.11	0.66±0.15	0.81±0.39	1.28±0.55
Peak acceleration (mm/s ²)	687±90	867±116	1464±170	1283±174	2288±460	2506±159
Peak systolic velocity (mm/s)	20.1±1.0	26.2±1.6	45.5±2.9	49.7±5.1	70.6±14.0	82.1±7.7

Results are expressed as mean ± SD; n = 10 for all stages.

Discussion

The validation study of our 20 MHz directional pulsed Doppler velocity meter showed that there is a close relationship between Doppler velocity and calibrated velocity. The regression line was found to be $y = 1.18x - 3.24$, $r^2 = 0.99$, standard error of the estimate = 1.38 mm/s. As can be seen in figure 1, velocities below 5 mm/s will be underestimated due to a non-linearity around zero, a finding that has already been discussed in the literature (Mills 1972).

Flow velocity wave forms were collected up to stage 35 (day 8 of incubation). In previous studies, embryonic wave forms have been obtained up to stage 29 only (Hu and Clark 1982, 1989). The present results show a high reproducibility for all flow velocity parameters.

A marked increase in mean dorsal aortic velocity and vessel area was observed, resulting in a 17-fold rise in mean dorsal aortic blood flow. Heart rate increased 2-fold and stroke volume 9-fold. These data resemble those reported by Hu and Clark (1989) and reflect rapid embryonic growth. Because the embryonic weight was not determined, the exact relationship between dorsal aortic blood flow and embryonic growth could not be established.

The observed increase in heart rate cannot be explained by parasympathetic or sympathetic neuron activity, because neither is functional until stage 42 (Pappano 1977; Higgins and Pappano 1981). However, circulating adrenergic and cholinergic agents, as well as such other peptides as atrial natriuretic factor may play a role in these heart rate changes (Hu and Clark 1989). The embryonic heart rates observed in the present study are somewhat lower than those reported by Hu and Clark (1989). One explanation may be a slight difference in environmental temperature at which the hemodynamic recordings were carried out; a reduction in the environmental temperature is associated with a decrease in heart rate (Nakazawa et al. 1985). Dunnigan et al. (1987) reported a heart rate of 210 bpm just prior to hatching. We found a heart rate of 239 bpm at stage 35, which suggests considerable plateauing of heart rate during remaining embryonic development.

The stage-related rise in peak systolic and mean velocities could be accounted for by increased volume flow, raised cardiac contractility, and a reduction in afterload. The latter could not be properly addressed since no pressure measurements were available. Our study shows that the stage-related rise in peak systolic and mean velocities is not coupled with major changes in the flow velocity wave form. The observed stage-related rise in peak acceleration suggests an increase in cardiac contraction force with advancing embryonic development.

Normal cardiovascular development, as expressed by the relationship between form and function, is important for an understanding of congenital heart disease. The hemodynamic and morphologic data presented in this study may serve as a basis for flow velocity wave form investigation and interpretation in developmental stages of cardiac malformations.

3.3 References

- Allen LD, Tynan M, Campbell S, Anderson RH (1981) Identification of congenital cardiac malformations by echocardiography in midtrimester fetus. *Br Heart J* 46:358-362.
- Broekhuizen MLA, Wladimiroff JW, Tibboel D, Poelmann RE, Wenink ACG, Gittenberger-de Groot AC (1992) Induction of cardiac anomalies with all-trans retinoic acid in the chick embryo. *Cardiol Young* 2:311-317.
- Chien KR, Zhu H, Knowlton KU, Miller-Hance W, van-Bilsen M, O'Brien TX, Evans SM (1993) Transcriptional regulation during cardiac growth and development. *Annu Rev Physiol* 55:77-95.
- Clark EB, Hu N (1982) Developmental hemodynamic changes in the chick embryo from stage 18 to 27. *Circ Res* 51:810-815.
- Clark EB, Hu N, Frommelt P, Vandekieft JL, Tomanek RJ (1989) Effect of increased ventricular pressure on heart growth in the chick embryo. *Am J Physiol* 257:H1-7.
- Clark EB, Hu N, Turner DR, Litter JE, Hansen J (1991) Effect of chronic verapamil treatment on ventricular function and growth in the chick embryo. *Am J Physiol* 261:H166-171.
- Dunnigan A, Hu N, Benson W JR, Clark EB (1987) Effect of heart rate increase on dorsal aortic flow in the stage 24 chick embryo. *Pediatr Res* 22:442-444.
- Fishman NH, Hof RB, Rudolph AM, Heyman MA (1978) Models of congenital heart disease in fetal lambs. *Circulation* 58:354-364.
- Hamburger V, Hamilton HL (1951) A series of normal stages in the development of the chick embryo. *J Morph* 88:49-92.
- Hartley CJ, Cole JS (1974) An ultrasonic pulsed Doppler system for measuring blood flow in small vessels. *J Appl Physiol* 37:626-629.
- Higgins D, Pappano A (1981) Development of transmitter secretory mechanisms in adrenergic neurons in the embryonic chick heart ventricle. *Dev Biol* 87:148-162.

Hu N and Clark EB (1989) Hemodynamics of stage 12 to stage 29 chick embryos. *Circ Res* 65:1665-1670.

Kleinman CS, Hobbins JC, Jaffe CC, Lynch DC and Talner NS (1980) Echocardiographic studies of the human fetus: prenatal diagnosis of congenital heart disease and cardiac dysrhythmias. *Pediatrics* 65:1059-1064.

Knaapen MWM, Vrolijk BCM, Wenink ACG (1996) Nuclear and cellular size of myocytes in the different segments of the developing rat heart. *Anat Rec* 244:118-125.

Marcus M, Wright C, Doty D, Eastham C, Laughlin D, Krumm P, Fastenow C, Brody M (1981) Measurements of coronary velocity and reactive hyperemia in the coronary circulation of humans. *Circ Res* 49:877-891.

Mills CH (1972) Measurement of pulsatile flow and flow velocity. In: Bergel DH (ed) *Cardiovascular Fluid Dynamics*. Academic Press, New York, pp 51-90.

Nakazawa M, Clark EB, Hu N, Wispe J (1985) Effect of environmental hypothermia on vitelline artery blood pressure and vascular resistance in the stage 18, 21, 24 chick embryo. *Pediatr Res* 19:651-654.

Pappano AJ (1977) Ontogenic development of autonomic neuroeffector transmission and transmitter reactivity in embryonic and fetal hearts. *Pharmacol Rev* 29:3-33.

Rakusan K (1984) Cardiac growth, maturation and aging. In: Zak R (ed) *Growth of the heart in health and disease*. Raven Press, New York, pp 131-164.

Schneider MD, Parker TG (1993) Molecular mechanisms of cardiac growth and hypertrophy: Myocardial growth factors and proto-oncogenes in development and disease. In: Roberts R (ed) *Molecular basis of cardiology*. Blackwell Scientific Publications, Bosten, pp 13-134.

Sharland GK, Lockhart SM, Chita SK, Allen LD (1990) Factors influencing the outcome of congenital heart disease detected prenatally. *Archives of Disease in Childhood* 65:284-287.

Sperelakis N, Pappano AJ (1983) Physiology and pharmacology of developing heart cells. *Pharm Ther* 22:1-39.

Stewart PA (1989) Fetal echocardiography: A review of six years experience. *Fetal Ther* 2:222-231.

Stewart PA, Wladimiroff JW (1993) Fetal echocardiography and colour Doppler flow mapping; The Rotterdam experience. *Ultrasound in Obstet Gynaecol*, 3:168-175.

Zak R (1984) Overview of growth process. In: Zak R (ed) Growth of the heart in health and disease. Raven Press, New York, pp 1-24.

CHAPTER 4

HEMODYNAMIC EVALUATION OF THE PREINNERVATED CHICK EMBRYONIC HEART THE RETINOIC ACID MODEL

4.1 Introductory remarks

Embryonic cardiovascular morphogenesis and function are related. Previously, it was established that the heart is sensitive to retinoic acid acting as cardiac teratogen, leading eventually to a spectrum of double outlet right ventricle at stage 34 (day 8 of incubation) (Broekhuizen et al 1992; Bouman et al. 1995).

During the early stages of cardiac development, the heart has no functional innervation, has primitive atrioventricular and outflow tract cushions, and has no functioning conduction system or coronary arteries. Therefore, the embryonic cardiovascular system responds to increasing hemodynamic demand using load sensitive, integrated tissue and cellular mechanisms.

In order to study the interaction between form and function in abnormal development of the heart, the hemodynamic profile was determined of stage 24 chick embryos before innervation of the heart, after retinoic acid treatment. Dorsal aortic flow velocity and pressure parameters will be discussed (4.2).

In addition to the assessment of hemodynamic parameters, a pilot study was conducted to pursue in this stage the feasibility of measuring cardiac function directly, through the pressure-volume loop recording. In collaboration with Dr. B.B. Keller (Department of Pediatric Cardiology, Rochester, New York), pressure-volume loops were assessed. The acquisition and analysis of pressure-volume loops will be discussed (4.3).

4.2 Hemodynamic parameters of the stage 24 chick embryo

Retinoic acid treatment

Fertilized white Leghorn chick eggs were incubated (blunt end up) at 38°C and staged according to Hamburger and Hamilton (1951). The material was subdivided into groups of embryos treated with a solution of all-trans retinoic acid and the solvent dimethylsulphoxide, embryos treated with only the solvent (sham-operated embryos) and control embryos.

At stage 15 (d 2½ of a 21-d incubation) each embryo, with exception of the controls, was exposed by creating a window in the shell followed by removal of the overlying membranes. Either a solution containing 1.0 µg all-trans retinoic acid or only the solvent 2% dimethylsulphoxide was deposited on the vitelline membrane of the embryo using a Hamilton syringe (Broekhuizen et al. 1992). After administration of the solution, the window was sealed with tape and the egg reincubated.

Assessment of hemodynamic parameters

Physiologic measurements were performed at stage 24 (day 4 of incubation) because there is no autonomic innervation of the heart in this stage. An egg was removed from the incubator and positioned on the stage of a dissecting microscope. Each embryo was exposed either by removing the tape of the all-trans retinoic acid treated and sham-operated embryos or making a window in the shell and removing the overlying membranes of the controls. Only live embryos with the right side up and without any sign of bleeding were included in the final analysis.

We simultaneously measured blood pressures, and flow velocities in the dorsal aorta in 20 embryos treated with 1.0 µg all-trans retinoic acid and in 7 sham-operated and 8 control embryos. The temperature of the embryo during the measurement was regulated by a thermoelement and was maintained at 37°C.

Blood pressure was measured in the dorsal aorta with a servo-null system (model 900A, World Precision Instruments, Inc., Sarasota, FL) and a 10 µm glass micropipette. This pressure system was validated to be accurate from -5 mm Hg to 40 mm Hg ($y=1.14x+0.25$, $r^2=0.99$, standard error of the estimate = 0.12 mm Hg) (Broekhuizen et al. 1995). Zero trans-tip pressure was obtained by immersing the tip of the micropipette in the extraembryonic fluid at the level of the measured site (Hu and Clark 1989).

Mean dorsal aortic blood flow velocities were measured with a 20 MHz directional pulsed Doppler velocity meter (model 545C-4 by Bioengineering, University of Iowa).

In a previous study (Broekhuizen et al. 1993), this equipment had been validated to be accurate above 5 mm/s. The Doppler probe consisting of a 750- μ m piezoelectric crystal was positioned at a 45° angle to the dorsal aorta at the level of the sinus venosus as described in earlier reports (Hu and Clark 1989; Broekhuizen et al. 1993, 1995).

The internal diameter of the dorsal aorta was measured at the same level with a filar micrometer eyepiece which was calibrated against a 10- μ m engraved glass standard. The vessel area was calculated from the equation $area = \pi d^2/4$ where d is the aortic diameter (mm).

Hemodynamic Parameters

The analog wave forms were sampled at 300 Hz by a Lab Master data acquisition analog-digital board (Axon Instruments Inc., Burlingame, CA) linked to a Commodore PC40 computer. The converter offered 12 bits at an input range of -10 to 10 Volt. Data were stored in a 5¼-inch 90 megabyte Bernoulli disk cartridge (Iomega Corp., Roy, UT).

Within each embryo a 2-min wave form recording was made. A technically high-quality wave form recording of 10 s was selected for analysis. Each 10 s recording contained 20 to 40 wave forms.

Peak-systolic, end-diastolic and mean blood pressures were determined. Dorsal aortic dP/dt (mm Hg/s) was derived from the analog pressure signal by digital differentiation. Mean dorsal aortic blood flow (mm³/s) was calculated as the product of the mean velocity and the area of the dorsal aorta (Broekhuizen et al. 1993, 1995). By measuring the cycle length between pulse waves and converting this into beats per minute (bpm), the heart rate was calculated. The peak acceleration dV/dt (mm/s²) was derived from the dorsal aortic velocity V(t) by means of digital differentiation. Stroke volume (mm³) was determined from the quotient of mean dorsal aortic blood flow and heart rate multiplied by 60. Cardiac work (mm³*mm Hg) is the product of stroke volume and mean arterial pressure. Vascular resistance [mm Hg/(mm³/s)] is the quotient of mean arterial pressure and mean dorsal aortic blood flow.

Morphologic Examination

After the wave form recordings were collected all 35 embryos were removed from the egg and evaluated macroscopically. Subsequently, the hearts were routinely processed for histologic sectioning by fixing in Bouin and embedding in paraffin. The embryos including the hearts were serially sectioned. The sections were 5 μ m thick and stained with Mayer's hematoxylin/eosin (Broekhuizen et al. 1992).

Scanning electron microscopy

Selected specimen (n=5) were processed for scanning electron microscopy. Hearts of stage 15 and 24 were perfusion fixed in half strength Karnovsky's fixative (1965) for at least 1 hr. They were then rinsed in 0.1 M sodium-cacodylate buffer (pH 7.2) and postfixed for 2 hrs at 4°C in 1% OsO₄ in the same buffer, followed by dehydration in graded ethanol. The preparations were critical point dried over CO₂ by conventional methods, sputter-coated with gold for 3 min (Balzers MED 010) and studied in the scanning electron microscope (Philips SEM 525M) and photographed.

Statistical analysis

Finally, the hemodynamic data were correlated with the morphology. The distribution of hemodynamic parameters was non-Gaussian. Therefore, a non-parametric statistical analysis was carried out. The data are presented as characteristics of the frequency distribution of the hemodynamic parameters by medians and ranges (minimum, maximum). Statistical comparison was done by the Kruskal-Wallis test, whereas the Mann-Whitney test was used to determine significant differences between control and experimental values. An exact trend test in a 3 X 2 cross-table was used for the dorsal aortic area because this parameter only had three ordered levels. The statistical significance level was defined as a *p* value of less than 1% (*p*<0.01) because several parameters were tested.

Results

Morphology

The stage 15 normal embryonic heart shows a ventricular loop that is positioned rightward and ventral to the atrioventricular canal (Figure 1a). Control and sham-operated stage 24 embryos showed normal cardiac morphology (Figure 1b). The heart in this stage is further looped than in stage 15. The majority of stage 24 retinoic acid treated embryos displayed malformed hearts. The outflow tract was dislocated to the right (Figure 1c). Furthermore, these hearts were not properly looped. The macroscopic diagnosis was confirmed at microscopy.

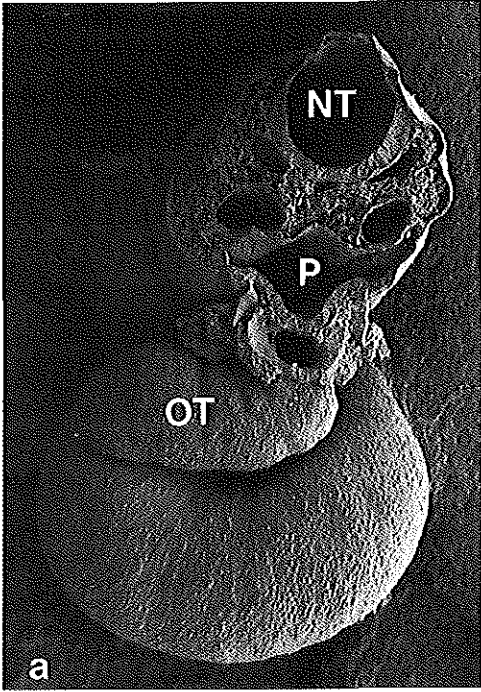
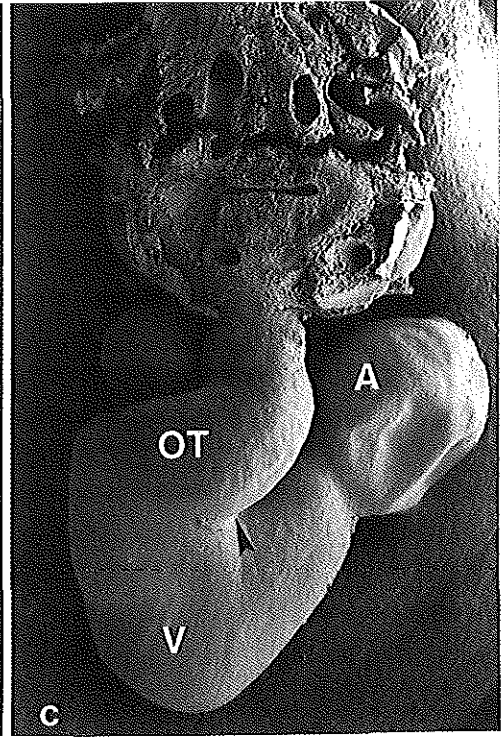
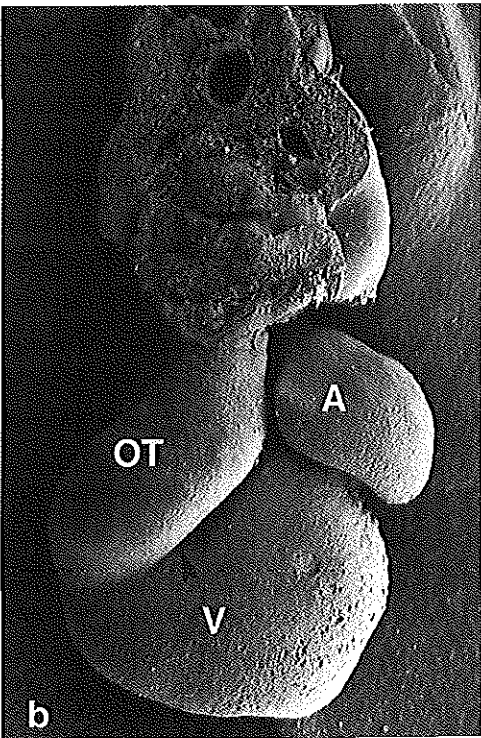


Figure 1. Scanning electron micrographs of chick embryo hearts.

a. Anterior view of a normal stage 15 embryo. (NT: neural tube; P: pharynx; OT: outflow tract)

b. Anterior view of a normal stage 24 embryo. The inner curvature is indicated by an arrow. (A: atrium; V: ventricle; OT: outflow tract)

c. Anterior view of a abnormal looped stage 24 embryo after retinoic acid treatment. The inner curvature (arrow) is positioned more ventrally compared to the normal situation (b). (A: atrium; V: ventricle; OT: outflow tract)



Hemodynamics

The characteristics of the frequency distribution of selected dorsal aortic wave form parameters of control embryos, sham-operated embryos, and embryos treated with all-trans retinoic acid can be seen in Figure 2a-d. There was no significant discrepancy in hemodynamics of control and sham-operated embryos. Heart rate was the only parameter that was significantly reduced in retinoic acid treated embryos compared to control and sham-operated embryos (Figure 2a). There was no significant difference in peak systolic and mean velocities, peak systolic and mean blood flows, and peak acceleration and stroke volume ($p > 0.01$).

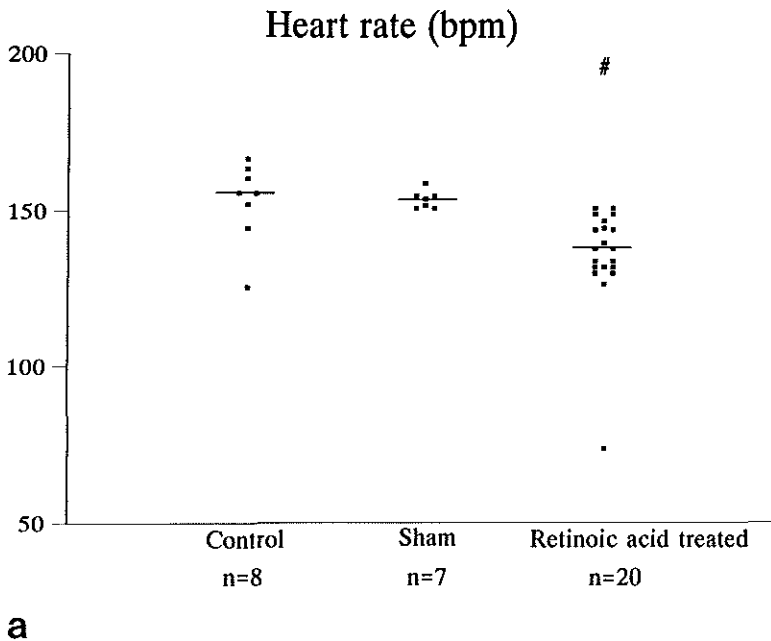


Figure 2. a. The characteristics of the frequency distribution of heart rate. #, Significantly different from control and sham-operated embryos ($p < 0.01$).

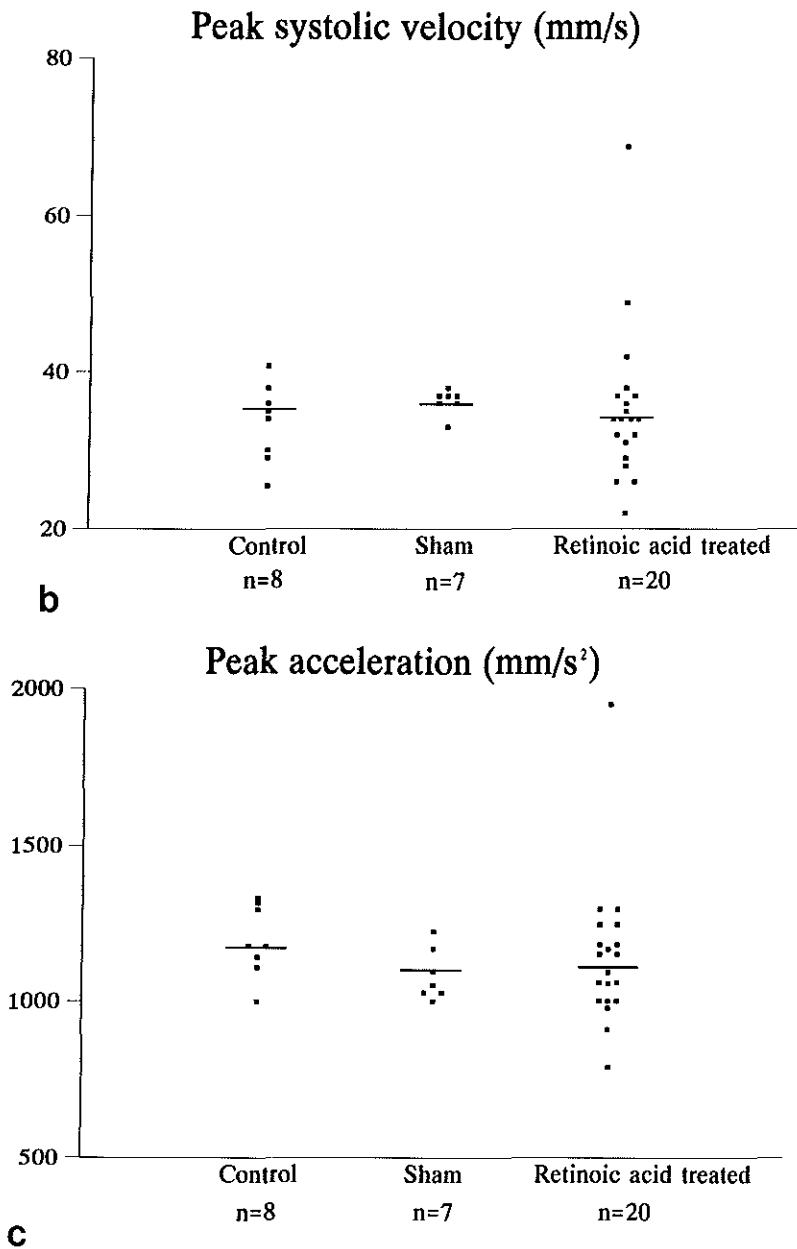


Figure 2. b-c. The characteristics of the frequency distribution of (b) peak systolic velocity, (c) peak acceleration.

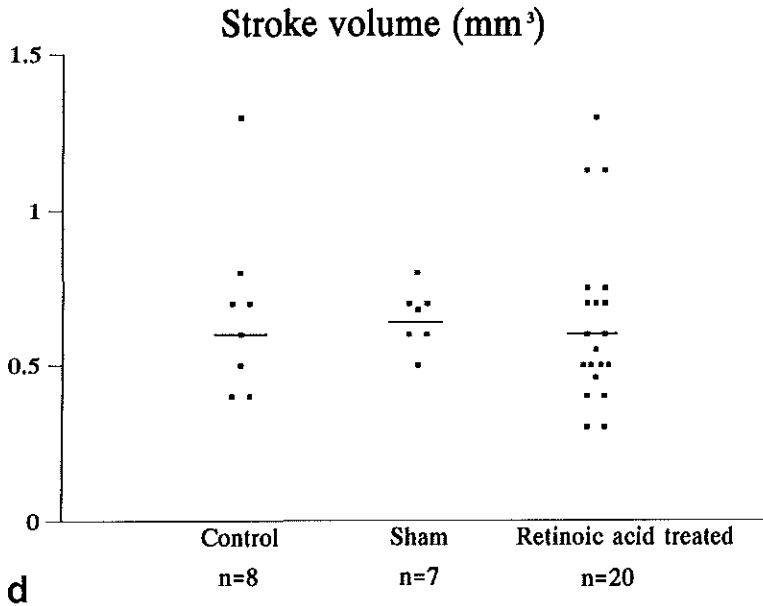


Figure 2. d. The characteristics of the frequency distribution of stroke volume.

A cross-table of the dorsal aortic area is presented in Table 1. The exact trend test in a 3 x 2 cross-table determined that this parameter was reduced in retinoic acid treated embryos.

Table 1. A cross-table of dorsal aortic area by control and experimental stage 24 chick embryos

	Control n=8	Sham n=7	Retinoic acid treated n=21 ($p<0.01$)
Dorsal aortic area (mm ²)			
0.09	0	0	8
0.13	2	5	9
0.15	6	2	3

The peak systolic and end-diastolic blood pressures measured in the dorsal aorta showed no significant difference between the three groups (Table 2). This was also the case for vascular resistance and cardiac work (Table 3).

Table 2. Characteristics of the frequency distribution of the dorsal aortic pressure parameters of control and experimental stage 24 chick embryos, $p > 0.01$

	Control (n=8)	Sham (n=7)	<u>Retinoic acid treated</u> (n=21)
Peak systolic pressure (mm Hg)			
minimum	0.9	1.0	1.0
median	1.4	1.6	1.7
maximum	1.9	1.8	4.3
End-diastolic pressure (mm Hg)			
minimum	0.2	0.09	0.1
median	0.5	0.5	0.5
maximum	0.8	0.8	3.0
Mean pressure (mm Hg)			
minimum	0.5	0.4	0.5
median	0.9	0.9	1.1
maximum	1.1	1.4	3.5
dP/dt max (mm Hg/s)			
minimum	11.2	13.3	5.7
median	17.7	24.0	30.4
maximum	40.0	30.3	6.3

Table 3. *Vascular resistance and cardiac work of control and experimental stage 24 chick embryos, $p > 0.01$*

	Control (n=8)	Sham (n=7)	<u>Retinoic acid treated</u> (n=21)
Vascular resistance [mm Hg/(mm ³ /s)]			
minimum	0.3	0.2	0.2
median	0.5	0.6	1.0
maximum	1.2	0.8	2.1
Cardiac work (mm ³ xmm Hg)			
minimum	0.3	0.2	0.2
median	0.6	0.5	0.7
maximum	1.1	1.1	2.4

Discussion

In this study dorsal aortic flow velocity and pressure wave forms were recorded in stage 24 embryos treated with retinoic acid, sham-operated embryos and control embryos. Hemodynamics of control and sham-operated embryos showed no significant differences. The hearts of these embryos revealed no abnormal cardiac morphology.

Hemodynamics of retinoic acid treated embryos and control and sham-operated embryos were compared with each other. In spite of abnormal morphology of the majority of retinoic acid treated embryos, hemodynamic evaluation displayed solely a significant decrease in heart rate without compensatory increase of stroke volume. In addition, the dorsal aortic area, that was determined from the vessel diameter, was reduced in these embryos. Pressure readings were not significantly different between control and experimental embryos. Furthermore, vascular resistance and cardiac work were similar for the three embryo groups.

The observed decrease in heart rate without compensatory increase of stroke volume, in retinoic acid treated embryos, suggests both pacemaker and contractile dysfunction. It has to be taken into account that this stage shows no innervation of the heart. Parasympathetic innervation can be first identified in the outflow tract of the heart in stage 27 (Kirby et al. 1980; Kirby and Stewart 1983).

The embryonic sinus venosus functions as the dominant pacemaker during cardiac development (Kamino 1981). Moreover, recent investigations have identified beat to beat variations of dorsal aortic and vascular impedance in the chick embryo before innervation is completed (Kempinski et al. 1993). They speculate that this modulation is the manifestation of a preinnervated hemodynamic control mechanism. This control mechanism suggests a feed-back between ventricular function and vascular bed (Kempinski 1995). This control mechanism could be disrupted after treatment with all-trans retinoic acid.

Retinoic acid could also have an effect on the myocardium directly as suggested in chapter 2. Contraction of the myofibrils of the heart occurs through an interaction between the contractile proteins, i.e. actin and myosin, regulatory proteins, calcium ions, and chemical energy (Pelouch 1995). Cardiac looping is related to the development of myofibrils and myofibril structure (Manasek et al. 1986; Itasaki et al. 1991; Shiaishi et al. 1992). It is described that retinoic acid has multiple effects on growth and differentiation of cardiac myocytes, including an inhibition of cell proliferation, development of heart contractions, and delay in α -actin synthesis (Wiens et al. 1992). Pexieder et al. (1995) showed that all-trans retinoic acid can modify cardiac contractile proteins and alter myocardial contractility. An interaction of retinoic acid and contractile proteins could cause a disturbance in the myofibrillogenesis or myofibril arrangement and result in myocardial dysfunction accompanied by abnormal cardiac looping.

In conclusion, retinoic acid treated stage 24 embryos displayed altered cardiac morphology accompanied with malfunction of the heart. Therefore, retinoic acid likely affects both vascular and myocardial function simultaneously in the preinnervated chick embryonic heart.

4.3 Pressure-volume relationship of the stage 21 and stage 24 chick embryo: technology and methodology

Introduction

It has been established that cardiac output increases geometrically during primary cardiovascular development (Hu and Clark 1989; Broekhuizen et al. 1993). At the time of birth there is a right to left shift of systemic circulation accompanied by changes in pulmonary and systemic vascular resistance and prompt changes in ventricular growth (Teitel et al. 1991). Later the fully developed cardiovascular system also adjusts to altering hemodynamic demands of individual lifestyles, disease, and aging (Yin 1987).

The development and validation of measures of cardiac function have been performed primarily in the mature human heart through pressure-volume analysis (Sagawa et al. 1988). It is described that the cardiovascular system operates as a closed-loop system. It is because of this that interactions between ventricles and vascular bed can be defined using pressure-volume data (Sunagawa et al. 1987).

In the chick embryo, information on cardiac function can be assessed indirectly through dorsal aortic flow velocities and pressure wave form recordings (Hu and Clark 1989; Clark et al. 1983, 1991; Broekhuizen et al. 1993, 1995). However, direct information on cardiac function can be assessed using pressure-volume analysis (Keller et al. 1991, 1994). In stage 16, 18 and 21 chick embryos they established that stroke volume increased linearly with end-diastolic volume. Arterial elastance decreased with growth of the embryo. Pressure-volume loop area, an index of consumption of energy, doubled between the embryonic stages.

To pursue the feasibility of this technique for our research, a pilot study was performed in collaboration with Dr. B.B. Keller (Department of Pediatric Cardiology, Rochester, New York), pressure-volume loops were assessed. Technical assistance was provided by J. Tinney. Pressure-volume analysis was performed in stage 21 and 24 retinoic acid treated embryos ($n=7$; $n=5$), sham-operated embryos ($n=4$; $n=1$) and control embryos ($n=9$; $n=1$). However, due to small numbers of embryos, data analysis is not yet complete.

Technique

Video images of the embryonic cardiac ventricle were acquired through a stereophotomicroscope, and a video camera. The video camera generates 60 sequential video fields per second. Real time is recorded on each field with time and date generator. A 100 μ m scale scribed-glass standard was recorded after imaging the embryonic heart.

Simultaneous measurement of intraventricular pressure was carried out with a servo-null pressure system. A fluid filled 5-10 μm diameter tip glass cannula was positioned using a micromanipulator to puncture the embryonic ventricle. The analog signal was sampled at 500 Hz by an analog-digital board, and displayed on a computer monitor in digital oscilloscope mode. In addition, an analog device sampled the pressure wave form at 15.75 kHz and placed a marker proportional to instantaneous pressure onto each horizontal video line in real time. The device also placed zero and full scale markers onto video fields for calibration of the pressure scale. Zero transtip pressure was obtained by immersing the tip of the micropipette into the embryonic fluid. The combined video fields containing longitudinal images of the beating cardiac ventricle with simultaneous pressures were recorded on VHS tape using a video recorder. At least 10 initial baseline cardiac cycles were recorded. Then, to evaluate ventricular response to reduced venous return, a fourth order vitelline vein was incised to produce venous hemorrhage. The cardiac cycles after hemorrhage were also recorded. Finally, contracture of the heart with 2M NaCl took place, for analysis of cavity volume. The solution (1-3 μl) was applied directly on the ventricle. Individual video fields were analyzed using a Pentium computer, frame grabbing board, multipurpose video monitor, and JAVA video analysis software.

Protocol for measurement in each embryo: a. measurement software was calibrated for length (mm) and area (mm^2) with the scribed standard; b. video fields were traced for scalar ventricular pressure (mm Hg) and epicardial area (mm^2) for two consecutive cardiac cycles every 15-30 seconds for 180 seconds; c. ventricular volume (V_T) was derived from area (A_T) using a simplified ellipsoid geometric model: $V_T=0.65A_T^{3/2}$. The ellipsoid equation is derived from equations for the cross-sectional area of an ellipsoid, $A=\pi ab$, where a is the semi-major axis, and b is the semi-minor axis; the volume of an ellipsoid of revolution, $V=(4\pi ab^2)/3$; and assumed a fixed aspect ratio, $a/b=4/3$; d. cavity volume was calculated as total volume minus wall volume measured after contracture with 50 μl 2M NaCl; e. pressure data were transformed into hemodynamic data (mmHg); f. heart rate (beats per minute) was calculated from the cycle length (ms) of consecutive end-diastolic pressures; g. pressure and volume data were plotted as pressure-volume loops; h. end-diastole is identified at the onset of ventricular contraction, and end-systole at the maximum instantaneous pressure to volume ratio for each cardiac cycle; i. end-diastolic and end-systolic pressures (mmHg) and volumes (mm^3) were recorded continuously; j. systolic time (ms) was calculated from the number of video fields from end-diastole to end-systole; k. diastolic time (ms) was calculated as cycle length minus systolic time; l. stroke volume (mm^3) was calculated as the difference between end-diastolic and end-systolic volumes.

Data analysis protocol for each pressure-volume loop: 1. calculations of cycle length, diastolic, and systolic time intervals; 2. calculations of isometric contraction time as the time from end-diastole to 5% of end-systole to the positive deflection in the ventricular pressure waveform; 3. end-diastolic and end-systolic pressures and volumes for compliance and contractility indices respectively; 4. stroke volume as the difference between end-diastolic and end-systolic volumes; 5. arterial elastance was calculated as the ratio of end-systolic pressure to stroke volume (mmHg/m^3), to determine ventricular-arterial bed relationship.

As preliminary data do not allow statistical analysis it is not possible to determine the definite outcome. An example of pressure-volume loops of a stage 21 control embryo and a retinoic acid treated embryo can be seen in Figure 3a,b.

It can be concluded that the pressure-volume technique is feasible for further direct analysis of cardiac function.

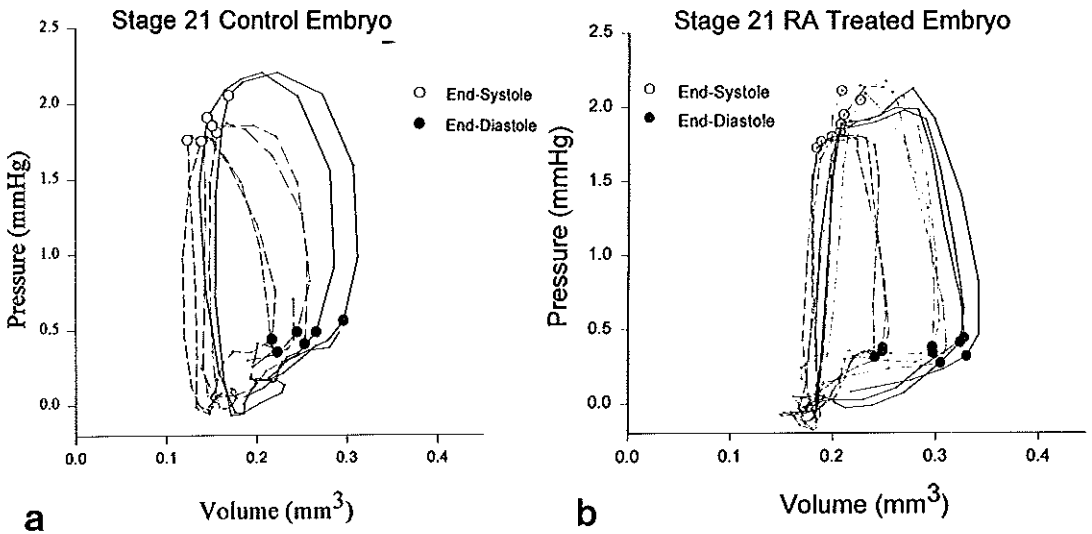


Figure 3. Pressure-volume loops of a control embryo (a) and a retinoic acid treated embryo (b).

4.4 References

- Bouman HGA, Broekhuizen MLA, Baasten MJ, Gittenberger-de Groot AC, Wenink ACG (1995) Spectrum of looping disturbances in stage 34 chicken hearts after retinoic acid treatment. *Anat Rec* 243:101-108.
- Broekhuizen MLA, Wladimiroff JW, Tibboel D, Poelmann RE, Wenink ACG, Gittenberger-de Groot AC (1992) Induction of cardiac anomalies with all-trans retinoic acid in the chick embryo. *Cardiol Young* 2:311-317.
- Broekhuizen MLA, Mast F, Struijk PC, Van der Bie W, Mulder PGH, Gittenberger-de Groot AC, Wladimiroff JW (1993) Hemodynamic parameters of stage 20 to stage 35 chick embryo. *Pediatr Res* 34:44-46.
- Broekhuizen MLA, Bouman HGA, Mast F, Mulder PGH, Gittenberger-de Groot AC, Wladimiroff JW (1995) Hemodynamic changes in HH stage 34 chick embryos after treatment with all-trans retinoic acid. *Pediatr Res* 38:342-348.
- Clark EB, Hu N, Dummett JL, Van de Kieft GK, Olson C, Tomanek R (1983) Ventricular function and morphology in chick embryo from stages 18-29. *Am J Physiol* 250:H407-H413.
- Clark EB, Hu N, Turner DR, Litter JE, Hansen J (1991) Effect of chronic verapamil treatment on the ventricular function and growth in chick embryos. *Am J Physiol* 261:H166-H171.
- Hu N, Clark EB (1989) Hemodynamics of stage 12 to stage 29 chick embryos. *Circ Res* 65:1665-1670.
- Itasaki N, Nakamura A, Sumida H, Yasuda M (1991) Actin bundles on the right side in the caudal part of the heart tube play a role in dextro-looping in the embryonic heart. *Anat Embryol* 183:29-39.
- Kamino K, Hirota A, Fujii S (1981) Localization of pacemaking activity in early embryo heart monitored using voltage-sensitive dye. *Nature* 260:595-597.
- Keller BB, Hu N, Serrino PJ, Clark EB (1991) Ventricular pressure-area loop characteristics in the stage 16 to 24 chick embryo. *Circ Res* 68:226-231.

Keller BB, Tinney JP, Hu N (1994) Embryonic ventricular diastolic and systolic pressure-volume relations. *Cardiol Young* 4:19-27.

Kempski MH, Kibler N, Blackburn JL, Dzakowic J, Hu N, Clark EB (1993) Hemodynamic regulation in the chick embryo. *Am Soc Mech Eng BED* 24:119-122.

Kempski MH (1995) Overview: Modeling and control of embryonic hemodynamics. In: Clark EB, Markwald RR, Takao A (eds) *Developmental Mechanisms of heart disease*. Futura publishing company, Inc, Armonk, New York, pp 421-434.

Kirby ML, Mckenzie JW, Weidman TA (1980) Developing innervation of the chick heart: a histofluorescence and light microscopic study. *Anat Rec* 196:333-340.

Kirby ML, Stewart D (1983) Neural crest origin of cardiac ganglion cells in the chick embryo: identification and extirpation. *Dev Biol* 97:433- 443.

Manasek FJ, Icardo J, Nakamura A, Sweeney (1986) Cardiogenesis: Developmental Mechanisms and Embryology. In: HA Fozzard et al. (eds) *The heart and cardiovascular system*. Raven Press, NY, pp 965-985.

Pelouch V (1995) Molecular aspects of regulation of cardiac contraction. *Physiol Res* 44:53-60.

Pexieder T, Blanc O, Pelouch V, Ostádalová I, Milerová M, Ostádal B (1995) Late fetal development of retinoic acid induced transposition of great arteries-morphology, physiology and biochemistry. In: Clark EB, Markwald RR, Takao A (eds) *Developmental Mechanisms of heart disease*. Futura Publishing Company, Armark, NY, pp 297-307.

Sagawa K, Maughan L, Suga H, Sunagawa K (1988) Historical overview. In: *Cardiac Contraction and the Pressure-Volume Relationship*. Oxford Press, NY, pp 3-41.

Shiraishi I, Takamatsu T, Minamikawa T, Fujita S (1992) 3-D observation of actin filaments during cardiac myofibrinogenesis in chick embryo using a confocal laser scanning microscope. *Anat Embryol* 185:401-408.

Sunagawa K, Sagawa K, Maughan WL (1987) Ventricular interaction with the vascular system in terms of pressure-volume relationships. In: Yin FCP (ed) *Ventricular Vascular Coupling: Clinical, Physiological, and Engineering Aspects*. Springer-Verlag, NY, pp 210-239.

Teitel DF, Klautz P, Steednijk P, van der Velde ET, van Bel F, Baan J (1991) The end-diastolic pressure-volume relationship in the newborn lamb: Effects of loading and inotropic interventions. *Pediatr Res* 29:473-482.

Wiens DJ, Mann TK, Fedderson DE, Rathmell WK, Franck BH (1992) Early heart development in the chick embryo: Effects of isoretinoin on cell proliferation, α -actin synthesis, and development of contractions. *Differentiation* 51:105-112.

Yin FCP (1987) Aging and vascular impedance. In: Yin FCP (ed) *Ventricular Vascular Coupling: Clinical, Physiological, and Engineering Aspects*. Springer-Verlag, NY, pp 115-139.

CHAPTER 5

HEMODYNAMIC EVALUATION OF THE STAGE 34 CHICK EMBRYO THE RETINOIC ACID MODEL

5.1 Introductory remarks

Hemodynamic data on normal cardiogenesis has been extensively studied from the onset of heart contractions to stage 29 chick embryo (Hu and Clark 1989) and to stage 35 (Broekhuizen et al. 1993). As for information on the interaction between form and function in later stages of cardiac development in the manipulated chick embryo, no data exist, until now.

In chapter 4 we elaborated on the altered cardiac form and function in the stage 24 retinoic acid treated chick embryo before innervation of the heart exits. At stage 34 it was established that retinoic acid treated embryos revealed the congenital heart malformation, double outlet right ventricle. To determine the effect of retinoic acid on the function of the four-chambered heart at this older stage, dorsal aortic flow velocities and vitelline artery blood pressures were assessed.

This chapter describes the interaction between form and function in the stage 34 chick embryo after exposure to all-trans retinoic acid.

5.2 Hemodynamic changes in stage 34 chick embryos after treatment with all-trans retinoic acid

*Monique L.A. Broekhuizen,¹ Hannie G.A. Bouman,² Frans Mast,³ Paul G.H. Mulder,⁴
Adriana C. Gittenberger-de Groot,² and Juriy W. Wladimiroff¹*

From the Department of Obstetrics and Gynecology¹ and Department of Epidemiology and Biostatistics,⁴ Academic Hospital Dijkzigt, Erasmus University, Rotterdam; Department of Anatomy and Embryology,² Leiden University; Department of Physiology,³ CARIM, Maastricht, The Netherlands

Summary

To obtain insight into the hemodynamics of abnormal cardiac development a chick embryo model was recently developed in which a spectrum of double outlet right ventricle was induced with all-trans retinoic acid. In Hamburger and Hamilton stage 34 white Leghorn chick embryos, we simultaneously measured dorsal aortic flow velocities with a 20-MHz directional-pulsed Doppler velocity meter, and vitelline artery blood pressures with a servo-null system. These measurements were performed in embryos treated at stage 15 with 1 µg all-trans retinoic acid (n=47), or with the solvent dimethylsulphoxide (n=15) and in control embryos (n=21). After the wave form recordings were collected, all embryos were examined histologically. Embryos treated with all-trans retinoic acid showed in 15 cases, hearts with a rightward positioned aorta with an additional subaortic ventricular septal defect and 32 cases without septation abnormalities of the heart. The hemodynamic data were correlated with the morphology. Statistical comparison was performed between control and experimental values. There was no significant discrepancy in hemodynamics of sham-operated and control embryos. Heart rate, peak systolic and mean velocities, peak systolic and mean blood flows, and peak acceleration and stroke volume were reduced in embryos treated with all-trans retinoic acid ($p<0.01$). Furthermore, in the presence of a subaortic ventricular septal defect the diameter of the dorsal aorta was reduced. Pressure readings were not statistically significant. Our findings suggest that the hemodynamic changes are the result of a decrease in cardiac contraction force.

Introduction

Cardiac development is a dynamic process involving complex structural changes accompanied by dramatic changes in hemodynamic function. Hemodynamics is concerned with the forces generated by the heart and the resulting motion of blood through the cardiovascular system. The multifaceted process of the interrelationship between form and function is a therefore major challenge to developmental biologists. Micro-Doppler and pressure studies in chick embryos have provided valuable information on this relationship in normal heart development (Hu and Clark 1989; Broekhuizen et al. 1993). To obtain insight into the hemodynamics in abnormal cardiac development, a chick embryo model was recently developed in which cardiac malformations as part of a continuous spectrum were induced with all-trans retinoic acid, a cardiac teratogen (Lammer et al. 1985; Pexieder et al. 1992). The heart malformations showed a spectrum of a rightward shift of the aorta. The rightward positioned aorta was still connected to the left ventricle in cases without a ventricular septal defect and were classified as having no septation abnormalities. In the presence of a ventricular septal defect, in combination with the rightward positioned aorta, this anomaly was diagnosed as double outlet right ventricle (Broekhuizen et al. 1992). This model will allow us to evaluate the cellular biological aspects of the influence of all-retinoic acid on cardiac morphogenesis as well as the assessment of the hemodynamic parameters involved.

The objective of the present study was to establish whether a difference in hemodynamics existed between embryos with a normally developing heart and embryos with a developing double outlet right ventricle following all-trans retinoic acid treatment. Stage 34 was selected because the cardiac defect was easy to diagnose in this stage (Broekhuizen et al. 1992).

Materials and Methods

Fertilized white Leghorn chick eggs were incubated (blunt end up) at 38°C and staged according to Hamburger and Hamilton (1951). The material was subdivided into groups of embryos treated with a solution of all-trans retinoic acid and the solvent dimethylsulphoxide, embryos treated with only the solvent (sham-operated embryos) and control embryos.

At stage 15 (day 2½ of a 21 day incubation) each embryo, with exception of the controls, was exposed by creating a window in the shell followed by removal of the overlying membranes. Either a solution containing 1.0 µg all-trans retinoic acid or only the solvent 2% dimethylsulphoxide was then deposited on the vitelline membrane of the embryo using a Hamilton syringe (Broekhuizen et al. 1992). After administration of the solution, the window was sealed with tape and the egg re-incubated.

Physiologic measurements were performed at stage 34 (day 8 of incubation) because the cardiac defect could be diagnosed with certainty in this stage (Broekhuizen et al. 1992). An egg was removed from the incubator and positioned on the stage of a dissecting microscope. Each embryo was exposed either by removing the tape of the all-trans retinoic acid treated and sham-operated embryos or making a window in the shell and removing the overlying membranes of the controls. Only live embryos with the right side up and without any sign of bleeding were included in the final analysis. We simultaneously measured blood pressures in the vitelline artery, and flow velocities in the dorsal aorta in 47 embryos treated with 1.0 μg all-trans retinoic acid and in 15 sham-operated and 21 control embryos. The temperature of the embryo during the measurement was regulated by a thermoelement and was maintained at 37°C.

Blood pressure was measured in the left vitelline artery with a servo-null system (model 900A, World Precision Instruments, Inc., Sarasota, FL) and a 10 μm glass micropipette. This pressure system was tested against a standing water column. A total of 26 measurements were performed. The relationship between the servo-null pressure system and the water column pressure was determined by regression analysis. The method was linear from -5 mm Hg to 40 mm Hg ($y=1.14x+0.25$, $r^2=0.99$, standard error of the estimate = 0.12 mm Hg). Zero trans-tip pressure was obtained by immersing the tip of the micropipette in the extraembryonic fluid at the level of the measured site (Hu and Clark 1989).

Mean dorsal aortic blood flow velocities were measured with a 20 MHz directional pulsed Doppler velocity meter (model 545C-4 by Bioengineering, University of Iowa). In a previous study (Broekhuizen et al. 1993), this equipment had been validated to be accurate above 5 mm/s. The Doppler probe consisting of a 750 μm piezoelectric crystal was positioned at a 45° angle to the dorsal aorta at the level of the sinus venosus as described in earlier reports (Hu and Clark 1989; Broekhuizen et al. 1993).

The internal diameter of the dorsal aorta was measured at the same level with a filar micrometer eyepiece which was calibrated against a 10- μm engraved glass standard. The vessel area was calculated from the equation $\text{area}=\pi d^2/4$ where d is the aortic diameter (mm).

Hemodynamic Parameters

The analog wave forms were sampled at 300 Hz by a Lab Master data acquisition analog-digital board (Axon Instruments Inc., Burlingame, CA) linked to a Commodore PC40 computer. The converter offered 12 bits at an input range of -10 to 10 Volt. Data were stored in a 5¼-inch 90 megabyte Bernoulli disk cartridge (Iomega Corp., Roy, UT).

Within each embryo a 2-min wave form recording was made. A technically high-quality wave form recording of 10 s was selected for analysis. Each 10 s recording contained 20 to 40 wave forms.

Peak-systolic, diastolic and mean blood pressures were determined. Vitelline artery dP/dt (mm Hg/s) was derived from the analog pressure signal by digital differentiation.

Mean dorsal aortic blood flow (mm^3/s) was calculated as the product of the mean velocity and the area of the dorsal aorta (Broekhuizen et al. 1993). By measuring the cycle length between pulse waves and converting this into beats per minute (bpm), the heart rate was calculated. The peak acceleration dV/dt (mm/s^2) was derived from the dorsal aortic velocity $V(t)$ by means of digital differentiation. Stroke volume (mm^3) was determined from the quotient of mean dorsal aortic blood flow and heart rate multiplied by 60. Cardiac work ($\text{mm}^3 \times \text{mm Hg}$) is the product of stroke volume and mean arterial pressure. Vascular resistance [$\text{mm Hg}/(\text{mm}^3/\text{s})$] is the quotient of mean arterial pressure and mean dorsal aortic blood flow.

Morphologic Examination

After the wave form recordings were collected all 83 embryos were removed from the egg and were processed for histologic sectioning in a routine way by fixing in Bouin and embedding in paraffin. Thereafter, the embryos including the hearts were serially sectioned. The sections were 5 μm thick and stained with Mayer's hematoxylin/eosin (Broekhuizen et al. 1992).

To exclude growth retardation at stage 34, the embryo, heart and extraembryonic vascular bed were weighed in an additional study of 32 embryos. These were subdivided into 17 embryos treated with all-trans retinoic acid, 7 sham-operated embryos and 8 controls. For this purpose the vitelline membrane was stripped away from the yolk, and each tissue was removed and rinsed with chick Ringer's solution. The specimen was placed on Parafilm and gently blotted to remove excess water and weighed on a Mettler balance accurate to $\pm 100 \mu\text{g}$. The ventricles and atria including the great vessels were weighed after the vessels distal to the aorta and pulmonary trunk were trimmed off.

Statistical Analysis

From each control embryo an additional wave form recording of 10 heart cycles was selected to analyze the reproducibility of the blood pressure readouts. The reproducibility (r) was defined according to the equation: $r = \sigma^2_{\text{B}}/(\sigma^2_{\text{B}} + \sigma^2_{\text{W}})$, in which σ^2_{B} represents the between-embryo variance and σ^2_{W} the within-embryo variance. These variances were estimated from an analysis of variance. The reproducibility of the flow velocity parameters had been determined to be satisfactory (Broekhuizen et al. 1993).

Finally, the hemodynamic data were correlated with the morphology. The distribution of hemodynamic parameters was non-Gaussian. Therefore, a non-parametric statistical analysis was carried out. The data are presented as characteristics of the frequency distribution of the hemodynamic parameters by medians and ranges (minimum, maximum). Statistical comparison was done by the Kruskal-Wallis test, whereas the Mann-Whitney test was used to determine significant differences between control and experimental values. An exact trend test in a 3 X 2 cross-table was used for the dorsal aortic area because this parameter only had three ordered levels. The statistical significance level was defined as a p value of less than 1% ($p < 0.01$) because several parameters were tested.

Results

Morphology

After histologic analysis, the heart malformations showed a spectrum of a rightward shift of the aorta. In 32 out of 47 embryos, treated with all-trans retinoic acid, no septation abnormalities of the heart could be found. The remaining 15 hearts showed a rightward positioned aorta with an additional subaortic ventricular septal defect. Therefore, all 47 embryos treated with all-trans retinoic acid were subdivided into two major groups, those with a (subaortic) ventricular septal defect ($n=15$) and those without a ventricular septal defect ($n=32$). All hearts of the controls ($n=21$) and 13 hearts of sham-operated embryos were normal. Two hearts of the sham-operated embryos had a subaortic ventricular septal defect although different from the ventricular septal defect encountered in embryos treated with all-trans retinoic acid. The results of measurements of whole embryo, heart, and extraembryonic vascular bed wet weights are presented in Table 1. There was no significant difference between embryos treated with all-trans retinoic acid, sham-operated embryos, and control embryos.

Table 1. Embryo, Heart, and Extraembryonic Vascular Bed Wet Weights of stage 34 control and experimental chick embryos, $p > 0.01$

	Control	Sham	<u>Retinoic acid treated</u>	
	(n=8)	(n=7)	no VSD (n=10)	subaortic VSD (n=7)
Embryo (g)				
minimum	1.189	1.214	1.024	1.135
median	1.253	1.326	1.209	1.199
maximum	1.336	1.388	1.432	1.481
Heart (g)				
minimum	0.012	0.011	0.012	0.011
median	0.013	0.014	0.014	0.015
maximum	0.016	0.017	0.017	0.017
Extraembryonic vascular bed (g)				
minimum	0.975	0.927	0.935	0.630
median	1.434	1.198	1.065	0.985
maximum	1.963	1.364	1.466	1.352

VSD=ventricular septal defect

Hemodynamics

The characteristics of the frequency distribution of the dorsal aortic wave form parameters of control embryos, sham-operated embryos and embryos treated with all-trans retinoic acid can be seen in Figure 1a-g. There was no significant discrepancy in hemodynamics of control and sham-operated embryos. The two sham-operated embryos with a subaortic ventricular septal defect had normal hemodynamic parameters. Hemodynamics of control and sham-operated embryos were compared with all-trans retinoic acid treated embryos. Heart rate, peak systolic and mean velocities, peak systolic and mean blood flows, and peak acceleration and stroke volume were reduced in embryos after treatment with all-trans retinoic acid, i.e. embryos with and without a subaortic ventricular septal defect ($p < 0.01$). Moreover, when the latter two subgroups were compared with each other all parameters derived from the flow velocity wave form recording were significantly reduced ($p < 0.01$) in the presence of a subaortic ventricular septal defect except heart rate and peak acceleration.

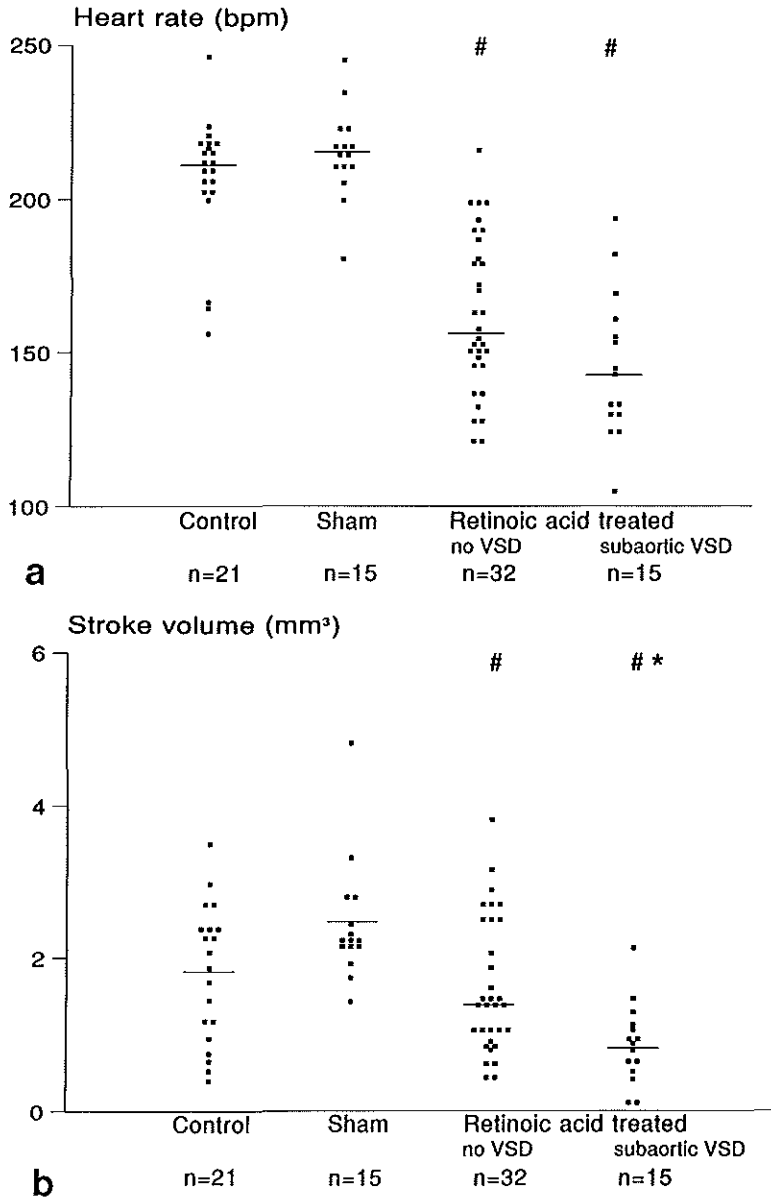


Figure 1. a-b. The characteristics of the frequency distribution of (a) heart rate, (b) stroke volume. #, Significantly different from control and sham-operated embryos ($p < 0.01$). *, Significantly different from embryos treated with all-trans retinoic acid without VSD ($p < 0.01$). VSD = ventricular septal defect.

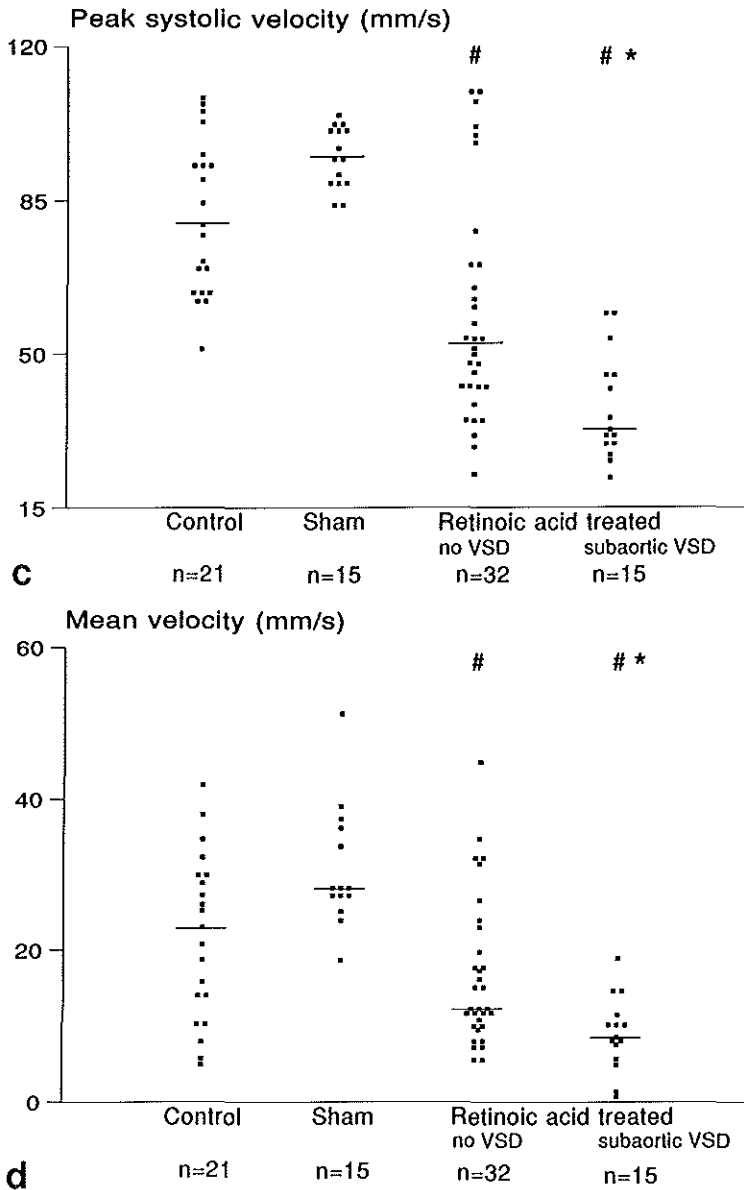


Figure 1. c-d. The characteristics of the frequency distribution of (c) peak systolic velocity, (d) mean velocity.

#, Significantly different from control and sham-operated embryos ($p < 0.01$).

*, Significantly different from embryos treated with all-trans retinoic acid without VSD ($p < 0.01$).

VSD = ventricular septal defect.

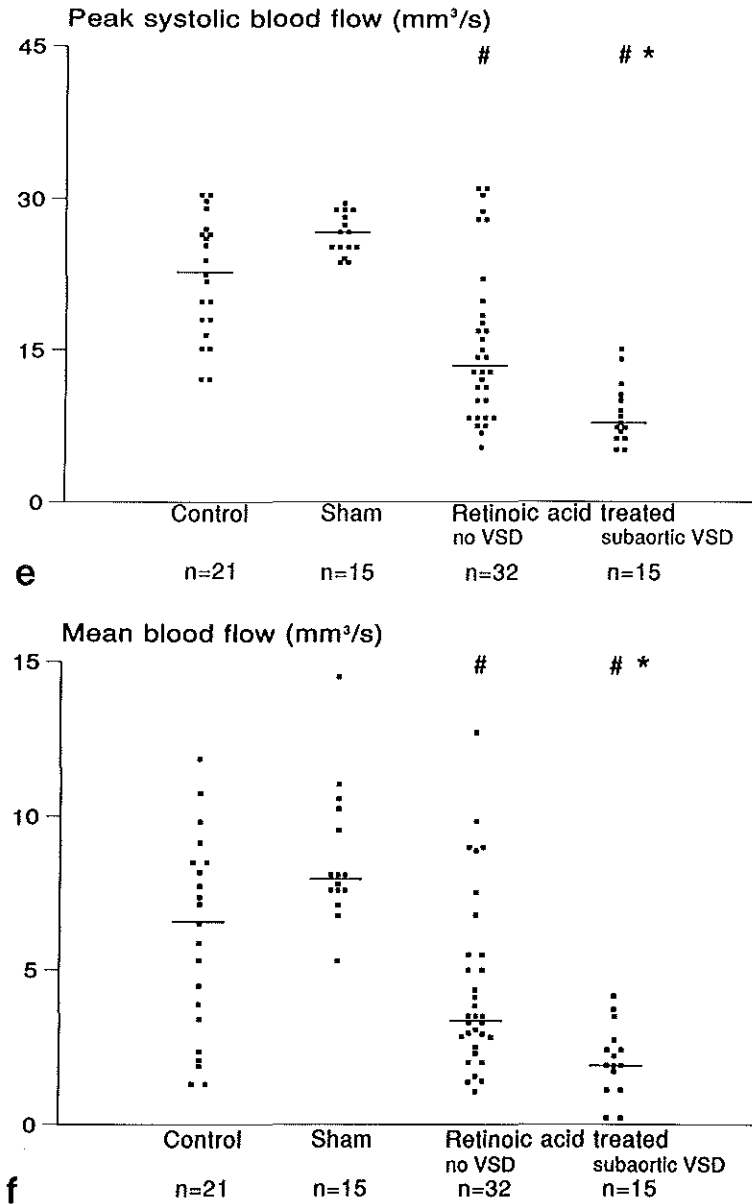


Figure 1. e-f. The characteristics of the frequency distribution of (e) peak systolic blood flow (f) mean blood flow.

#, Significantly different from control and sham-operated embryos ($p < 0.01$).

*, Significantly different from embryos treated with all-trans retinoic acid without VSD ($p < 0.01$).

VSD = ventricular septal defect.

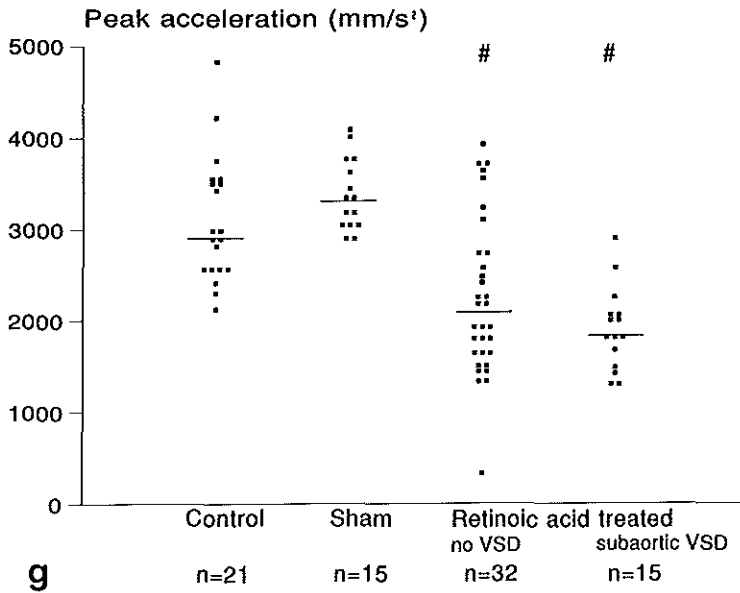


Figure 1. g. The characteristics of the frequency distribution of peak acceleration. #, Significantly different from control and sham-operated embryos ($p < 0.01$). VSD = ventricular septal defect.

An example of dorsal aortic flow velocity and pressure wave forms for a stage 34 control embryo, sham-operated embryo and an embryo treated with all-trans retinoic acid that appeared to have a subaortic ventricular septal defect, is shown in Figure 2. It is clear from this figure that there is a reduction in peak systolic velocity and peak acceleration in the embryo with a subaortic ventricular septal defect after treatment with all-trans retinoic acid compared with the control and sham-operated embryo. The vitelline artery pressure shows no significant difference between the three groups of embryos.

A cross table of the dorsal aortic area can be seen in Table 2. The exact trend test in a 3 X 2 cross table determined that this parameter was reduced in embryos with a subaortic ventricular septal defect after treatment with all-trans retinoic acid ($p < 0.01$).

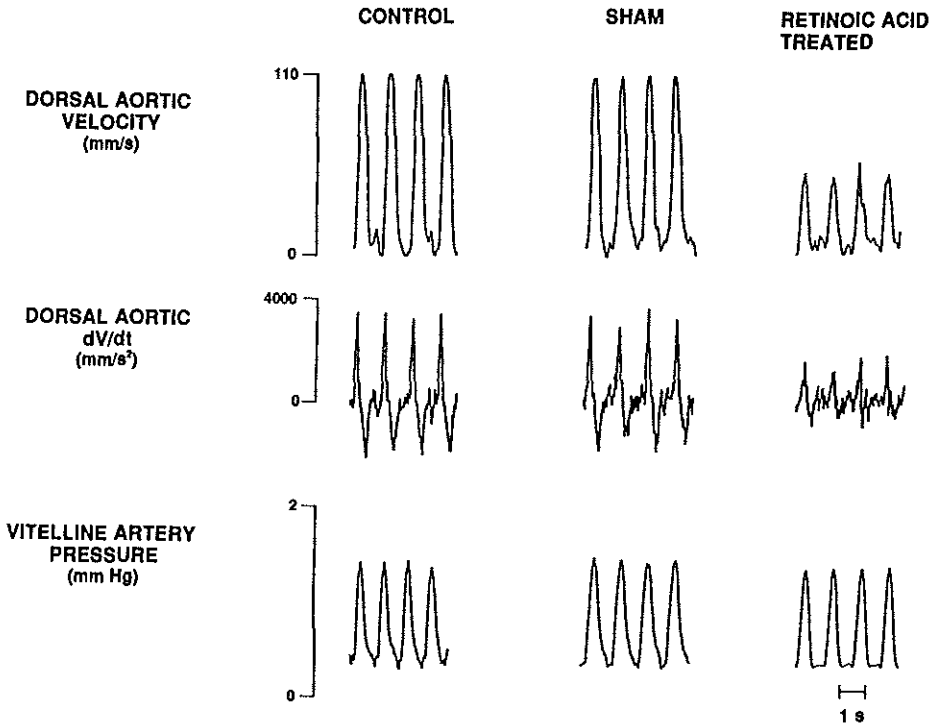


Figure 2. Flow velocity and pressure wave forms of a control embryo, sham-operated embryo and a retinoic acid treated embryo that appeared to have a subaortic ventricular septal defect.

Table 2. A cross-table of dorsal aortic area by control and experimental stage 34 chick embryos

	Control n=21	Sham n=15	Retinoic acid treated	
			no VSD n=32	subaortic VSD n=15 ($p<0.01$)
Dorsal aortic area (mm ²)				
0.19	1	0	3	4
0.23	4	1	11	10
0.28	16	14	18	1

VSD = ventricular septal defect

The peak-systolic and diastolic blood pressures measured in the left vitelline artery of control and sham-operated embryos and embryos treated with all-trans retinoic acid showed no significant difference (Table 3). The dP/dt showed a reduction in embryos treated with all-trans retinoic acid but was not significant. It was not possible to collect satisfactory pressures in all embryos because sometimes the tip of the glass micropipette was clogged up before an adequate pressure could be recorded.

Table 3. Characteristics of the frequency distribution of the vitelline arterial pressure parameters of control and experimental stage 34 chick embryos, $p > 0.01$

	Control (n=11)	Sham (n=11)	Retinoic acid treated	
			no VSD (n=27)	subaortic VSD (n=10)
Peak systolic pressure (mm Hg)				
minimum	0.8	0.7	0.5	0.9
median	2.9	1.8	2.2	1.7
maximum	4.2	4.1	6.4	2.7
Diastolic pressure (mm Hg)				
minimum	0.05	0.06	0.01	0.05
median	0.6	0.6	0.5	0.3
maximum	1.9	1.6	2.7	0.9
Mean pressure (mm Hg)				
minimum	0.3	0.4	0.03	0.2
median	1.1	0.9	1.1	0.8
maximum	2.9	2.1	3.2	1.4
dP/dt max (mm Hg/s)				
minimum	20.5	20.2	5.7	9.8
median	33.8	34.2	30.4	25.3
maximum	52.4	50.3	96.3	34.1

VSD = ventricular septal defect

The results of the analysis of variance for each of the pressure parameters is shown in Table 4. The correlation coefficient (*r*) that represents the reproducibility, using the average of 10 cycles as measurement outcome, was above 0.95.

Table 4. Results of analysis of variance

Pressure (mm Hg)	σ^2_{W} *	σ^2_{B} †	<i>r</i> ‡
Peak systolic	0.02	7.38	1.00
Diastolic	0.10	3.57	0.97
Mean	0.01	4.77	1.00

* Variance within embryos.

† Variance between embryos.

‡ Reproducibility (correlation coefficient).

The vascular resistance and cardiac work are shown in Figure 3 *a,b*. Vascular resistance was elevated and cardiac work reduced in embryos with a subaortic ventricular defect when compared with the sham-operated embryos ($p < 0.01$). Furthermore, in contrast with control embryos, embryos with a subaortic ventricular defect showed a significant decrease in cardiac work ($p < 0.01$). The degree of dextroposition of the aorta in embryos without ventricular septal defect, does not seem to have a significant impact on the hemodynamic parameters measured.

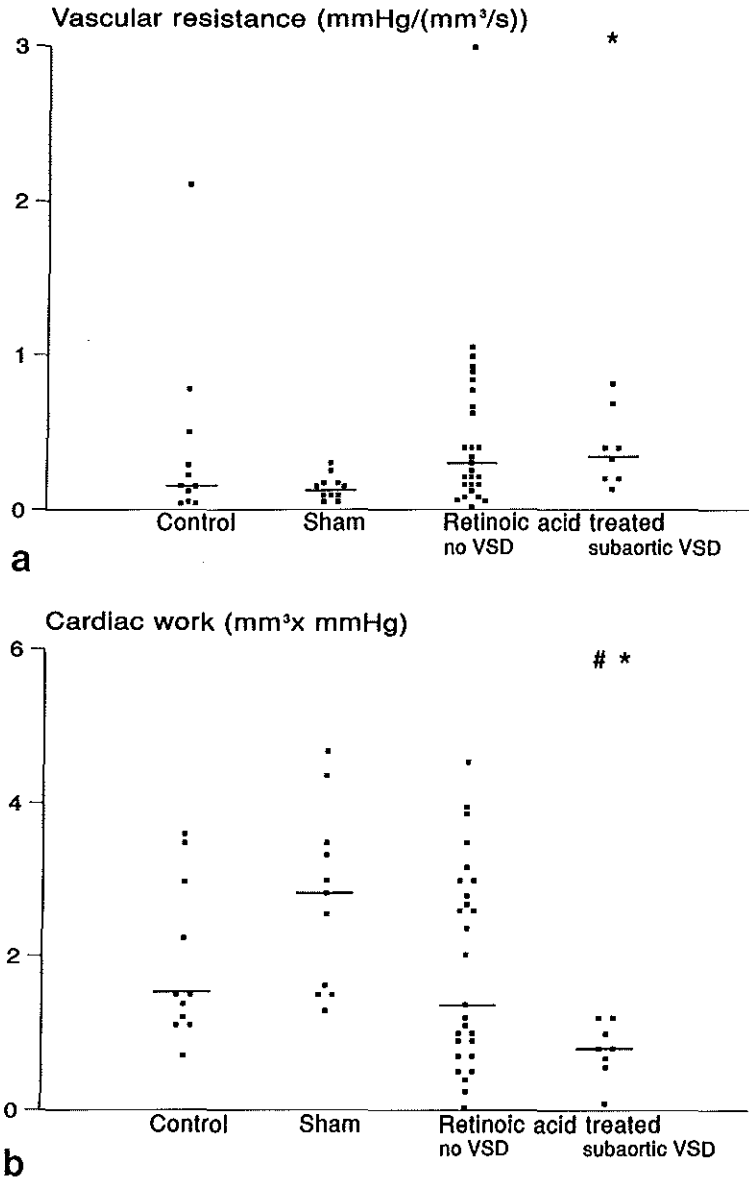


Figure 3. a-b. The characteristics of the frequency distribution of (a) vascular resistance, (b) cardiac work.

#, Significantly different from control embryos ($p < 0.01$).

* Significantly different from sham operated embryos ($p < 0.01$).

VSD=ventricular septal defect.

Discussion

In the present study dorsal aortic flow velocity and vitelline artery pressure wave forms were recorded in stage 34 (d 8 of incubation) embryos treated with all-trans retinoic acid, sham operated embryos and control embryos. Hemodynamics of control and sham-operated embryos showed no significant difference. The presence of a ventricular septal defect in 2 out of 15 sham operated embryos had no effect on hemodynamic outcome. The 13.3% incidence of this type of ventricular septal defect is in the range of spontaneous occurrence of 11.7% of cardiac malformations seen in the chick embryo and the majority closes before hatching (Kuhlman and Kolesari 1984). It is described that dimethylsulphoxide by itself can interfere with normal development by producing defects of head and limbs (Landauer and Salam 1972). As solvent it can produce very important changes in the teratogenic effectiveness of biologically active compounds. This could explain the 31.9% incidence and severity of the cardiac malformations seen after treatment with all-trans retinoic acid.

Hemodynamics of retinoic acid treated embryos, control and sham-operated embryos were compared with each other. A significant decrease in heart rate, peak systolic and mean velocities, peak systolic and mean blood flows, and peak acceleration and stroke volume was observed in embryos treated with all-trans retinoic acid. A comparison was also carried out between the two subgroups of embryos treated with all-trans retinoic acid. All parameters derived from the flow velocity wave form recording were significantly reduced in the presence of a subaortic ventricular septal defect except heart rate and peak acceleration. Moreover, the dorsal aortic area, that was determined from the vessel diameter, was reduced in these embryos. Pressure readings were not essentially different between control and sham-operated embryos and all embryos treated with all-trans retinoic acid. Therefore, the increase in vascular resistance and decrease in cardiac work in embryos with a subaortic ventricular defect can only be explained by the observed decrease in volume flow. The latter finding could not be the result of a possible growth retardation because the measurements of whole embryo, heart, and extraembryonic vascular wet weights showed no significant differences between retinoic acid treated embryos, sham-operated embryos, and control embryos.

The hemodynamic changes seen in retinoic acid treated embryos, in particular the reduced peak acceleration and stroke volume, suggest a decrease in cardiac contraction force. The peak acceleration was derived from the dorsal aortic velocity and indicates the contraction potential of the heart. Stroke volume was determined from mean dorsal aortic blood flow and heart rate. The decrease in heart rate may be caused by an immature impuls formation in the conduction system due to a delay in the maturation process of the heart. In a previous report we described the physiological increase of heart rate between stage 20 to stage 35 (Broekhuizen et al. 1993).

Comparison between the two subgroups of retinoic acid treated embryos revealed in embryos with a subaortic ventricular septal defect a significant reduction of all wave form parameters, except heart rate and peak acceleration. The latter suggests no significant difference in cardiac contraction force between the two subgroups. The abnormal morphology in combination with the decrease in cardiac contraction force could account for the impaired volume flow and could lead to the calculated reduction in vessel area in these embryos.

We propose that the hemodynamic changes presented in this study are mainly due to myocardial dysfunction and to a lesser extent to abnormal cardiac morphology in embryos that were treated with all-trans retinoic acid. A decrease in cardiac contraction force was found in these embryos regardless the presence of a ventricular septal defect.

Although the mechanism is unclear, we postulate that all-trans retinoic acid may have an indirect and a direct effect on the myocardium.

The indirect effect may result from an impaired parasympathetic innervation through a disturbance of the migration of cells from the neural crest. It is described that neural crest cells contribute to the cardiac ganglia (Kirby and Stewart 1983; Kirby 1993). Parasympathetic innervation of the heart via the cardiac ganglia could be impaired after treatment with retinoic acid. The effect of all-trans retinoic acid on the neural crest may be through cytotoxicity (Jelínek and Kistler 1981) or result from alterations in region-specific signals necessary for homing of neural crest cells or for their differentiation (Hart et al. 1990). Furthermore, *in vitro* mesenchymal cell migration is inhibited by retinoids (Thorogood et al. 1982; Smith-Thomas 1987). Impaired parasympathetic innervation could lead to an alteration of the tonus of the cardiac myocytes.

A direct effect cannot be excluded. Evidence exists that 13-cis retinoic acid and all-trans retinoic acid have multiple effects on growth and differentiation of cardiac myocytes, including an inhibition of cell proliferation, development of heart contractions, and delay in α -actin synthesis (Wiens et al. 1992). Retinoic acid may have direct effects on the myocytes by disruption of gap junctional communication (Mehta 1989) that could be mediated through retinoid binding proteins (Maden et al. 1989, 1991) and the nuclear receptors (Ruberte et al. 1991). Pexieder et al. (1995) showed that all-trans retinoic acid can modify cardiac contractility. In rat fetuses treated during early pregnancy with all-trans retinoic acid, a higher sensitivity towards extracellular calcium-ion variations was found. This could indicate a larger permeability (immaturity) of the sarcolemma and/or delayed development of the sarcoplasmic reticulum (Pexieder et al. 1995). Furthermore, they reported that all-trans retinoic acid significantly decreased the total amount of protein in morphologically normal mouse hearts and hearts that showed a double outlet right ventricle.

In these morphologically normal and abnormal hearts, the concentration of sarcoplasmic proteins was significantly increased and that of contractile proteins decreased. Results of our study coincide with their data that, in embryos treated with all-trans retinoic acid complementary with structural changes of the myocardium, the function of the embryonic heart is also affected. Both direct and indirect effects on the myocardium could generate myocardial dysfunction in various ways, and lead to the same result i.e., a decrease in cardiac contraction force.

In conclusion we put forward that the hemodynamic changes observed in embryos after treatment with all-trans retinoic acid are the result of a decrease in cardiac contraction force. Our results suggest there was no significant difference in contraction force between the two subgroups, embryos with and without ventricular septal defect, of retinoic acid treated embryos. The presence of a subaortic ventricular septal defect in combination with the myocardial dysfunction could account for impaired volume flow and could lead to the observed diminished dorsal aortic diameter in these embryos.

Regulation of cardiac growth, and function involves the orchestration of hemodynamic and cellular events. Further longitudinal studies will be conducted to evaluate the degree of altered myocardial contractility. These studies concern myocardial innervation and immunohistochemistry of the contractile apparatus.

5.3 References

- Broekhuizen MLA, Wladimiroff JW, Tibboel D, Poelmann RE, Wenink ACG, Gittenberger-de Groot AC (1992) Induction of cardiac anomalies with all-trans retinoic acid in the chick embryo. *Cardiol Young* 2:311-317.
- Broekhuizen MLA, Mast F, Struijk PC, Van der Bie W, Mulder PGH, Gittenberger-de Groot AC, Wladimiroff JW (1993) Hemodynamic parameters of stage 20 to stage 35 chick embryo. *Pediatr Res* 34:44-46.
- Hamburger V, Hamilton HL (1951) A series of normal stages in the development of the chick embryo. *J Morph* 88:49-92.
- Hart RC, McCue PA, Ragland WL, Winn KJ, Unger ER (1990) Avian model for 13-cis retinoic acid embryopathy: demonstration of neural crest related defects. *Teratology* 41:463-472.
- Hu N, Clark EB (1989) Hemodynamics of stage 12 to stage 29 chick embryo. *Circ Res* 65:1665-1670.
- Jelinek R, Kistler A (1981) Effect of retinoic acid upon the chick embryonic morphogenetic systems. The embryotoxicity range. *Teratology* 23:191-195.
- Kirby ML, Stewart D (1983) Neural crest origin of cardiac ganglion cells in the chick embryo: identification and extirpation. *Dev Biol* 97:433-443.
- Kirby ML (1993) Cellular and molecular contributions of the cardiac neural crest to cardiovascular development. *Trends Cardiovasc Med* 3:18-23.
- Kuhlmann RS, Kolesari GL (1984) The spontaneous occurrence of aortic arch and cardiac malformations in the white Leghorn chick embryo (*Gallus domesticus*). *Teratology* 30:55-59.
- Lammer EJ, Chen DT, Hoar RM, Angish ND, Benke PJ, Braun JT, Curry CJ, Fernhoff PM, Grix AW, Lott IT, Richard JM, Sun SC (1985) Retinoic acid embryopathy. *N Engl J Med* 313:837-841.

Landauer W, Salam N (1972) Aspects of dimethylsulphoxide as solvent for teratogens. *Dev Biol* 28:35-46.

Maden M, Ong DE, Summerbell D, Chytil F (1989) The role of retinoid-binding proteins in the generation of pattern in the developing limb, the regenerating limb and the nervous system. *Development* 107 (Supplement):109-119.

Maden M, Hunt P, Erikson U, Kuroiwa A, Krumlauf R, Summerbell D (1991) Retinoic acid-binding protein, rhombomeres and the neural crest. *Development* 111:35-44.

Mehta P, Bertram J, Loewenstein W (1989) The actions of retinoids on cellular growth correlate with their actions on gap junctional communication. *J Cell Biol* 108:1053- 1065.

Pexieder T, Pfiizenmaier R, Rousseil M, Prados-Frutos JC (1992) Prenatal pathogenesis of the transposition of great arteries. In: Vogel M, Bühlmeier K (eds) *Transposition of the great arteries 25 years after Rashkind balloon septostomy*. Steinkopff Verlag, Darmstadt, pp. 11-27.

Pexieder T, Blanc O, Pelouch V, Ostádalová I, Milerová M, Ostádal B (1995) Late fetal development of retinoic acid induced transposition of great arteries-morphology, physiology and biochemistry. In: Clark EB, Markwald RR, Takao A (eds) *Developmental mechanisms of heart disease*. Futura Publishing Company, Armark, New York, pp 297-307.

Ruberte E, Dollé P, Chambon P, Morriss-Kay G (1991) Retinoic acid receptors and cellular retinoid binding proteins. II. Their differential pattern of transcription during early morphogenesis in mouse embryos. *Development* 111:45-60.

Smith-Thomas L, Lott I, Bronner-Fraser M (1987) Effects of isotretinoin on the behavior of neural crest cells in vitro. *Dev Biol* 123:276-280.

Thorogood P, Smith L, Nicol A, McGinty R, Garrod D (1982) Effects of vitamin A on the behavior of migratory neural crest cells in vitro. *J Cell Sci* 57:331-350.

Wiens DJ, Mann TK, Feddersen DE, Rathmell WK, Franck BH (1992) Early heart development in the chick embryo: effects of isotretinoin on cell proliferation, α -actin synthesis, and development of contractions. *Differentiation* 51:105-112.

CHAPTER 6

**ALTERED PARASYMPATHETIC INNERVATION
AFTER
RETINOIC ACID TREATMENT**

6.1 Introductory remarks

The period of organogenesis is characterized by rapid embryo growth. Although the embryo weight doubles the heart grows less rapidly (Rakusan 1984). Growth in response to functional demands is a fundamental feature of the heart. Increasing myocardial contractility is related to embryonic myocardial growth that occurs by cell proliferation or hyperplasia (Knaapen et al. 1996), and is responsive in part to environmental factors (Clark 1989, 1991). The events of growth, increasing contractility correlate with the appearance of functional autonomic nervous system (Serelakis and Pappano 1983).

Treatment with all-trans retinoic acid leads to a decrease cardiac contraction force in stage 34 chick embryos which suggests myocardial dysfunction (Broekhuizen et al. 1995). Previously we hypothesized that retinoic acid could both have a direct and indirect effect on the myocardium. The indirect effect may result from an abnormal parasympathetic innervation through a disturbance of neural crest cell migration.

This chapter discusses the possible effects of retinoic acid on the stage 34 embryonic chick heart. The hearts were studied with immunohistochemical markers that are considered to be markers for neuronal differentiation.

6.2 Impaired neural crest derived parasympathetic innervation of embryonic chick hearts in the presence of altered hemodynamics after treatment with all-trans retinoic acid

*Monique L. A. Broekhuizen¹, Adriana C. Gittenberger-de Groot², Mieke J. Baasten²,
Juriy W. Wladimiroff¹, Robert E. Poelmann²*

From the Department of Obstetrics and Gynecology¹, Academic Hospital Rotterdam, Erasmus University, Rotterdam, Department of Anatomy and Embryology², Leiden University, Leiden
The Netherlands

Summary

To obtain more insight into underlying mechanisms of decrease of hemodynamic parameters after all-trans retinoic acid treatment, neural crest derived parasympathetic innervation patterning of the developing avian heart was studied. In stage 34 white Leghorn chick embryos, we simultaneously measured dorsal aortic flow velocities with a 20 MHz directional pulsed Doppler velocity meter, and vitelline artery blood pressures with a servo-null system. These measurements were performed in embryos treated at stage 15 with 1 µg all-trans retinoic acid (n=11), or with the solvent dimethylsulphoxide (sham-operated embryos, n=8), and in control embryos (n=8). After the waveform recordings were collected all embryos were examined with a dissecting microscope. The hearts were removed and whole-mount stained with anti-HNK-1-antibody. All hearts of retinoic acid treated embryos showed an impaired parasympathetic distribution over the heart. The parasympathetic innervation was not altered in the sham-operated embryos compared to controls. Hemodynamic data were correlated with the morphology. A decrease in cardiac contraction force was found in all embryos that displayed abnormal parasympathetic branching over the heart, regardless the presence of a morphologically detectable intracardiac anomaly, being a double outlet right ventricle in 3 out of 11 cases. Control and sham-operated embryos showed normal hemodynamics.

A separate set of hearts of retinoic acid embryos, sham-operated and control embryos, was devised for serial sectioning and staining with anti-HNK-1-antibody. This revealed a similar diminished parasympathetic distribution compared to the whole mounts. Our findings suggest that impaired parasympathetic development may contribute to myocardial dysfunction in all-trans retinoic acid treated embryos.

Introduction

During embryonic development a widespread migration of neural crest cells gives rise to neuronal cell populations of the autonomic nervous system. The vagal postganglionic parasympathetic innervation of the outflow tract of the heart has been described in the chick embryo (Kirby et al. 1980; Kirby and Stewart 1983). Neural crest ablation studies revealed that a part of the vagal neural crest, "cardiac neural crest", contributes to cardiac ganglia and to the formation of the outflow tract (Kirby 1987). A morphologic study on the development of cardiac innervation by the vagus nerve in whole-mount specimens of chick embryos stained with anti-neurofilament protein antibody (Kuratani and Tanaka 1990) indicated that the final configuration of the vagus nerve is established at stage 34. The vagal branches can be classified into two categories, i.e., the branches which are primarily related to the pharyngeal arch system, and the intestinal arborization derivatives which are associated primarily with the primitive gut. The branchial portion of the vagus nerve consists of the superior cardiac branch innervating the truncus arteriosus of the heart. The intestinal portion of the vagus nerve consists of the sinoatrial branch, pulmonary branches as well as the recurrent nerve and the other intestinal branches (Kuratani and Tanaka 1990). The autonomic nervous system can be detected by a monoclonal antibody HNK-1. The distribution and characterization of the HNK-1 antigen has been studied in the developing avian heart (Luiders et al. 1993). HNK-1 expression was particularly observed in morphologically dynamic regions such as the outflow tract cushions and the developing valves, the developing conduction system and the autonomic nervous system of the heart.

Recently a chick embryo model was developed in which cardiac anomalies were induced with all-trans retinoic acid (Broekhuizen et al. 1992, 1995). The heart malformations showed a spectrum of increasing rightward shift of the aorta. The category with a rightward positioned aorta and no ventricular septal defect was classified as having no septation abnormalities. In the presence of a ventricular septal defect, combined with the rightward positioned aorta, the anomaly was diagnosed as double outlet right ventricle. Furthermore, hemodynamic changes were encountered in the retinoic acid treated embryos (Broekhuizen et al. 1995). The observed changes suggest a decrease in cardiac contraction force regardless the presence of a ventricular septal defect. It was thus proposed that the altered hemodynamics in all-trans retinoic acid treated embryos, were predominantly due to myocardial dysfunction and to a lesser extent to abnormal intracardiac morphology. We hypothesize that retinoic acid may affect the myocardium through impaired parasympathetic innervation. The latter is a result of disturbed neural crest cell migration.

The objective of the present study was to establish whether a difference in innervation patterns exists between hearts of control, sham-operated and retinoic acid treated embryos. Stage 34 was selected for two reasons, 1) because of the marked altered hemodynamics encountered in a previous study (Broekhuizen et al. 1995), and 2) because the vagal nerve should have reached its final arborization pattern (Kuratani and Tanaka 1990). The hearts were studied with immunohistochemical markers that are considered to be markers for neuronal differentiation.

Materials and Methods

Fertilized white Leghorn chick eggs were incubated (blunt end up) at 38°C and staged according to Hamburger and Hamilton (1951). The material was subdivided into three groups, embryos treated with a solution of all-trans retinoic acid and dimethylsulphoxide (n=11), embryos treated with only the solvent dimethylsulphoxide (sham-operated embryos, n=8) and control embryos (n=8).

At stage 15 (day 2½ of a 21 day incubation period) each embryo, with exception of the controls, was exposed by creating a window both in the shell and in the overlying membranes. Either a solution containing 1.0 µg all-trans retinoic acid or only the solvent 2% dimethylsulphoxide was deposited on the vitelline membrane of the embryo using a Hamilton syringe (Broekhuizen et al. 1992). Subsequently, the window was sealed with tape and the egg reincubated.

Hemodynamics

Physiological measurements were performed at stage 34 (day 8 of incubation). The egg was removed from the incubator and positioned on the stage of a stereo-dissecting microscope. The embryo was exposed by removing the tape of the all-trans retinoic acid treated and sham-operated embryos or by making a window in the shell and the overlying membranes of the controls. Only live embryos with the right side up and without any sign of bleeding were included in the final analysis. We measured simultaneously blood pressure in the vitelline artery and flow velocity in the dorsal aorta. Temperature of the embryo during the measurement was regulated by a thermoelement and was maintained at 37°C (Broekhuizen et al. 1995). Blood pressure was measured in the left vitelline artery with a servo-null system (model 900A, World Precision Instruments, Inc., Sarasota, Florida) and a 10 µm glass micropipette. Mean dorsal aortic blood flow velocities were measured with a 20 MHz directional pulsed Doppler velocity meter (model 545C-4, Bioengineering, University of Iowa). The Doppler probe consisting of a 750 µm piezoelectric crystal was positioned at a 45° angle to the dorsal aorta at the level of the sinus venosus as described earlier (Broekhuizen et al. 1993, 1995).

Peak-systolic, end-diastolic and mean blood pressures were determined. Vitelline artery dP/dt (mmHg/s) was derived from the analog pressure signal by digital differentiation. Mean dorsal aortic blood flow (mm^3/s) was calculated as the product of the mean velocity and the area of the dorsal aorta (Broekhuizen 1993, 1995). By measuring the cycle length between pulse waves and converting this into beats per minute (bpm), the heart rate was calculated. The peak acceleration dV/dt (mm/s^2) was derived from the dorsal aortic velocity $V(t)$ by means of digital differentiation. Stroke volume (mm^3) was determined from the quotient of mean dorsal aortic blood flow and heart rate multiplied by 60.

Following the hemodynamic measurements hearts of the embryos were removed and subjected to whole-mount staining with anti-HNK-1-antibody. To determine the presence of a cardiac anomaly, these hearts were serially sectioned for morphologic evaluation.

Immunohistochemistry on whole hearts

At stage 34 (day 8 of incubation) embryos were removed from the eggs. The hearts were perfusion fixed with phosphate buffered 4% paraformaldehyde for 10 min. After 24 h immersion fixation in the same fixative, the hearts were processed for whole-mount staining with anti-HNK-1-antibody.

The hearts were first dehydrated in alcohol 70% through 100% and treated with a solution of 3% hydrogen peroxide (H_2O_2) in 100% methanol to block endogenous peroxidase activity. The next day the hearts were rehydrated and rinsed with phosphate-buffered saline (PBS). After washing in PBS containing 0.05% Tween-20 (PBST) the hearts were incubated with the primary antibody diluted 1/10 in PBST containing 1% Ovalbumine (PBST-OVA) overnight. The primary antibody was directed against the HNK-1 epitope (American type tissue connection, Abo and Balch 1981). The specimen were washed in PBS and in PBST for several hours, and incubated with the secondary antibody, peroxidase-labeled rabbit anti-mouse (Dako P260) diluted 1/200 in PBST-OVA overnight. After washing in PBS and Tris-maleate buffer the hearts were preincubated in diaminobenzidine (DAB). After thorough washing, the hearts were developed with DAB- H_2O_2 , rinsed with PBS and stored in alcohol 70%. The hearts were examined under a dissecting microscope. In particular, the arterial trunk and the base of the heart with the distribution of nerve branches were studied.

Morphology of whole-mount stained hearts

To determine the morphology of the whole-mount stained hearts, with emphasis on the presence or absence of a ventricular septal defect, stained hearts were embedded in paraffin, and sectioned serially. The 5 μm thick sections were counterstained with Mayer's hematoxylin/eosin (Broekhuizen et al. 1992). However, this material was not suitable to study the detailed nerve patterning in deeper layers, due to poor penetration of antibodies. Therefore, a separate set of hearts was devised for direct HNK-1 staining on serial sections.

Immunohistochemistry on serial sections

To explore in depth the parasympathetic distribution in the heart, a separate set of hearts of retinoic acid treated embryos, sham-operated and control embryos, was selected for serial sectioning and staining of the slides with anti-HNK-1-antibody. Embryos were fixed in ethanol-acetic acid for 24-72 h and embedded in paraffin. Serial sections of 5- μm were incubated in 1% H_2O_2 / methanol to inhibit endogenous peroxides. Both incubation with the HNK-1-antibody (undiluted) and the secondary rabbit-anti-mouse immunoglobulin conjugated with peroxidase, 100 times diluted, were performed for 1 hr at room temperature. The tissue sections were stained with DAB- H_2O_2 , rinsed with PBST for 5 min at room temperature and briefly counterstained with Mayer's hematoxylin.

Results

Hemodynamics

Control and sham-operated embryos showed similar hemodynamics. Retinoic acid treated embryos displayed a decrease of all parameters derived from the flow velocity wave form recording (Table 1). Figure 1 (*a-d*) depicts heart rate (bpm), stroke volume (mm^3), peak systolic velocity (mm/s), peak acceleration (mm/s^2). Pressure readings showed no significant difference between the three embryo groups (Table 2).

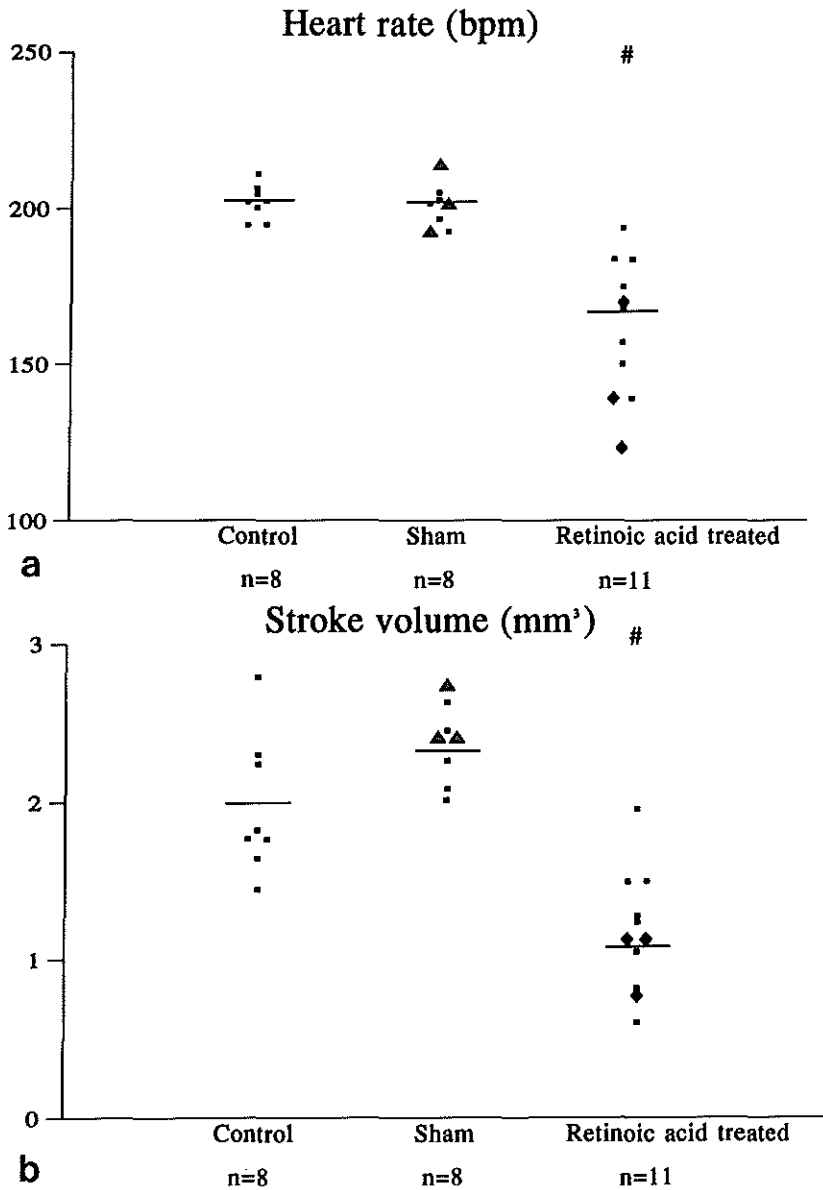


Figure 1. a-b. The characteristics of the frequency distribution of (a) heart rate and (b) stroke volume, of control and experimental stage 34 chick embryos. The Mann-Whitney test was used to determine significant differences between control and experimental values.

#, Significantly different from control and sham-operated embryos ($p < 0.01$).

diamond: hearts with double outlet right ventricle; triangle: hearts with muscular ventricular septal defect.

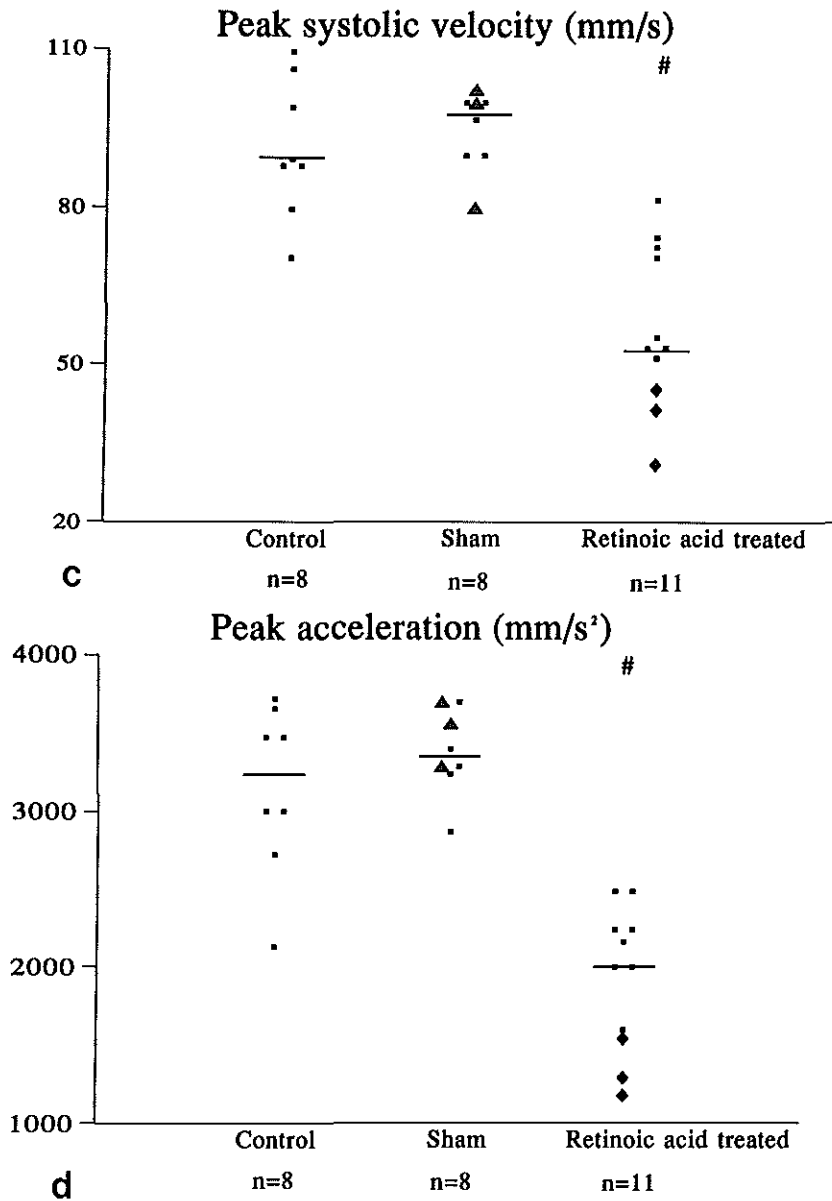


Figure 1. c-d. The characteristics of the frequency distribution of (c) peak systolic velocity and (d) peak acceleration, of control and experimental stage 34 chick embryos. The Mann-Whitney test was used to determine significant differences between control and experimental values.

#, Significantly different from control and sham-operated embryos ($p < 0.01$).

diamond: hearts with double outlet right ventricle; triangle: hearts with muscular ventricular septal defect.

Table 1. Characteristics of the frequency distribution of the dorsal aortic wave form parameters of control and experimental stage 34 chick embryos

	Control	Sham	Retinoic acid treated ($p < 0.01$)
Heart rate (bpm)			
Minimum	194.6	192.7	123.1
Median	202.7	202.0	168.0
Maximum	211.5	214.6	194.3
Peak systolic velocity (mm/s)			
Minimum	70.4	79.9	30.9
Median	88.7	98.5	53.2
Maximum	109.7	102.5	81.6
Mean velocity (mm/s)			
Minimum	17.2	23.5	7.3
Median	21.7	27.7	13.7
Maximum	32.1	30.6	17.4
Peak systolic blood flow (mm ³ /s)			
Minimum	19.9	22.5	7.3
Median	25.1	27.8	13.1
Maximum	31.0	34.0	23.0
Mean blood flow (mm ³ /s)			
Minimum	4.8	6.6	1.5
Median	6.1	8.0	3.2
Maximum	9.0	9.2	4.9
Stroke volume (mm ³)			
Minimum	1.4	2.0	0.6
Median	1.9	2.4	1.1
Maximum	2.8	2.8	1.9
Peak acceleration (mm/s ²)			
Minimum	2126	2868	1175
Median	3238	3343	1998
Maximum	3722	3722	2486

Table 2. Characteristics of the frequency distribution of the vitelline arterial pressure parameters of control and experimental stage 34 chick embryos, $p > 0.01$.

	Control	Sham	Retinoic acid treated
Peak systolic pressure (mmHg)			
Minimum	1.1	1.5	1.4
Median	2.1	1.9	2.8
Maximum	3.6	4.1	4.6
End-diastolic pressure (mmHg)			
Minimum	0.2	0.1	0.2
Median	0.5	0.6	0.8
Maximum	0.7	2.0	1.2
Mean pressure (mmHg)			
Minimum	0.6	0.9	0.7
Median	1.1	1.0	1.8
Maximum	2.0	3.1	2.1
dP/dt max (mmHg/s)			
Minimum	18.6	21.3	15.9
Median	26.0	34.2	27.5
Maximum	76.4	49.7	72.2

Morphology of whole-mount stained hearts

A study of sections showed no septation defects of the heart in 8 out of 11 embryos, treated with all-trans retinoic acid. The remaining 3 hearts showed a double outlet right ventricle. All hearts of the controls ($n=8$) and 5 hearts of sham-operated embryos were normal which included also the arterial trunk. Three hearts of the sham-operated embryos displayed a muscular ventricular septal defect in combination with a normal arterial trunk.

The outcome of the morphologic evaluation of the whole-mount stained hearts is also indicated in Figure 1 (*a-d*).

Immunohistochemistry on whole hearts.

Examining hearts of control and sham-operated embryos, whole-mount stained for HNK-1 revealed a comparable staining pattern. The parasympathetic branches of the vagus nerve, descend ventrally along the left side of the pulmonary trunk to the base of the heart. The nerve branches cross the atrioventricular sulcus and spread over the shoulders of the ventricles towards the ventral face of the heart (Figure 2a). The dorsal view displays two ganglia from which cardiac branches arise and communicate, thus forming a nerve plexus that innervates the dorsal (posterior) surface of the ventricles (Figure 2b).

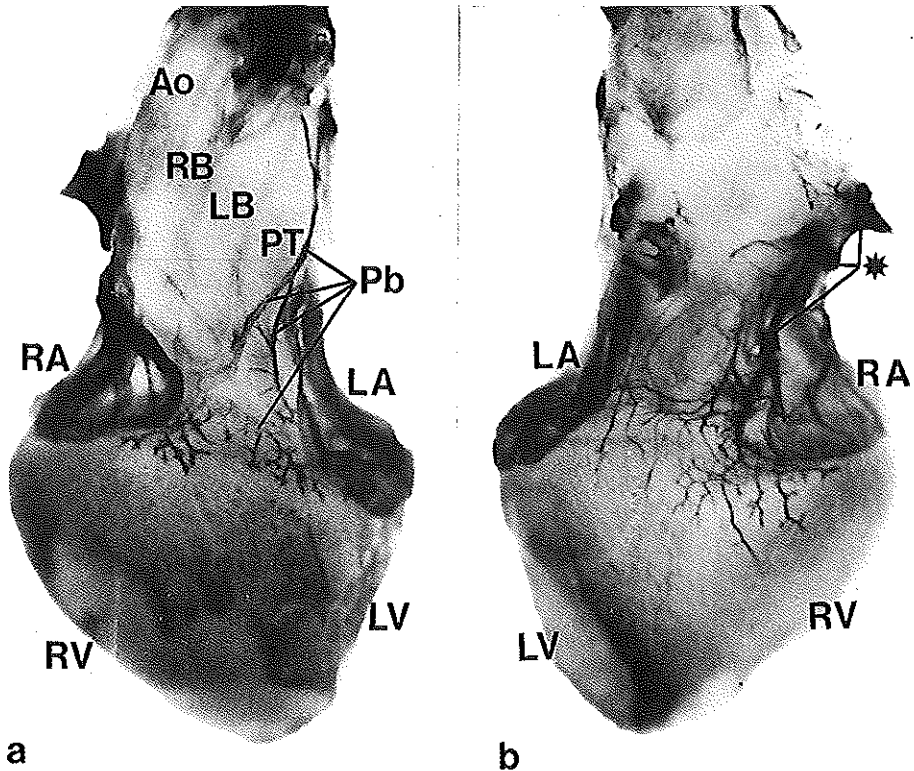


Figure 2. a-b. Whole-mount staining with anti-HNK-1-antibody.

a. Anterior view of a normal heart (stage 34).

The parasympathetic branches of the vagus nerve (Pb), descend ventrally along the left side of the pulmonary trunk (PT). The nerve branches cover the shoulders of the ventricles (arrowhead), close to the atrioventricular sulcus. (RA/LA: right/left atrium; RV/LV: right/left ventricle; Ao: Aorta)

b. Dorsal view of same heart as 1a. Two ganglia (*) can be distinguished from which cardiac branches arise that communicate.

(RA/LA: right/left atrium; RV/LV: right/left ventricle)

Hearts of all-trans retinoic acid treated embryos showed an abnormal branching. Ventrally, the parasympathetic branch over the pulmonary trunk was very thin and inconspicuous. The number of branches over the ventricles was reduced. Moreover, the complexity of the network was less intricate compared to normal hearts (Figure 2c). The reduction of branches was also seen dorsally (Figure 2d). This impaired parasympathetic distribution was seen in all embryos treated with all-trans retinoic acid regardless the presence of intracardiac malformations.

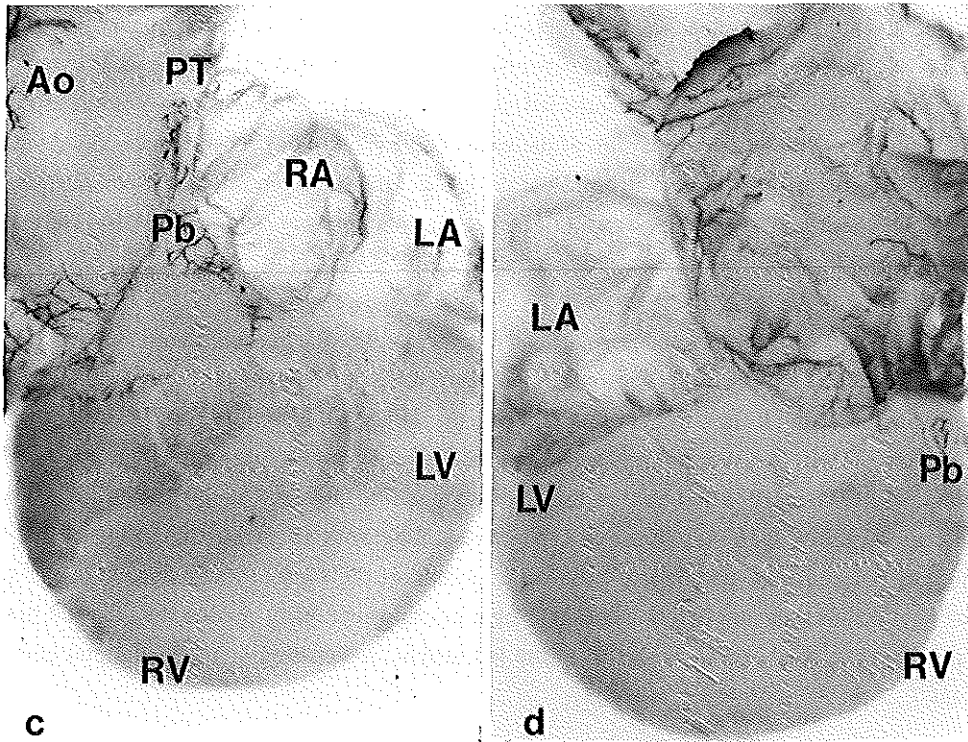


Figure 2. c-d. Whole-mount staining with anti-HNK-1-antibody.

c. Anterior view of an abnormal heart of a stage 34 embryo after treatment with all-trans retinoic acid. The aorta and brachiocephalic arteries are displaced to the right. This heart was diagnosed as double outlet right ventricle. The parasympathetic branch (Pb) over the pulmonary trunk (PT) is very thin and incomplete. The distribution over the ventricles is inconspicuous.

(RA/LA: right/left atrium; RV/LV: right/left ventricle; Ao: Aorta)

d. Dorsal view of same heart as 1c. The thin branches (Pb) reduced in number are also observed dorsally. (RA/LA: right/left atrium; RV/LV: right/left ventricle)

Immunohistochemistry on serial sections.

HNK-1 immunoreactivity was observed in many regions of the heart, including endocardium, epicardium and valve tissue. In this study the neuronal distribution is described in the heart of a control and a sham-operated embryo and in two retinoic acid treated embryos. Control and sham-operated embryos showed comparable HNK-1 positive neuronal cells and branches, particularly in the subepicardial mesenchyme and the atrioventricular sulcus. Other branches penetrate the myocardium and accompany the coronary arteries. Two large branches (dorsal and ventral) and one smaller branch (left lateral) originate from the branchial part of the vagus nerve and can be seen just above the level of the semilunar valves (Figure 3a). At the level of the aorto-pulmonary septum the branches fuse together and form a ventral network (Figure 4a). The network of branches covers only the upper portion of the ventricles (Figure 5a). At the level of the oesophagus two branches could be distinguished as the intestinal portion of the vagus nerve (Figure 6a). The branches divide at the level of the dorsal mesocardium. The branch at the level of the sinus venosus is characterized as the sinoatrial branch and innervates the dorsal wall of the right atrium and ventricle (Figure 6a). These data correlate with the whole-mount data presented earlier.

The hearts of the two retinoic acid treated embryos were diagnosed in both cases as double outlet right ventricle. These hearts showed similar distribution of HNK-1 positive neuronal cells. The staining pattern differed from hearts of control and sham-operated embryos. Just above the level of the semilunar valves two short branches could be distinguished which appear to be thin (Figure 3b). In contrast with control embryos, the branches do not fuse together at the level of the aorto-pulmonary septum (Figure 4b). There is a sparse ventral network as can be seen in Figure 5b. The number of branches that cover part of the upper portion of the ventricles is reduced. At the level of the oesophagus there are two branches, the right branch is distinctly smaller than the left branch (Figure 6b). The sinoatrial branch is shifted to the left atrium. A subaortic ventricular septal defect is present.

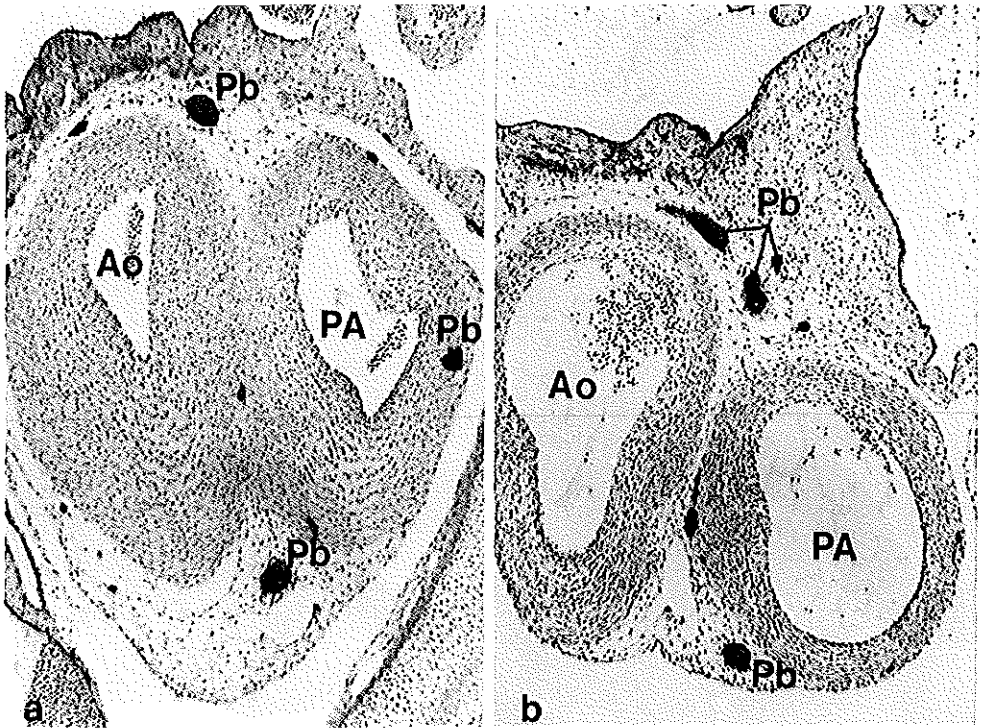


Figure 3. Serial sections of anti-HNK-1-antibody stained hearts. Cross section above level of semilunar valves of a normal heart (a) and a heart with double outlet right ventricle after retinoic acid treatment (b). Only two small parasympathetic branches (Pb) can be distinguished in this abnormal heart. (Ao: Aorta; Pulmonary artery PA)

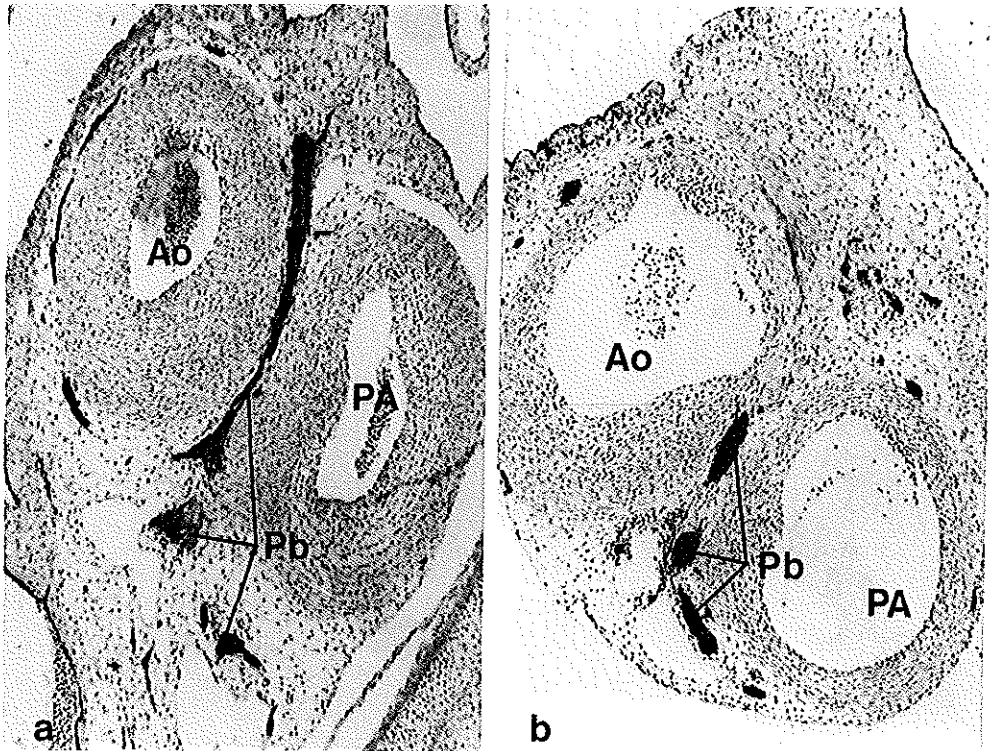


Figure 4. Serial sections of anti-HNK-1-antibody stained hearts. Cross section at the level of the aorto-pulmonary septum of a normal heart (a) and a heart with double outlet right ventricle after retinoic acid treatment (b). In this heart there is no connection between dorsal and ventral branches. The parasympathetic fibers are reduced compared to heart (a). (Ao: Aorta; Pulmonary artery PA)

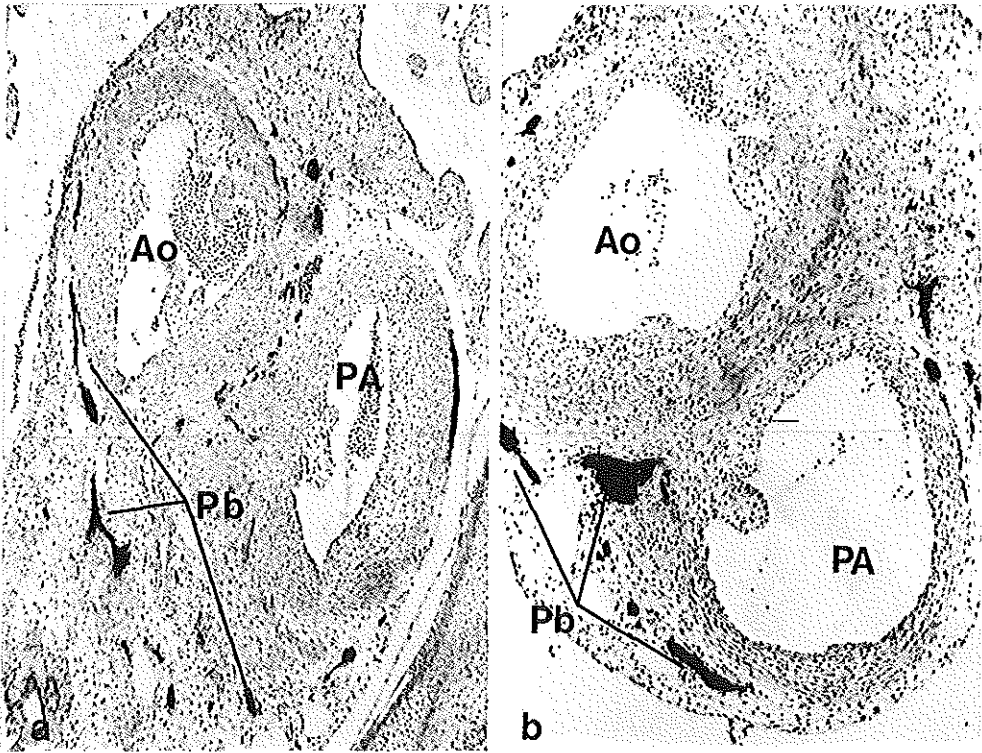


Figure 5. Serial sections of anti-HNK-1-antibody stained hearts. Cross section of upper part of ventricles in detail, of a normal heart (a) and a heart with double outlet right ventricle after retinoic acid treatment (b). (Ao: Aorta; Pulmonary artery PA)

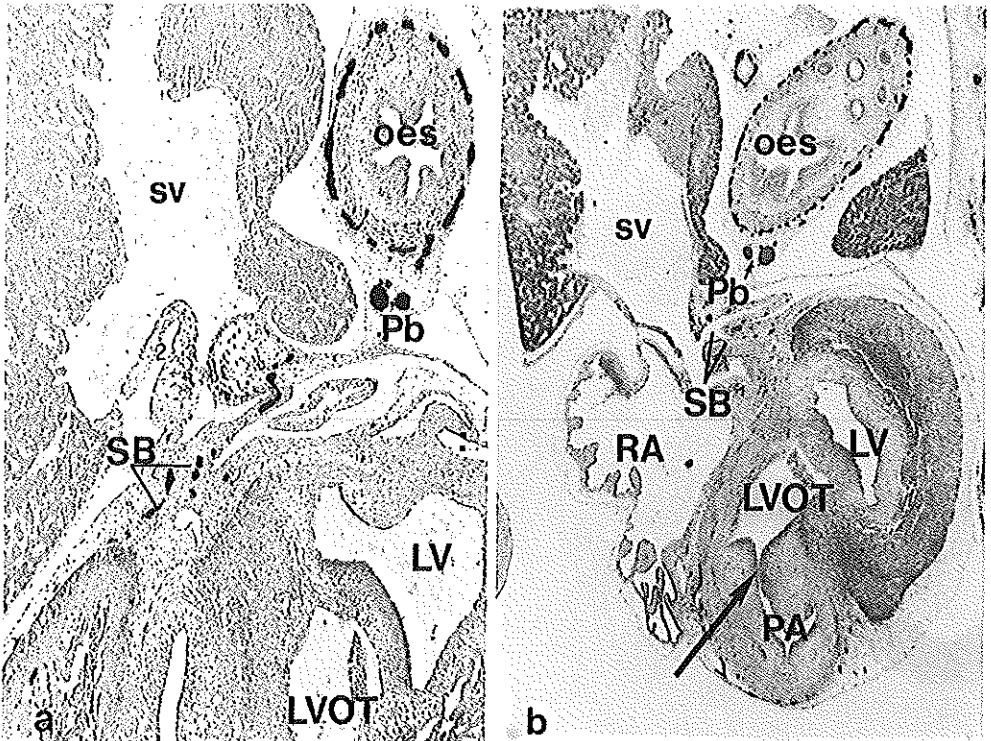


Figure 6. Serial sections of anti-HNK-1-antibody stained hearts. Cross section at the level of the sinus venosus of a normal heart (a) and heart with double outlet right ventricle after retinoic acid treatment (b). The subaortic ventricular septal defect is indicated by an arrow. At the level of the oesophagus (oes) there are two branches (Pb). The right is distinctly smaller than the left branch. The sinoatrial branch (SB) appears to be shifted to the left.

(Pulmonary artery PA; RA: right atrium; LV: Left ventricle; LVOT: Left ventricular outflow tract; SB: Sinoatrial branch; sv: sinus venosus; Pb: Parasympathetic branch)

Discussion

Cardiac development is an example of the intricate interrelationship of function and form. The mechanical forces that bring about the short-term shape change during the heart cycle and the long-term shape change during development are generated within the developing myocardium. Hemodynamic function during cardiac morphogenesis has been defined in the normal stage 20 (day 3) to stage 35 (day 9) chick embryo (Broekhuizen et al. 1993). There is a stage-related rise in heart rate, peak systolic velocity, mean velocity, and peak acceleration. The latter indirectly suggests an increase in cardiac contraction force with advancing embryonic development. To study the role of hemodynamics during abnormal cardiogenesis a chick embryo model was developed in which cardiac malformations as part of a continuous spectrum were induced with all-trans retinoic acid (Broekhuizen et al. 1992). Altered hemodynamics were encountered in stage 34 retinoic acid treated embryos regardless the presence of a ventricular septal defect (Broekhuizen et al. 1995). A decrease in cardiac contraction force was found in these embryos. We hypothesized that the hemodynamic changes could be due to myocardial dysfunction. It was proposed that retinoic acid may have an effect on the myocardium that could result from impaired parasympathetic innervation through a disturbance of neural crest cell migration.

The present study concerns immunohistochemistry of myocardial parasympathetic innervation accompanied by hemodynamic evaluation. A decrease in cardiac contraction force as expected on the basis of Doppler flow measurements was matched with the pattern seen in both a whole mount and serial section staining with anti-HNK-1-antibody, as an indication for neuronal branches and ganglionic cells. These are mainly derived from the neural crest.

The origin of the autonomic nervous system from the rhombencephalic neural crest (Narayanan and Narayanan 1980) showed the origin of the proximal ganglionic neurons and satellite cells in the glossopharyngeal and vagus nerves. Neural crest ablation studies have revealed that the parasympathetic innervation is mediated via the cardiac ganglia and can be identified in the outflow tract of the heart in stage 27 (day 5 of incubation) (Kirby et al. 1980; Kirby and Stewart 1983). Furthermore, the normal morphologic development of cardiac innervation by the vagus nerve (Kuratani and Tanaka 1990) showed two categories in which the vagal nerve can be subdivided. The branchial part consisting of the superior cardiac branch innervating the truncus arteriosus of the heart, was also seen in our study of whole-mount stained hearts of sham-operated and control embryos. Moreover, the intestinal portion of the vagus nerve was clearly seen in the separate set of stained serially sectioned hearts of sham-operated and control embryos. In particular, the sinoatrial branch innervating the dorsal wall of the right atrium and ventricle is of importance.

In our study, retinoic acid treated embryos showed an underdevelopment of cardiac branches by an abnormal staining pattern and a reduction of parasympathetic branches. Using a similar whole-mount nerve staining technique, Kuratani et al. (1991) have encountered alterations in the patterning of cardiac nerve branches after ablation of the cardiac neural crest. The nerve trunks of the glossopharyngeal and vagus nerves were poorly developed and often consisted of several thin bundles like our retinoic acid treated embryos. Furthermore, our embryos displayed a decrease of all parameters derived from the dorsal aortic flow velocity wave form recording as seen in a previous study (Broekhuizen et al. 1995).

Although the mechanism has yet to be resolved, the effect of all-trans retinoic acid on cardiac function may result from an abnormal parasympathetic innervation through a disturbance of the migration of cells from the neural crest. The effect on the neural crest may be through cytotoxicity (Jelínek and Kistler 1981). Alternatively it may result from alterations in region-specific signals necessary for homing and differentiation of neural crest cells (Hart et al. 1990). Impaired parasympathetic innervation could lead to an alteration of the tonus of the cardiac myocytes and generate myocardial dysfunction.

It has to be taken into account that parasympathetic innervation can be first identified in the outflow tract of the heart in stage 27 (Kirby et al. 1980; Kirby and Stewart 1983). Therefore, a stage 24 embryo is not innervated yet. Recent investigations have identified beat to beat variations of dorsal aortic and vascular impedance in the chick embryo before innervation is completed (Kempski et al. 1993). They speculate that this modulation is the manifestation of a preinnervated hemodynamic control mechanism. This control mechanism suggests a feed-back between ventricular function and vascular bed (Kempski 1995). Late in development, beyond stage 29 (day 6 of incubation), neural crest related autonomic control can be assessed through heart rate variability analysis. Hemodynamic regulation in the embryo seems therefore to shift from biomechanical to neuronal mediation at this stage of cardiovascular development. This regulation mechanism could be disrupted after treatment with all-trans retinoic acid.

Therefore, a biomechanical effect as a result of retinoic acid treatment on the embryonic heart that is not related with the neural crest must be considered. Preliminary data in the stage 24 (day 4 of incubation) chick embryo displayed malfunction of the embryonic heart complementary with structural changes of the myocardium (Broekhuizen, unpublished data). Heart rate was decreased in retinoic acid treated embryos at stage 24, without compensatory increase of stroke volume suggesting both pacemaker and contractile dysfunction (Broekhuizen, unpublished data).

Contraction of the myofibrils of the heart occurs through an interaction between the contractile proteins, i.e. actin and myosin, regulatory proteins, calcium ions, and chemical energy (Pelouch 1995). Cardiac looping is related to the development of myofibrils and myofibril structure (Manasek et al. 1986; Itasaki et al. 1991; Shiaishi et al. 1992). It is described that retinoic acid has multiple effects on growth and differentiation of cardiac myocytes, including an inhibition of cell proliferation, development of heart contractions, and delay in α -actin synthesis (Wiens et al. 1992). Pexieder et al. (1995) showed that all-trans retinoic acid can modify cardiac contractility. In rat fetuses treated during pregnancy with all-trans retinoic acid, a higher sensitivity toward extracellular calcium ion variations was found. This could indicate an increased permeability of the sarcolemma and/or delayed development of the sarcoplasmic reticulum (Pexieder et al. 1995). Furthermore, they reported that all-trans retinoic acid significantly decreased the total amount of protein in morphologically normal mouse hearts and hearts that showed double outlet right ventricle. In these morphologically normal and abnormal hearts, the concentration of sarcoplasmic proteins was significantly increased and that of contractile proteins decreased. An interaction of retinoic acid and contractile proteins could cause a disturbance in the myofibrillogenesis or myofibril arrangement and result in myocardial dysfunction accompanied by abnormal cardiac looping.

In conclusion a difference in innervation of hearts was found between control, sham-operated and retinoic acid treated embryos in stage 34. We put forward the hypothesis, that in the innervated embryo, cardiac dysfunction may be due to impaired parasympathetic development, through an indirect effect of retinoic acid on the neural crest cell migration. In the preinnervated embryo myocardial dysfunction could be the result of an indirect effect of retinoic acid on the hemodynamic regulation mechanism. Furthermore, a direct effect of retinoic acid on the cardiac myocytes could result in myocardial dysfunction accompanied by abnormal cardiac looping culminating in morphologically abnormal hearts. Further studies in combining biomechanical and morphological approaches are needed and will contribute to a better understanding of the genesis of embryonic cardiac defects.

6.3 References

- Abo T, Balch CM (1981) A differentiation antigen of human NK and K cells identified by a monoclonal antibody (HNK-1). *J Immunol* 127:1024-1029.
- Broekhuizen MLA, Wladimiroff JW, Tibboel D, Poelmann RE, Wenink ACG, Gittenberger-de Groot AC (1992) Induction of cardiac anomalies with all-trans retinoic acid in the chick embryo. *Cardiol Young* 2:311-317.
- Broekhuizen MLA, Mast F, Struijk PC, van der Bie W, Mulder PGH, Gittenberger-de Groot AC, Wladimiroff JW (1993) Hemodynamic parameters of stage 20 to stage 35 chick embryo. *Pediatr Res* 34:44-46.
- Broekhuizen MLA, Bouman GA, Mast F, Mulder PGH, Gittenberger-de Groot AC, Wladimiroff JW (1995) Hemodynamic changes in HH stage 34 chick embryos after treatment with all-trans retinoic acid. *Pediatr Res* 38:342-348.
- Clark EB, Hu N, Frommelt P, Vandekieft JL, Tomanek RJ (1989) Effect of increased ventricular pressure on heart growth in the chick embryo. *Am J Physiol* 257:H1-7.
- Clark EB, Hu N, Turner DR, Litter JE, Hansen J (1991) Effect of chronic verapamil treatment on ventricular function and growth in the chick embryo. *Am J Physiol* 261:H166-171.
- D'Amico-Martel A, Noden DM (1983) Contributions of placodal and neural crest cells to avian cranial peripheral ganglia. *Am J Anat* 166:445-468.
- Hamburger V, Hamilton HL (1951) A series of normal stages in the development of the chick embryo. *J Morph* 88:49-92.
- Hart RC, McCue PA, Ragland WL, Winn KJ, Unger ER (1990) Avian model for 13-cis retinoic acid embryopathy: demonstration of neural crest related defects. *Teratology* 41:463-472.
- Itasaki N, Nakamura A, Sumida H, Yasuda M (1991) Actin bundles on the right side in the caudal part of the heart tube play a role in dextro-looping in the embryonic chick heart. *Anat Embryol* 183:29-39.

Jelínek R, Kistler A (1981) Effect of retinoic acid upon the chick embryonic morphogenetic systems. The embryotoxicity range. *Teratology* 23:191-195.

Kempski MH, Kibler N, Blackburn JL, Dzakowic J, Hu N, Clark EB (1993) Hemodynamic regulation in the chick embryo. *Am Soc Mech Eng BED* 24:119-122.

Kempski MH (1995) Overview: Modeling and control of embryonic hemodynamics. In: Clark EB, Markwald RR, Takao A (eds) *Developmental Mechanisms of heart1 disease*. Futura publishing company, Inc, Armonk, New York, pp 421-434.

Kirby ML, Mckenzie JW, Weidman TA (1980) Developing innervation of the chick heart: a histofluorescence and light microscopic study. *Anat Rec* 196:333-340.

Kirby ML, Stewart D (1983) Neural crest origin of cardiac ganglion cells in the chick embryo: identification and extirpation. *Dev Biol* 97:433-443.

Kirby ML (1987) Cardiac Morphogenesis-recent reasearch advances. *Pediatr Res* 21:219-224.

Knaapen MWM, Vrolijk BCM, Wenink ACG (1996) Nuclear and cellular size of myocytes in the different segments of the developing rat heart. *Anat Rec* 244:118-125.

Kuratani S, Tanaka S (1990) Peripheral development of the avian vagus nerve with special reference to the morphological innervation of heart and lung. *Anat Embryol* 182:435-445.

Kuratani SC, Miyagawa-Tomita S, Kirby ML (1991) Development of cranial nerves in the chick embryo with special reference to the alterations of cardiac branches after ablation of the cardiac neural crest. *Anat Embryol* 183:501-51410.

Luider TM, Bravenboer N, Meijers C, van der Kamp AWM, Tibboel D (1993) The distribution and characterization of HNK-1 antigens in the developing heart. *Anat Embryol* 188:307-316.

Manasek FJ, Icardo J, Nakamura A, Sweeney (1986) *Cardiogenesis: Developmental Mechanisms and Embryology*. In: H.A. Fozzard et al. (eds) *The heart and cardiovascular system*. Raven Press, NY, pp 965-985.

Narayanan CH, Narayanan Y (1980) Neural crest and placodal contribution in the development of the glossopharyngeal-vagal complex in the chick. *Anat Rec* 196:71-82.

Pelouch V (1995) Molecular aspects of regulation of cardiac contraction. *Physiol Res* 44:53-60.

Pexieder T, Blanc O, Pelouch V, Ostádalová I, Milerová M, Ostádal B (1995) Late fetal development of retinoic acid induced transposition of great arteries: Morphology, physiology and biochemistry. In: Clark EB, Markwald RR, Takao A (eds) *Developmental Mechanisms of Heart Disease*. Futura Publishing Company, Armark, NY, pp 297-307.

Rakusan K (1984) Cardiac growth, maturation and aging. In: Zak R (ed) *Growth of the heart in health and disease*. Raven Press, New York, pp 131-164.

Shiraishi I, Takamatsu T, Minamikawa T, Fujita S (1992) 3-D observation of actin filaments during cardiac myofibrinogenesis in chick embryo using a confocal laser scanning microscope. *Anat Embryol* 185:401-408.

Sperelakis N, Pappano AJ (1983) Physiology and pharmacology of developing heart cells. *Pharm Ther* 22:1-39.

Wiens DJ, Mann TK, Feddersen DE, Rathmell WK, Franck BH (1992) Early heart development in the chick embryo: Effects of isotretinoin on cell proliferation, α -actin synthesis, and development of contractions. *Differentiation* 51:105-112.

CHAPTER 7

**HEMODYNAMIC EVALUATION
OF CHICK EMBRYOS
AFTER VENOUS CLIP**

7.1 Introductory remarks

In chapters 4 to 6, data were discussed of primary morphologic interference, the retinoic acid model, followed by hemodynamic evaluation. The role of blood flow on cardiac development could not be extracted from these data. In a previous study by Hogers et al. (1995), intracardiac flow patterns were studied. Laminar flow depends on the interaction between velocity, viscosity and tube diameter (Coulter and Pappenheimer 1949; Little 1989). A minimal velocity is necessary to start laminar flow (Coulter and Pappenheimer 1949; Jaffee 1966). The heart starts to beat at stage 9 (Fuji et al. 1981) and laminar flow can be observed from stage 12 onward. In the pumping heart blood flow remains laminar regardless irregularities in the inner wall such as trabeculae, endocardial cushions, and developing septa (Hogers et al. 1995). Their experiments showed that blood from specific yolk sac regions follow a specific stage-dependent intracardiac route. The development of the vitelline vessels is related to the intracardiac flow pattern. Moreover, they assumed that this change in intracardiac flow pattern is probably important for normal heart development. Interfering with the normal development of intracardiac flow by manipulating the venous inflow of the heart may result in abnormal heart morphogenesis. To fully understand the effect of blood flow on heart development the venous clip model was devised that changes blood flow without changing neural crest, cervical flexure, blood volume or oxygen content (Hogers et al. submitted). This chapter will discuss the interaction of hemodynamics and morphology after venous clip.

7.2 Altered hemodynamics in chick embryos after clipping the vitelline vein

*Monique L. A. Broekhuizen¹, Bianca Hogers², Marco C. DeRuiter², Robert E. Poelmann²,
Adriana C. Gittenberger-de Groot¹, Juriy W. Wladimiroff²*

From the Department of Obstetrics and Gynecology¹, Academic Hospital Dijkzigt, Erasmus University, Rotterdam; Department of Anatomy and Embryology², Leiden University
The Netherlands

Summary

To obtain insight into hemodynamics of abnormal cardiac development a chick model was recently developed in which a spectrum of double outlet right ventricle in combination with atrioventricular anomalies and/or pharyngeal arch artery malformations was induced through venous clip at stage 17 (70 hrs of incubation). In white Leghorn chick embryos, we simultaneously measured dorsal flow velocities with a 20 MHz pulsed Doppler velocity meter, and dorsal aortic (stage 24) and vitelline artery (stage 34) blood pressures with a servo-null system. These measurements were performed in control and venous clip embryos. After the wave form recordings were collected, all embryos were examined histologically. In addition immunohistochemistry was performed on selected specimen to evaluate parasympathetic innervation of the heart. At stage 24, venous clip embryos showed a dislocation of the outflow tract in 6/11 cases. At stage 34, 5/18 hearts were normal. A spectrum of double outlet right ventricle was encountered in 13/18 cases. The parasympathetic innervation of the heart was similar to controls. The hemodynamic data were correlated with the morphology. Statistical comparison was performed between control and experimental values. Peak acceleration was decreased at stage 24 after venous clip. At stage 34 heart rate was reduced. However, peak systolic and mean velocities, peak systolic and mean blood flows and stroke volume were increased after venous clip ($p < 0.01$). Pressure readings showed no statistically significant differences between control and experimental embryos. Our findings suggest that the hemodynamic changes seen in venous clip embryos reflect the presence of a compensatory mechanism.

Introduction

Embryonic blood flow is distributed between the embryonic and extraembryonic circulations in the chick embryo, and between the embryo and placenta in mammals. The distribution of blood flow through the embryonic heart has been of major interest to developmental biologists for many years (Rychter 1962; Yoshida et al. 1983). Although these studies describe experiments in which blood from the yolk sac circulation is visualized through the heart or pharyngeal arch arteries, none were performed by injection of dye into the smallest venules of particular yolk sac regions.

During normal development, stage-specific intracardiac blood flow patterns are described and the localization of these various currents is determined by the origin in the six yolk sac areas (Hogers et al. 1995). A consistent but continuously changing pattern of intracardiac blood flow during development, is related to growth of the yolk sac to meet the increasing demands of the developing embryo.

Hemodynamics is the complex of forces generated by the heart and the resulting motion of blood through the cardiovascular system. The relationship between form and function is a multifaceted process. Measurement of embryonic cardiovascular function in chick embryos has provided valuable information on this relationship in normal heart development (Hu and Clark 1989; Broekhuizen et al. 1993). Recently a hemodynamic study was performed in embryos with a spectrum of double outlet right ventricle induced by all-trans retinoic acid (Broekhuizen et al. 1995) that serves as a morphogen in physiological concentrations, but as a teratogen in higher amounts. This model demonstrates the effect of retinoic acid on cardiac function. However, the role of blood flow on cardiac formation could not be extracted from these data.

The long-term effect of blood flow on cardiovascularogenesis has been studied through mechanical manipulation of various arterial and heart segments resulting in a variety of cardiac outflow tract malformations (Rychter 1962; Colvee and Hurler 1983; Clark et al. 1984). Mechanical interference in the pharyngeal arch region could restrict the migration of e.g. cardiac neural crest cells which might lead to cardiac abnormalities as shown after neural crest ablation (Kirby and Waldo 1990; Leatherbury et al. 1993). It has to be kept in mind that manipulation in the head and neck region of the embryo could interfere with normal embryonic morphogenetic processes. To bypass intervention side effects at the arterial side of the heart, venous blood flow has been manipulated through trans-section (Rychter and Lemez 1965) or ligation (Orts Llorca et al. 1980). However, the survival rate of the embryos was very low and the survival time was rather short.

Recently an intervention model was designed to obtain insight into the hemodynamics of the long term effect of mechanical manipulation at the venous pole of the heart. Cardiac malformations were induced by permanent obstruction of the right lateral vitelline vein with a microclip, the venous clip model (Hogers et al. submitted).

The heart malformations displayed a spectrum of outflow tract anomalies varying from ventricular septal defect in combination with abnormal semilunar valves and/or pharyngeal arch artery malformations. In the presence of a rightward shift of the aorta in combination with a ventricular septal defect, this anomaly was diagnosed as double outlet right ventricle. The venous clip model will allow us to evaluate biologic aspects of the influence of blood flow on cardiac morphogenesis as well as the hemodynamic parameters involved.

The objective of the present study was to establish whether a difference in hemodynamics existed between embryos with a normally developing heart and embryos with a developing double outlet right ventricle after venous clip.

Materials and Methods

Fertilized White Leghorn chick eggs were incubated (blunt end up) at 38°C and staged according to Hamburger and Hamilton (1951). The material was subdivided into venous clipped embryos, and control embryos. All experiments were performed in ovo.

At stage 17 (70 hrs of a 21 day incubation) the egg shell was cleaned with ethanol 70%. Each embryo was exposed by creating a window in the shell followed by removal of the overlying membranes. The egg was kept warm in isolated foil. All manipulations were performed using a stereo-dissecting microscope. Above the chosen clip site the vitelline membrane was removed and a small incision was made with a tungsten needle in the yolk sac membrane, adjacent to the vitelline vein. Microclips have been devised from a nickel carrier grid, otherwise used for transmission electron microscopy. A microclip was used to clip the right lateral vitelline vein. Cessation of blood flow proximal to the microchip was confirmed. After venous clip the window was sealed with tape and the egg reincubated until stage 24 and stage 34 (day 4 and day 8 of incubation).

Physiological measurements were performed at stage 24 and stage 34 in controls (n=8; n=21), and venous clip embryos (n=11; n=18). An egg was removed from the incubator and positioned on the stage of a dissecting microscope. Each embryo was exposed either by removing the tape of the experimental embryos or making a window in the shell and removing the overlying membranes of the controls. Only live embryos with the right side up and without any sign of bleeding were included in the final analysis. Simultaneous measurement of blood pressures in the dorsal aorta at stage 24 and in the vitelline artery at stage 34, and flow velocities in the dorsal aorta was performed. Temperature of the embryo during the measurement was regulated by a thermoelement and was maintained at 37°C.

Blood pressure was measured, in the dorsal aorta at stage 24 and in the left vitelline artery at stage 34, with a servo-null system (model 900A, World Precision Instruments, Inc., Sarasota, Florida) and a 10 µm glass micropipette.

Due to development of the embryonic thoracic wall the vitelline artery was chosen to obtain pressure measurements at stage 34. Zero trans-tip pressure was obtained by immersing the tip of the micropipette in the extraembryonic fluid at the level of the measured site (Broekhuizen et al. 1995).

Mean dorsal aortic blood flow velocities were measured with a 20 MHz directional pulsed Doppler velocity meter (model 545C-4 by Bioengineering, University of Iowa). The Doppler probe consisting of a 750 micron piezoelectric crystal was positioned at a 45° angle to the dorsal aorta at the level of the sinus venosus as described in earlier reports (Hu and Clark 1989; Broekhuizen et al. 1993, 1995). The internal diameter of the dorsal aorta was measured at the same level with a filar micrometer eyepiece which was calibrated against a 10 µm engraved glass standard. The vessel area was calculated from the equation $area = \pi d^2/4$ where d is the aortic diameter (mm).

Hemodynamic parameters

The analog wave forms were sampled at 300 Hz by a Lab Master data acquisition analog-digital board (Axon Instruments Inc., Burlingame, CA) linked to a Compaq Prolinea 4/66 computer. The converter offered 12 bits at an input range of -10 to 10 Volt. Data were stored in a 5¼-inch 90 megabyte Bernoulli disk cartridge (Iomega Corp., Roy, UT).

Peak-systolic, end-diastolic and mean blood pressures were determined. Dorsal aortic and vitelline artery dP/dt (mm Hg/s), in stage 24 and stage 34 respectively, were derived from the analog pressure signal by digital differentiation.

Mean dorsal aortic blood flow velocity (mm^3/s) was calculated as the product of the mean velocity and the area of the dorsal aorta (Broekhuizen et al. 1993, 1995). By measuring the cycle length between pulse waves and converting this into beats per minute (bpm), the heart rate was calculated. The peak acceleration dV/dt (mm/s^2) was derived from the dorsal aortic velocity $V(t)$ by means of digital differentiation. Stroke volume (mm^3) was determined from the quotient of dorsal aortic blood flow and heart rate multiplied by 60. Cardiac work ($mm^3 \times mmHg$) is the product of stroke volume and mean arterial pressure. Vascular resistance ($mmHg/[mm^3/s]$) is the quotient of mean arterial pressure and mean dorsal aortic blood flow.

Morphological examination

After the wave form recordings were collected all 58 embryos were removed from the egg and were processed for histologic sectioning in a routine way by fixing in Bouin and embedding in paraffin. Thereafter, the embryos including the hearts were serially sectioned. The sections were 5 µm thick and stained with Mayer's hematoxylin/eosin.

Scanning electron microscopy

Selected specimen (n=10) were processed for scanning electron microscopy. Hearts were perfusion fixed in half strength Karnovsky's fixative (1965) for at least 1 hr and opened frontally with iridectomy scissors. They were rinsed in 0.1 M sodium-cacodylate buffer (pH 7.2) and postfixed for 2 hrs at 4°C in 1% OsO₄ in the same buffer, followed by dehydration in graded ethanol. The preparations were critical point dried over CO₂ by conventional methods, sputter-coated with gold for 3 min (Balzers MED 010) and studied in the scanning electron microscope (Philips SEM 525M) and photographed.

Immunohistochemistry

A third set of embryos (n=10) was evaluated for the development of the parasympathetic innervation of the heart using an anti-HNK-1 antibody staining technique. This immunohistochemical technique was performed on whole hearts which were serially sectioned afterwards. At stage 34, embryos were removed from the eggs. The hearts were perfusion fixed with phosphate buffered 4% paraformaldehyde. After 24 h fixation the hearts were processed for whole-mount staining with anti-HNK-1 antibody.

The hearts were first dehydrated in alcohol 70% through 100% and treated with a solution of 3% hydrogen peroxide (H₂O₂) in 100% methanol. The next day the hearts were rehydrated and rinsed with phosphate-buffered saline (PBS). After washing in PBS containing 0.05% Tween-20 (PBST) the hearts were incubated with the primary antibody diluted 1/10 in PBST containing 1% Ovalbumine (PBST-OVA) overnight. The primary antibody was directed against the HNK-1 epitope (American type tissue connection, Abo and Balch 1981). The specimen were washed in PBS and in PBST for several hours, and incubated with the secondary antibody, peroxidase-labeled rabbit anti-mouse (Dako P260) diluted 1/200 in PBST-OVA overnight. After washing in PBS and Tris-maleate buffer the hearts were preincubated in diaminobenzidine (DAB). After thorough washing, the hearts were developed with DAB-H₂O₂, and rinsed with PBS and stored in alcohol 70%. The hearts were examined under a dissecting microscope.

In particular, the arterial trunk and the base of the heart with the distribution of nerve branches were studied. To explore in depth the parasympathetic distribution in the heart and to obtain insight into the morphology of the whole-mount stained hearts, with emphasis on the presence or absence of a ventricular septal defect, stained hearts were embedded in paraffin, and sectioned serially. The 5 µm thick sections were counterstained with Mayer's hematoxylin.

Statistical Analysis

The hemodynamic data were correlated with the morphology. The distribution of hemodynamic parameters was non-Gaussian. Therefore, a non-parametric statistical analysis was carried out. The data are presented as characteristics of the frequency distribution of the hemodynamic parameters by medians and ranges (minimum, maximum). An exact trend test in a 3 x 2 cross-table was used for the dorsal aortic area because this parameter had only three ordered levels. Statistical comparison was done by the Kruskal-Wallis test whereas the Mann-Whitney test was used to determine significant differences between control and experimental values. The statistical significance level was defined as a p value of less than 1% ($p < 0.01$).

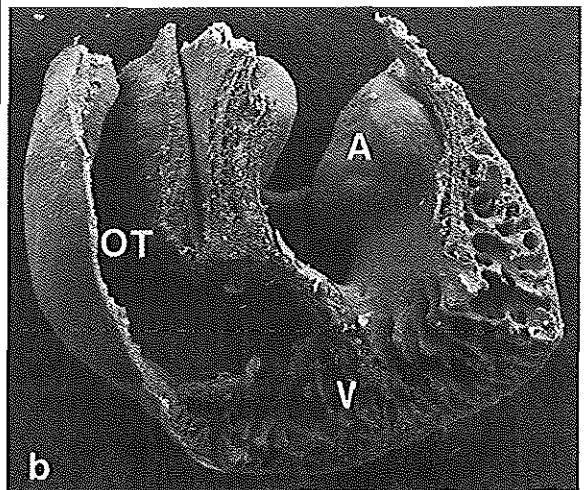
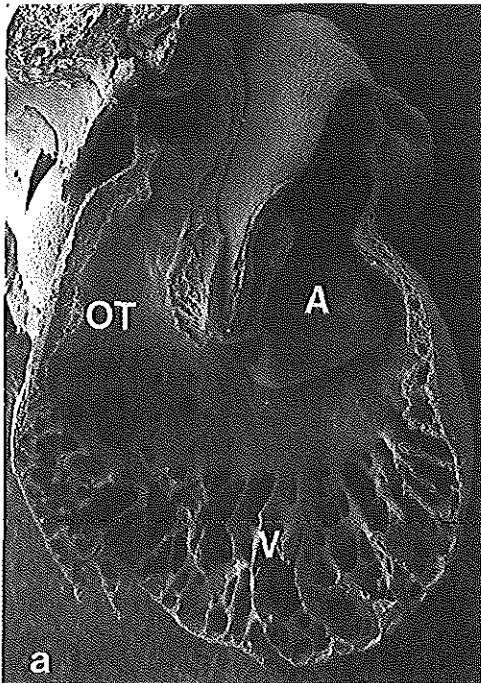
Results

Morphology

Stage 24

Outflow tract anomalies were observed macroscopically in 6 out of 11 venous clip embryos. The outflow tract appeared to be dislocated to the right. Histologic examination confirmed macroscopy. Figure 1 displays scanning electron micrographs of hearts of a stage 24 control (*a*) and venous clip embryo (*b*).

Figure 1. a. Scanning electron micrograph of a normal heart of a stage 24 control embryo. Right oblique frontal view. b. Scanning electron micrograph of an abnormal heart of a stage 24 embryo after venous clip. Right oblique frontal view heart. The outflow tract is dislocated to the right. (A: posterior atrioventricular cushion; V: ventricle; OT: outflow tract)



Stage 34

After histological analysis, 5 out of 18 embryos with a venous clip displayed normal hearts. In the remaining 13 cases, anomalies of the heart and pharyngeal arch arteries were encountered. A spectrum of outflow tract malformations was seen, ranging from ventricular septal defect (n=13), in combination with abnormal semilunar valves (6/13), and/or with pharyngeal arch artery malformations (7/13). In the presence of a rightward shift of the aorta in combination with a ventricular septal defect, this anomaly was diagnosed as double outlet right ventricle (6/13). Control embryos showed no abnormalities.

Figure 2 shows scanning electron micrographs of the heart of a stage 34 control embryo (*a*), and a venous clip embryo (*b*) that was diagnosed as double outlet right ventricle. The subaortic ventricular septal defect is indicated by an arrow.

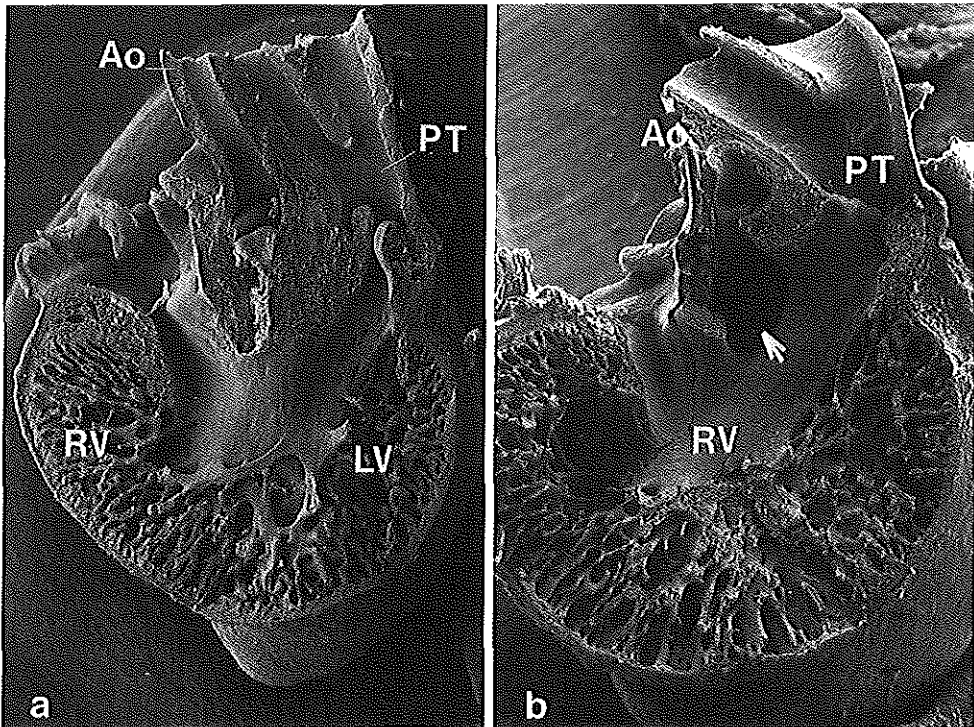


Figure 2. *a.* Scanning electron micrograph of a normal heart of a stage 34 control embryo. Right oblique frontal view. (Ao: aorta; PT: pulmonary trunk; RV: right ventricle; LV: left ventricle)
b. Scanning electron micrograph of an extreme form of double outlet right ventricle of a stage 34 embryo after venous clip. This is a right oblique frontal view of the right ventricle (RV) including the arterial pole. The ventricular septal defect is indicated by an arrow. (Ao: aorta; PT: pulmonary trunk)

Immunohistochemistry on whole hearts of stage 34 embryos

Examining hearts of control and venous clip embryos, whole-mount stained for HNK-1, revealed a comparable staining pattern. The parasympathetic branches of the vagus nerve, descend ventrally along the left side of the pulmonary trunk to the base of the heart. The nerve branches cross the atrioventricular sulcus and spread over the shoulders of the ventricles (Figure 3a,b). The dorsal view (Figure 3c,d) displays two ganglia from which cardiac branches arise and communicate, thus forming a nerve plexus that innervates the dorsal (posterior) surface of the ventricles.

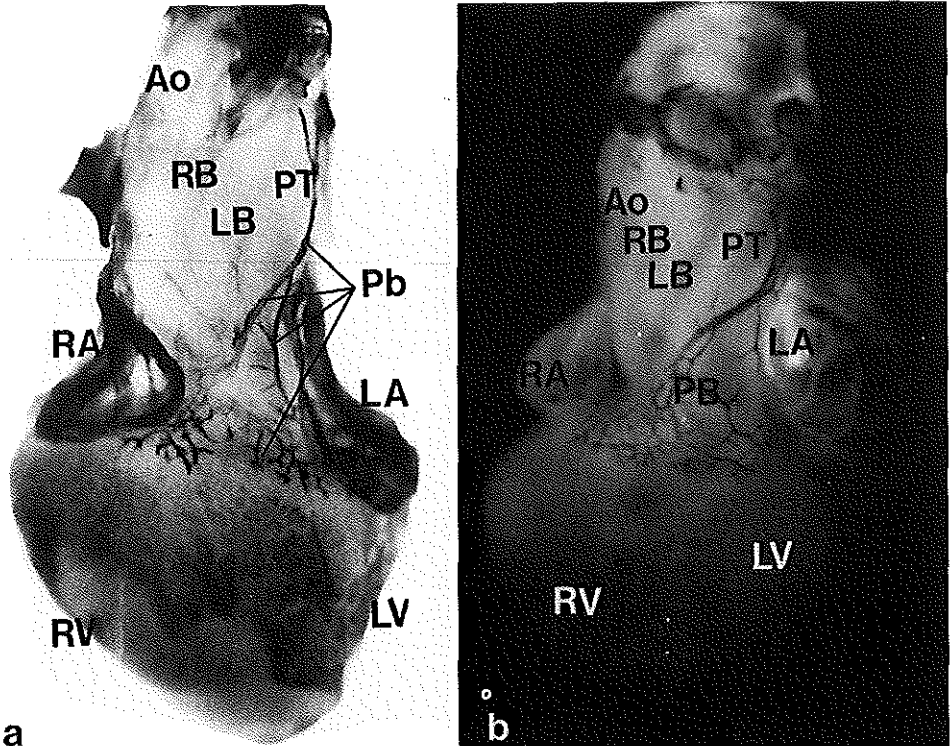


Figure 3. Whole-mount staining with anti-HNK-1-antibody.

Anterior view of a heart (stage 34) of a control (a) and venous clip embryo (b).

The parasympathetic branches of the vagus nerve (Pb), descend ventrally along the left side of the pulmonary trunk (PT). The nerve branches cover the shoulders of the ventricles, close to the atrioventricular sulcus.

(RA/LA: right/left atrium; RV/LV: right/left ventricle; Ao: Aorta; PT: Pulmonary trunk)

Serial sections of stage 34 whole-mount hearts

HNK-1 immunoreactivity was observed in many regions of the heart, including endocardium, epicardium and valve tissue. Control and venous clip embryos showed comparable HNK-1 positive neuronal cells and branches, particularly in the subepicardial mesenchyme and the atrioventricular sulcus. Other branches penetrate the myocardium or accompany the coronary arteries. These data correlate with the whole-mount data presented in this study.

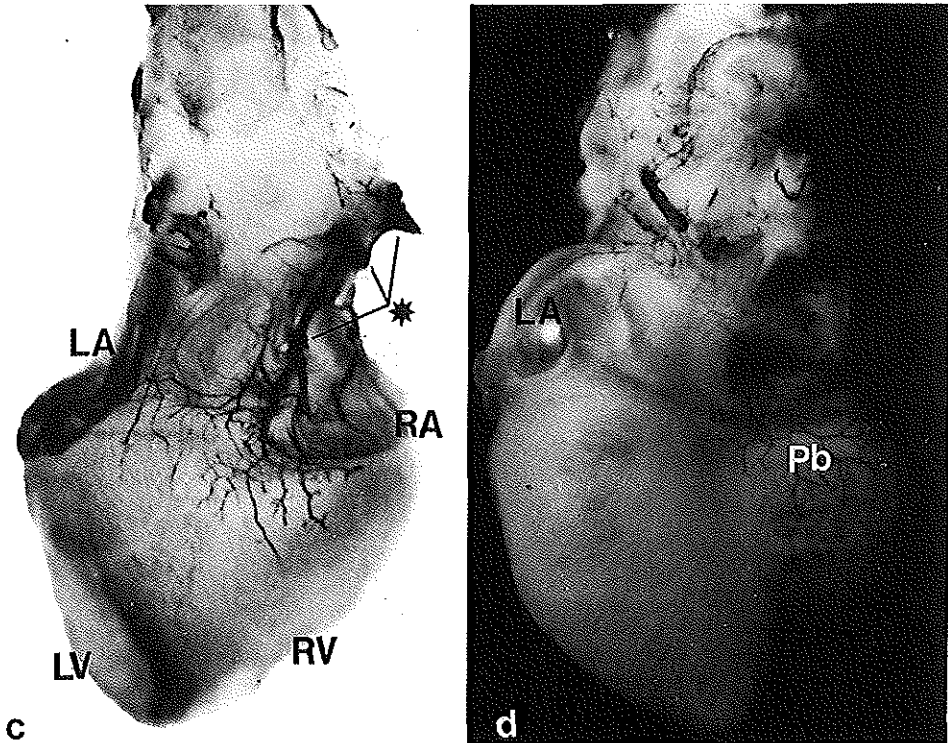


Figure 3. Whole-mount staining with anti-HNK-1-antibody.

Dorsal view of same heart as a,b. Control (c) and venous clip embryo (d). Two ganglia () can be distinguished from which cardiac branches arise that communicate.*

(RA/LA: right/left atrium; RV/LV: right/left ventricle; Ao: Aorta; PT: Pulmonary trunk; Pb: parasympathetic branches)

Hemodynamics

The characteristics of the frequency distribution of the dorsal aortic wave form parameters of stage 24 and stage 34 control embryos, and venous clip embryos are presented in Figure 4 a-g and Figure 5 a-b. Hemodynamics of control embryos were compared with venous clip embryos.

Stage 24

Heart rate was similar for controls and venous clip (Figure 4a). Moreover, no significant difference was found in peak systolic and mean velocities, peak systolic and mean blood flows and stroke volume after venous clip (Figure 4b-f). However, the peak acceleration was reduced in venous clip embryos (Figure 4g). Dorsal aortic diameter showed no significant difference in the two embryo groups (Table 1). Dorsal aortic pressures were similar in all control and both experimental groups (Table 2). The vascular resistance and cardiac work are shown in Figure 5 a,b. There were no significant changes after venous clip.

Stage 34

Heart rate was decreased after venous clip (Figure 4a). Peak systolic and mean velocities, peak and mean blood flows, stroke volume were increased following venous clip (Figure 4b-f). Peak acceleration was increased but was not statistically significant (Figure 4g).

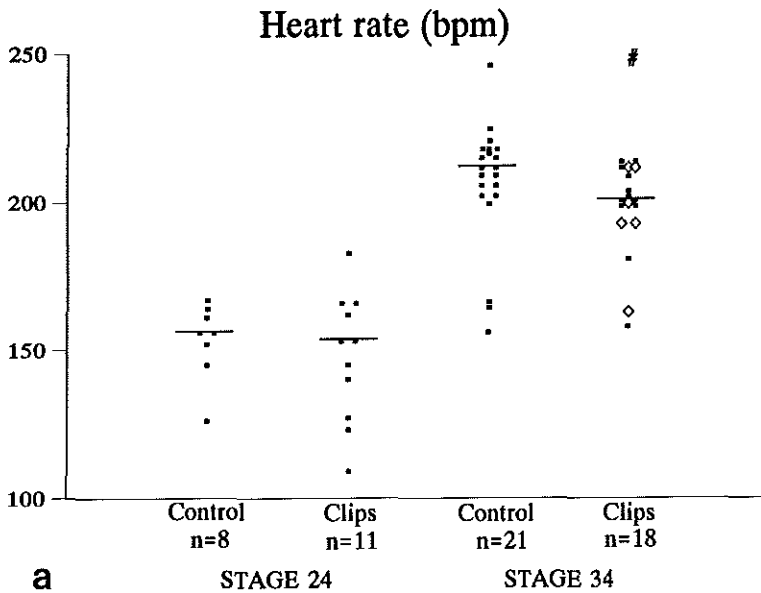


Figure 4. a. The characteristics of the frequency distribution of heart rate, of stage 24 and stage 34 control and venous clip embryos.

Significantly different from control embryos; ($p < 0.01$).

The diamond indicates the embryos with a double outlet right ventricle.

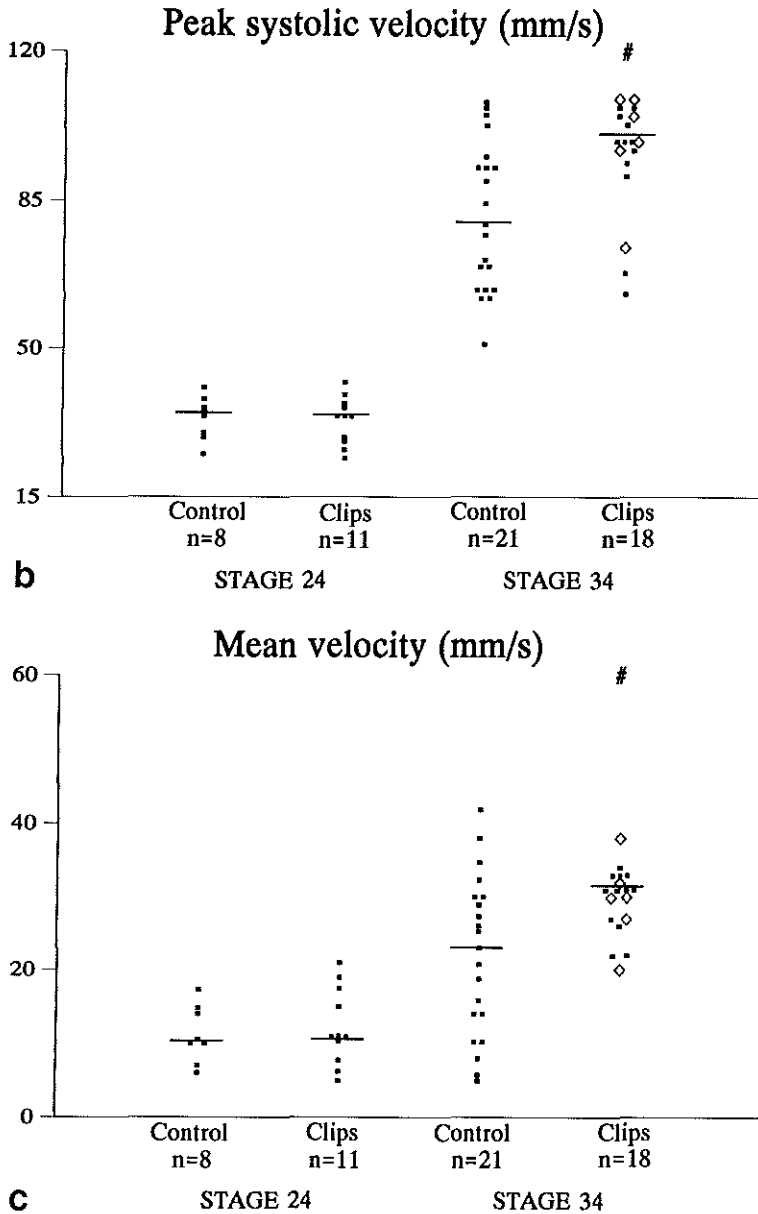


Figure 4. b-c. The characteristics of the frequency distribution of (b) peak systolic velocity and (c) mean velocity, of stage 24 and stage 34 control and venous clip embryos.

Significantly different from control embryos; ($p < 0.01$).

The diamond indicates the embryos with a double outlet right ventricle.

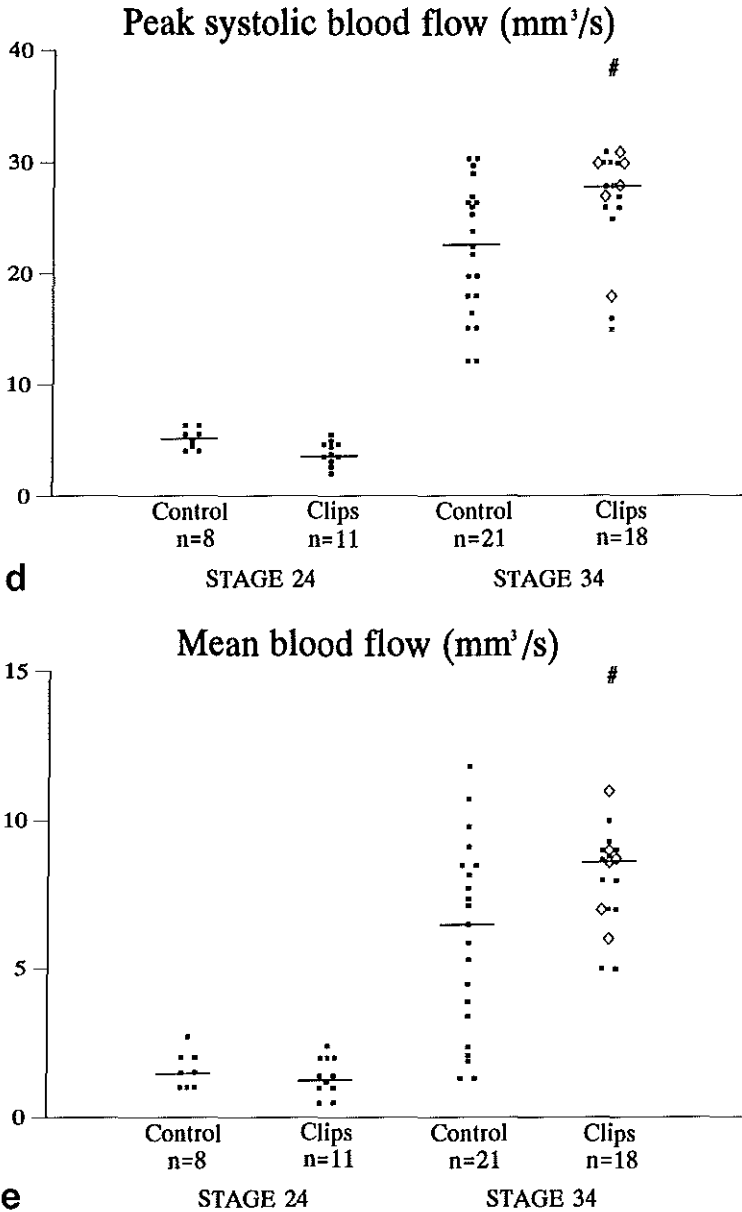


Figure 4. d-e. The characteristics of the frequency distribution of (d) peak systolic blood flow and (e) mean blood flow, of stage 24 and stage 34 control and venous clip embryos.

Significantly different from control embryos; ($p < 0.01$).

The diamond indicates the embryos with a double outlet right ventricle.

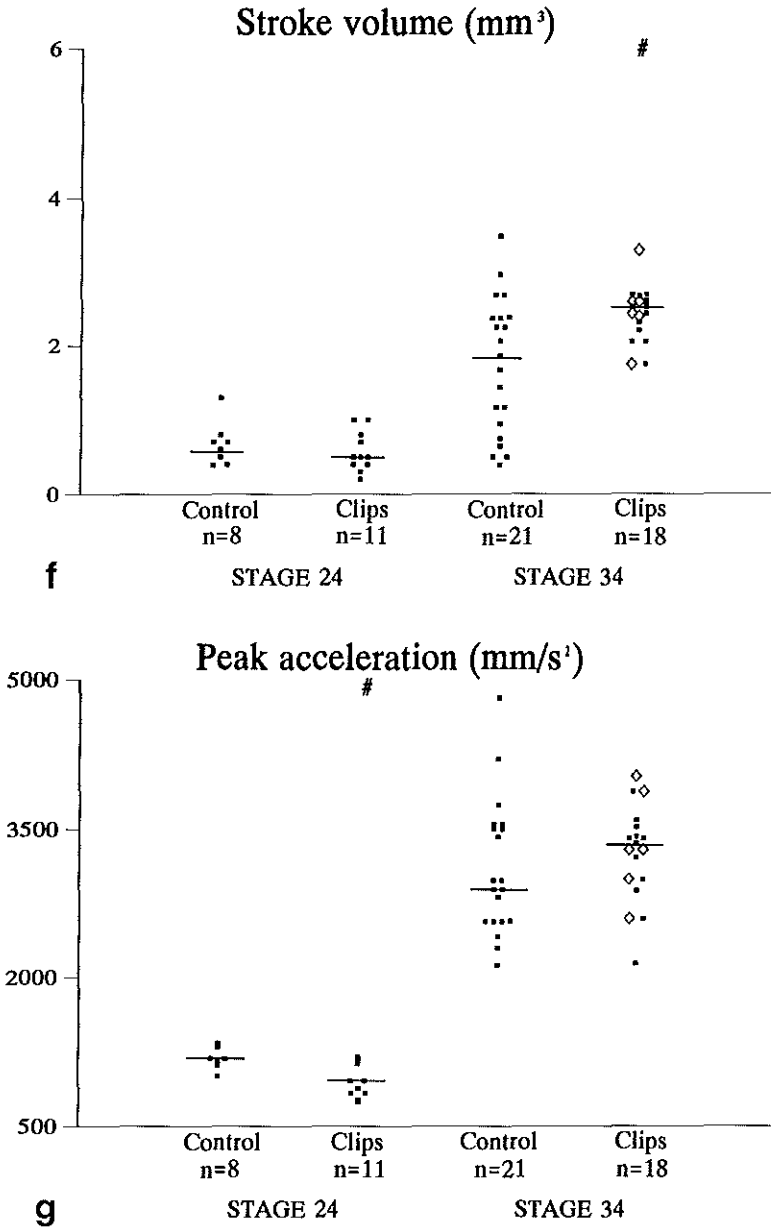


Figure 4. f-g. The characteristics of the frequency distribution of (f) stroke volume and (g) peak acceleration, of stage 24 and stage 34 control and venous clip embryos.

Significantly different from control embryos; ($p < 0.01$).

The diamond indicates the embryos with a double outlet right ventricle.

Chapter 7

Dorsal aortic diameter displayed no significant differences in the two embryo groups (Table 1). Vitelline artery pressures were not statistically different (Table 2).

Table 1. A Cross-table of dorsal aortic area by control and experimental stage 24 and stage 34 chick embryos, $p > 0.01$

Dorsal aortic area (mm ²)	stage 24		stage 34	
	Control (n=8)	Clips (n=11)	Control (n=21)	Clips (n=18)
0.09		3		
0.13	2	8		
0.16	6			
0.19			1	
0.23			4	4
0.28			16	14

Table 2. Characteristics of the frequency distribution of the dorsal aortic and vitelline arterial pressure parameters of control and experimental stage 24 and stage 34 chick embryos respectively, $p > 0.01$

	stage 24		stage 34	
	Control (n=8)	Clips (n=11)	Control (n=11)	Clips (n=8)
Peak systolic pressure (mmHg)				
Minimum	0.9	1.0	0.8	0.8
Median	1.4	1.3	2.9	2.7
Maximum	1.9	2.9	4.2	4.6
End-diastolic pressure (mmHg)				
Minimum	0.2	0.9	0.05	0.06
Median	0.5	0.5	0.6	0.7
Maximum	0.9	1.6	1.9	3.2
Mean pressure (mmHg)				
Minimum	0.5	0.5	0.3	0.5
Median	0.9	0.9	1.1	1.3
Maximum	1.2	2.2	2.9	2.2
dP/dt max (mmHg/s)				
Minimum	11.2	13.9	20.5	17.7
Median	17.7	19.0	33.8	29.6
Maximum	39.9	29.1	52.4	47.6

Vascular resistance was not altered after venous clip (Figure 5a). However, cardiac work was elevated in venous clip embryos (Figure 5b).

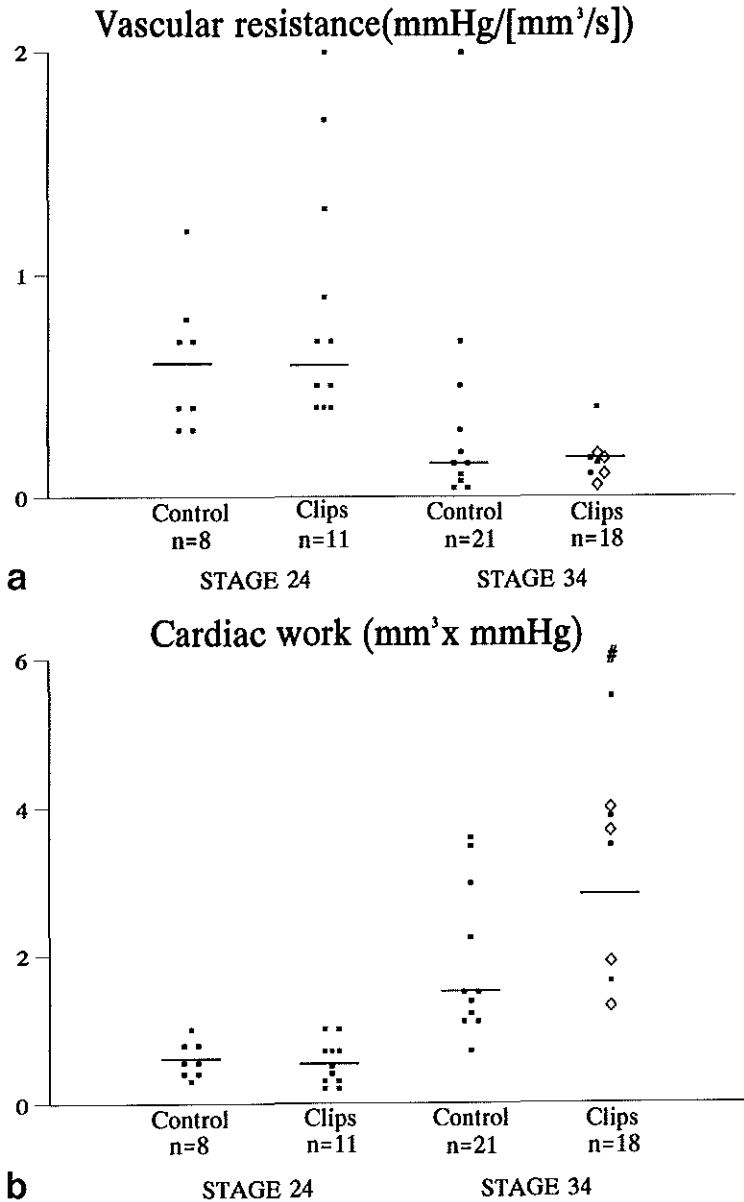


Figure 5. a-b. The characteristics of the frequency distribution of (a) vascular resistance and (b) cardiac work, of stage 24 and 34 control and venous clip embryos. # Significantly different from control embryos; ($p < 0.01$).

Discussion

Rerouting of blood occurs after venous clip (Hogers et al. submitted). They have demonstrated that changes in intracardiac blood flow patterns lead to cardiac malformations. In stage 24 as well as in stage 34 outflow tract anomalies were observed.

In the present study dorsal aortic flow velocity, dorsal aortic, and vitelline artery pressure wave forms were recorded in stage 24 and stage 34 respectively (day 4 and day 8 of incubation) control and venous clip embryos. Heart rate was altered at stage 34 after venous clip. Peak acceleration was decreased at stage 24 but displayed no change at stage 34. A significant increase in peak systolic and mean velocities, peak systolic and mean blood flows, and stroke volume was observed at stage 34 after venous clip. Dorsal aortic area, that was determined from the vessel diameter, was not altered in both embryonic stages. Furthermore, pressure readings were not essentially different between control and venous clip embryos. As the arterial pressure was not altered and stroke volume was increased in stage 34 venous clip embryos, the observed increase in cardiac work goes without saying. Vascular resistance displayed no significant changes after venous clip in both stages. There is a drop in vascular resistance from stage 24 to stage 34. This drop is due to an increase in the number of resistance vessels as the extra embryonic and embryonic bed expand (Hu and Clark 1989).

The hemodynamic changes seen in venous clip embryos reflect the presence of a compensatory mechanism. It appears that at stage 24, in spite of anatomic alterations due to venous clip, hemodynamic regulation compensates to maintain hemodynamic homeostasis. At stage 34 the compensatory mechanism is more evident. Cardiovascular function is controlled by variations in heart rate, preload, afterload and myocardial contractility (Clark 1990). In the chick embryo heart rate increases with development (Hu and Clark 1989; Broekhuizen et al. 1993) and may reflect the need to maintain coupling between preload, ventricular function and afterload (Zahka et al. 1989).

Acute changes in heart rate profoundly influence cardiac output. The chick embryo is susceptible to environmental temperature (Nakazawa et al. 1985). It is described that as heart rate slows with cooling, there is a decrease in cardiac output while stroke volume remains constant and vascular resistance increases. In our study, embryonic temperature was maintained at 37°C. Heart rate remained unchanged at stage 24 after venous clip. However, stage 34 venous clip embryos, displayed a decrease in heart rate which is associated with an increase in cardiac output and stroke volume. Stroke volume in the embryo is mainly determined by the length of the cardiac muscle fibers, and this effect is independent of innervation. The force of contraction of cardiac muscle is dependent upon its preloading and its afterloading. The length-tension relationship in cardiac muscle has been defined by Frank-Starling and the mechanism is functional in the chick embryo heart (Wagman et al. 1990).

Stroke volume is also dependent on the contractility of the myocardium. The ventricular myocyte is submitted to remarkable changes during morphogenesis of the heart (Forbes 1985). Intra and extracellular factors may regulate the pattern of contractile element development (Sugi and Lough 1992). Intracellular forces are generated by the contractile apparatus and organelles forming within myocyte and endocardial cells. The extracellular forces are generated by the extracellular matrix and the stress strain relationship of changing wall tension during the cardiac cycle (Taber et al. 1993).

In addition to the assessment of hemodynamic parameters in venous clip embryos, the autonomic nervous system of the heart was studied. The autonomic nervous system can be detected by a monoclonal antibody directed against the HNK-1 epitope. The anti-HNK-1 antibody staining of controls and venous clip embryos was comparable. The parasympathetic innervation was normal. Although cardiac anomalies induced by venous clip are remarkably similar to malformations after retinoic acid treatment (Broekhuizen et al. 1992), the parasympathetic innervation and hemodynamics differed. Anti-HNK-1-antibody staining of whole hearts and serial sections of retinoic acid treated embryos showed abnormal patterning of the parasympathetic innervation (Broekhuizen et al. 1996). Moreover, this was accompanied by altered hemodynamics suggesting myocardial dysfunction. In venous clip embryos the observed hemodynamic changes suggest no myocardial dysfunction but rather a compensatory mechanism.

Cardiac anomalies after venous clip also resemble anomalies after neural crest ablation (Nishibitake et al. 1987; Kirby 1993; Leatherbury et al. 1993; Gittenberger-de Groot et al. 1995). Using a similar whole mount nerve staining technique as anti-HNK-1 antibody, Kuratani et al. (1991) have encountered alterations in the patterning of cardiac nerve branches after ablation of the cardiac neural crest similar to the patterning seen after retinoic acid. In a hemodynamic study using microcinephotography, compensatory mechanisms have been encountered in chick embryos after neural crest ablation (Leatherbury et al. 1991) before cardiac malformations occur (Bockman et al. 1989; Leatherbury et al. 1993). Cardiac output was similar between control and neural crest ablated embryos. It appeared that the experimental embryos compensated for decreased contractility (decreased ejection fraction) by ventricular dilation (Leatherbury et al. 1991).

Although a similarity in cardiac malformations is seen between cardiac neural crest ablation, retinoic acid treated embryos and venous clip embryos, the hemodynamic profile of these various models is different. Defining new models of cardiovascular dysmorphogenesis may help us understand mechanisms which relate form and function during cardiovascular development and may aid in interpreting the underlying etiologies of congenital heart disease.

7.3 References

- Bockman DE, Redmond ME, Kirby ML (1989) Alteration of early vascular development after ablation of cranial neural crest. *Anat Rec* 225:209-217.
- Bouman HGA, Broekhuizen MLA, Baasten MJ, Gittenberger-de Groot AC, Wenink ACG (1995) Spectrum of looping disturbances in stage 34 chicken hearts after retinoic acid treatment. *Anat Rec* 243:101-108.
- Broekhuizen MLA, Mast F, Struijk PC, Van der Bie W, Mulder PGH, Gittenberger-de Groot AC, Wladimiroff JW (1993) Hemodynamic parameters of stage 20 to stage 35 chick embryo. *Pediatr Res* 34:44-46.
- Broekhuizen MLA, Bouman HGA, Mast F, Mulder PGH, Gittenberger-de Groot, Wladimiroff JW (1995) Hemodynamic changes in HH stage 34 chick embryos after treatment with all-trans retinoic acid. *Pediatr Res* 38:342-348.
- Clark EB, Hu N, Rosenquist GC (1984) Effect of conotruncal constriction on aortic-mitral valve continuity in the stage 18, 21 and 24 chick embryo. *Am J Cardiology* 53:324-327.
- Clark EB (1990) Hemodynamic control of the embryonic circulation. In: Clark EB, Takao A (eds) *Developmental Cardiology: Morphogenesis and Function* Mount Kisco, NY, Futura Publishing Co., Inc., pp 291-303.
- Colvee E, Hurler JM (1983) Malformations of semilunar valves produced in chick embryos by mechanical interference with cardiogenesis. *Anat Embryol* 168:59-71.
- Coulter NA, Pappenheimer JR (1949) Development of turbulence in flowing blood. *Am J Physiol* 159:401-408.
- Forbes MS (1985) T tubules and sarcoplasmic reticulum of mammalian heart. In: Ferrans VJ, Rosenquist GC, Weinstein C (eds). *Cardiac Morphogenesis* NY, Elsevier, pp 11-123.
- Fujii S, Hirota A, Kamino K (1981) Optical indication of pace-maker potential and rhythm generation in early chick heart. *J Physiol (Lond)* 312:253-263.

Gittenberger-de Groot AC, Bartelings MM, Oddens JR, Kirby ML, Poelmann RE (1995) Coronary artery development and neural crest. In: Clark EB, Markwald RR, Takao A (eds) *Developmental Mechanisms of Heart Disease*. Futura Publishing Company, Armark, NY, pp 291-296.

Hamburger V, Hamilton HL (1951) A series of normal stages in the development of the chick embryo. *J Morph* 88:49-92.

Hogers B, DeRuiter MC, Baasten AMJ, Gittenberger-de Groot, Poelmann RE (1995) Intracardiac blood flow patterns related to the yolk sac circulation of the chick embryo. *Circ Res* 76:871-877.

Hu N, Clark EB (1989) Hemodynamics of stage 12 to stage 29 chick embryo. *Circ Res* 65:1665-1670.

Hu N, Clark EB (1990) Effect of changes in circulating blood volume on cardiac output and arterial and ventricular blood pressure in the stage 18, 24 and 29 chick embryo. *Circ Res* 67:187-192.

Jaffee OC (1966) Hemodynamic analysis of experimentally produced cardiac malformations. *Anat Rec* 154:509. Abstract.

Karnovsky MJ (1965) A formaldehyde-glutaraldehyde fixative of high osmolarity for use in electron microscopy. *J Cell Biol* 27:137A.

Kirby ML, Waldo KL (1990) Role of neural crest in congenital heart disease. *Circulation* 82:332-340.

Kirby ML (1993) Cellular and molecular contributions of the cardiac neural crest to cardiovascular development. *Trends Cardiovasc Med* 3:18-23.

Kirby ML, Waldo KL (1995) Neural crest and cardiovascular patterning. *Circ Res* 77:211-215.

Leatherbury L, Connuck DM, Gauldin HE, Kirby ML (1991) Hemodynamic changes and compensatory mechanisms during early cardiogenesis after neural crest ablation in chick embryos. *Pediatr Res* 30:509-512.

Leatherbury L, Connuck DM, Kirby ML (1993) Neural crest ablation versus sham surgical effects in a chick embryo model of defective cardiovascular development. *Pediatr Res* 33:628-631.

Leatherbury L, Waldo K (1995) Visual understanding of cardiac development: the neural crest's contribution. *Cell Mol Biol Res* 41:279-291.

Little RC, Little WC (1989) Hemodynamics. In: Physiology of the heart and circulation. Chicago, III: Year Book Medical Publishers, Inc, pp 219-234.

Männer J, Seidl W, Steding G (1993) Correlation between the embryonic head flexures and cardiac development. An experimental study in chick embryos. *Anat Embryol* 188:269-285.

Nakazawa M, Clark EB, Hu N, Wispe J (1985) Effect of environmental hypothermia on vitelline artery blood pressure and vascular resistance in the stage 18, 21, and 24 chick embryo. *Pediatr Res* 19:651-654.

Nishibitake M, Kirby ML, van Mierop L (1987) Pathogenesis of persistent truncus arteriosus and dextroposed aorta in the chick embryo after neural crest ablation. *Circulation* 75:255-264.

Orts Llorca F, Puerta Fonolla J, Sobrado Perez J (1980) The morphogenesis of the ventricular flow pathways in man. *Arch Anat Hist Embr norm et exp* 63:5-16.

Rychter Z (1962) Experimental morphology of the aortic arches and the heart loop in chick embryos. *Adv Morphol* 2:333-371.

Rychter Z, Lemez L (1965) Changes in localization in aortic arches of laminar blood streams of main venous trunks to heart after exclusion of vitelline vessels on second day of incubation. *Fed Proc Transl Suppl* 24:815-820.

Sugi Y, Lough J (1992) Onset of expression and regional deposition of alpha-smooth and sarcomeric actin during avian heart development. *Dev Dyn* 1992;193:116-124.

Taber LA, Hu N, Pexieder T, Clark EB, Keller BB (1993) Residual strain in the ventricle of the stage 16-24 chick embryo. *Circ Res* 72:455-462.

Wagman AJ, Hu N, Clark EB (1990) Effect of changes in circulating blood volume on cardiac output and arterial and ventricular blood pressure in the stage 18, 24 and 29 chick embryo. *Circ Res* 67:187-192.

Yoshida H, Manasek F, Arcilla RA (1983) Intracardiac flow patterns in early embryonic life. A reexamination. *Circ Res* 53:363-371.

Zahka KG, Hu N, Brin KP, Yin FCP, Clark EB (1989) Arterial impedance and hydraulic energy in stage 18 to 29 chick embryo. *Circ Res* 64:1091-1095.

CHAPTER 8

SUMMARY
AND
GENERAL DISCUSSION

Introduction

The aim of this study was to relate hemodynamics and morphology in normal and abnormal cardiac development. In order to study abnormal cardiogenesis it is essential to have animal models with specific and reproducible cardiac malformations. Spontaneous anomalies do not provide the necessary reproducible sequence of stages for hemodynamic studies. In the chick embryo two models were developed (chapter 2). The retinoic acid model and the venous clip model. Both lead to the same spectrum of congenital heart malformations, specifically, double outlet right ventricle. Although these two models generate similar heart defects, the effect on cardiac function could be different.

Mechanisms underlying morphogenetic processes

It was proposed that retinoic acid could have both a direct and an indirect effect on the myocardium. The indirect effect may result from an impaired parasympathetic innervation through a disturbance of the migration of cells from the neural crest. It is described that neural crest cells contribute to the cardiac ganglia (Kirby and Stewart 1983; Kirby 1993). Parasympathetic innervation of the heart via the cardiac ganglia is impaired after treatment with retinoic acid. The effect of all-trans retinoic acid on the neural crest is through cytotoxicity (Jelínek and Kistler 1981) or results from alterations in region-specific signals necessary for homing of neural crest cells or for their differentiation (Hart et al. 1990). The action of retinoic acid at the cellular level is linked to the fact that neural crest cells show particular expression of retinoic acid binding protein (CRABP) (Maden et al. 1991). Retinoic acid receptors (RARs) and CRABPs play an important role in the mechanism of gene expression (Gudas 1992; Morris-Kay 1992; Ross 1993), but their specific spatiotemporal patterns of expression, are extremely complex (Morris-Kay 1992; Ross 1993). The study of Lohnes et al. (1994) and the accompanying study of Mendelsohn et al. (1994) of RAR double mutant mouse fetuses show that RARs are involved in the ontogenesis of many organs and that the cardiac malformations in these mutant mice are comparable to those in cardiac neural crest ablated chickens (Kirby and Waldo 1990). Furthermore, in-vitro mesenchymal cell migration is inhibited by retinoids (Thorogood et al. 1982; Smith-Thomas 1987). Impaired parasympathetic innervation through a disturbance in neural crest cell migration leads to an alteration of the tonus of the cardiac myocytes.

Retinoic acid affects the cardiac myocytes directly by interfering with the looping process. Cardiac looping is related to the development of myofibrils and myofibril structure (Manasek et al. 1986; Itasaki et al. 1991; Shiraishi et al. 1992). It is described that retinoic acid has multiple effects on growth and differentiation of cardiac myocytes, including an inhibition of cell proliferation, development of heart contractions, and delay in α -actin synthesis (Wiens et al. 1992).

Furthermore, it has been shown that excess of retinoic acid can alter integrin expression in the embryonic heart, which ultimately leads to congenital malformations (Hierck 1996). Integrins have important functions in cell-cell and cell-matrix adhesion processes as well as in signal transduction (Hierck 1996). Pexieder et al. (1995) showed that all-trans retinoic acid can modify cardiac contractility. In rat fetuses treated during pregnancy with all-trans retinoic acid, a higher sensitivity toward extracellular calcium ion variations was found. This indicates an increased permeability of the sarcolemma and/or delayed development of the sarcoplasmic reticulum (Pexieder et al. 1995). Furthermore, they reported that all-trans retinoic acid significantly decreased the total amount of protein in morphologically normal mouse hearts and hearts that showed double outlet right ventricle. In these morphologically normal and abnormal hearts, the concentration of sarcoplasmic proteins was significantly increased and that of contractile proteins decreased. An interaction of retinoic acid and contractile proteins causes a disturbance in the myofibrillogenesis or myofibril arrangement and results in myocardial dysfunction accompanied by abnormal cardiac looping.

Both direct and indirect effects on the myocardium generate myocardial dysfunction.

The mechanism underlying abnormal heart development after venous clip is considered to be different from the retinoic acid model. Venous clip induced specific cardiovascular malformations, as subaortic ventricular septal defect, rightward positioned aorta, semilunar valve anomalies, atrioventricular valve anomalies, and pharyngeal arch artery malformations (interruption of the aortic arch). Hemodynamic influence of intracardiac anomalies on the development of the aortic arch have been described in the human (Moulaert et al. 1975). It was proposed that diminished blood flow through the embryonic aorta is considered to be the common factor responsible for the different anomalies of the aortic arch as interruption of the aortic arch. Intracardiac and pharyngeal arch artery malformations observed after venous clip are due to the changed intracardiac flow patterns because there is no direct manipulation to any part of the embryo. The venous clip model was devised to study the long-term effect of blood flow on heart development without interfering with the neural crest. The myocardium after venous clip is not altered like the myocardium after retinoic acid. Moreover, the parasympathetic innervation of the heart is normal after venous clip.

Hemodynamic evaluation

Initially hemodynamic function during rapid cardiac morphogenesis was defined in a reproducible way in the dorsal aorta using a 20 MHz Doppler velocity meter in the stage 20 to stage 35 chick embryo with normally developed hearts (chapter 3). A marked increase in mean dorsal aortic velocity and vessel area was observed, resulting in a 17-fold rise in mean dorsal aortic blood flow. Heart rate increased 2-fold and stroke volume 9-fold. Furthermore there was a stage-related rise in peak acceleration suggesting an increase in cardiac contraction force with advancing embryonic development.

The retinoic acid model and venous clip model allowed assessment of hemodynamic parameters in embryos with congenital heart malformations. The evaluation of form and function in stage 24 embryos provided information on cardiac function in an early stage of abnormal cardiogenesis before innervation of the heart exists. At stage 34, embryos with the heart defect were easily diagnosed, therefore, a more detailed correlation between hemodynamics and morphology took place.

After retinoic acid treatment, at stage 24, embryos showed reduced heart rate without a compensatory increase in stroke volume suggesting pacemaker and contractile dysfunction (chapter 4). Although the heart is not innervated yet, beat to beat variations of dorsal aortic and vascular impedance have been identified suggesting the presence of a preinnervated hemodynamic control mechanism (Kempski et al. 1993). This control mechanism indicates a feed-back between ventricular function and vascular bed (Kempski 1995). This control mechanism is disrupted after treatment with all-trans retinoic acid and lead to the observed decrease of heart rate. As for the contractile dysfunction, in this stage, is explained by the direct effect of retinoic acid on the cardiac myocytes leading to a disturbance in the myofibrillogenesis or myofibril arrangement.

At stage 34, a dramatic decrease of all hemodynamic parameters derived from the dorsal aortic flow velocity wave form was established suggesting primary myocardial dysfunction (chapter 5). Besides the direct effect of retinoic acid on the cardiac myocytes, there is also the indirect effect on the myocardium, that is neural crest related, that has to be considered. Neural crest cells give rise to neuronal populations of the autonomic nervous system. The parasympathetic innervation of the heart was impaired after retinoic acid and lead to myocardial dysfunction. The use of the immunohistochemical markers that are considered to be markers for neuronal differentiation confirmed our hypothesis (chapter 6). Impaired parasympathetic innervation was seen in stage 34 retinoic acid treated embryos. Moreover, these embryos displayed as encountered before, reduced hemodynamic parameters.

After venous clip, stage 24 embryos displayed solely a decrease in peak acceleration. Heart rate was altered at stage 34. An increase was observed in hemodynamic parameters reflecting no sign of myocardial dysfunction but rather a compensatory mechanism (chapter 7).

Future research

In this thesis we found chick embryos that were subjected to the morphogen and teratogen retinoic acid or venous clip both induce the same structural congenital heart anomaly, but display a different hemodynamic profile. Retinoic acid treated embryos displayed primary myocardial dysfunction. A compensatory mechanism seems to be present in venous clip embryos. These observations are based on peripheral Doppler velocimetry which does not provide a direct insight into cardiac muscle mechanisms. In chapter 4 the technique of pressure-volume relationship has been introduced as a method to measure cardiac function directly. Ventricular pressure-volume curves depend primarily on average global properties. Although parameters of cardiovascular function can be directly measured, several crucial parameters, by definition, will necessitate mathematical evaluation. These mathematical models will allow the assessment of differences in wall stress, a parameter which may be critical in the regulation of myocardial growth. Furthermore, it is feasible to verify our hypothesis related to myocardial growth and function in manipulated embryos.

References

- Gudas LJ (1992) Retinoids, retinoid-responsive genes, cell differentiation, and cancer. *Cell Growth & Differentiation* 3:655-662.
- Hart RC, McCue PA, Ragland WL, Winn KJ, Unger ER (1990) Avian model for 13-cis retinoic acid embryopathy: demonstration of neural crest related defects. *Teratology* 41:463-472.
- Hierck B 1996 Integrins and Laminins in Heart development, Role of Retinoic acid. Thesis
- Itasaki N, Nakamura A, Sumida H, Yasuda M (1991) Actin bundles on the right side in the caudal part of the heart tube play a role in dextro-looping in the embryonic heart. *Anat Embryol* 183:29-39.
- Jelinek R, Kistler A (1981) Effect of retinoic acid upon the chick embryonic morphogenetic systems. I. The embryotoxicity dose range. *Teratology* 23:191-195.
- Kempinski MH, Kibler N, Blackburn JL, Dzakowic J, Hu N, Clark BB (1993) Hemodynamic regulation in the chick embryo. *Am Soc Mech Eng BED* 24:119-122.
- Kempinski MH (1995) Overview: Modeling and control of embryonic hemodynamics. In: Clark BB, Markwald RR, Takao A (eds) *Developmental Mechanisms of heart disease*. Futura publishing company, Inc, Armonk, New York, pp 421-434.
- Kirby ML, Stewart D (1983) Neural crest origin of cardiac ganglion cells in the chick embryo: identification and extirpation. *Dev Biol* 97:433- 443.
- Kirby ML, Waldo L (1990) Role of neural crest in congenital heart disease. *Circulation* 82:332-340.
- Kirby ML (1993) Cellular and molecular contributions of the cardiac neural crest to cardiovascular development. *Trends Cardiovasc Med* 3:18-23.
- Lohnes D, Mark M, Mendelsohn C, Dollé P, Dierich A, Gorry P, Gansmuller A, Chambon P (1994) Function of the retinoic acid receptors (RARs) during development. I. Craniofacial and skeletal abnormalities in RAR double mutants. *Development* 120:2713-2748.

Maden M, Hunt P, Eriksson U, Kuroiwa A, Krumlauf R, Summerbell D (1991) Retinoic acid-binding protein, rhombomeres and the neural crest. *Development* 111:35-44.

Manasek FJ, Icardo J, Nakamura A, Sweeney (1986) Cardiogenesis: Developmental Mechanisms and Embryology. In: HA Fozzard et al. (eds) *The heart and cardiovascular system*. Raven Press, NY, pp 965-985.

Mendelsohn C, Lohnes D, Décimo D, Lufkin T, LeMeur M, Chambon P, Mark M (1994) Function of the retinoic acid receptors (RARs) during development. II. Multiple abnormalities at various stages of organogenesis in RAR double mutants. *Development* 120:2749-2771.

Moulaert AJ, Bruijns CC, Oppenheimer-Dekker A (1976) Anomalies of the aortic arch and ventricular septal defects. *Circulation* 53:1011-1015.

Morriss-Kay G (1992) Retinoic acid and development. *Pathobiology* 60:264-270.

Pexieder T, Blanc O, Pelouch V, Ostádalová I, Milerová M, Ostádal B (1995) Late fetal development of retinoic acid induced transposition of great arteries-morphology, physiology and biochemistry. In: Clark EB, Markwald RR, Takao A (eds) *Developmental Mechanisms of heart disease*. Futura Publishing Company, Armark, NY, pp 297-307.

Ross AC (1993) Overview of retinoid metabolism. *J Nutr* 123:346-350.

Shiraishi I, Takamatsu T, Minamikawa T, Fujita S (1992) 3-D observation of actin filaments during cardiac myofibrinogenesis in chick embryo using a confocal laser scanning microscope. *Anat Embryol* 185:401-408.

Smith-Thomas L, Lott I, Bronner-Fraser M (1987) Effects of isotretinoin on the behavior of neural crest cells in-vitro. *Dev Biol* 123:276-280.

Thorogood P, Smith L, Nicol A, McGinty R, Garrod D (1982) Effects of vitamin A on the behavior of migratory neural crest cells in-vitro. *J Cell Sci* 57:331-350.

Wiens DJ, Mann TK, Feddersen DE, Rathmell WK, Franck BH (1992) Early heart development in the chick embryo: Effects of isotretinoin on cell proliferation, α -actin synthesis, and development of contractions. *Differentiation* 51:105-112.

**SAMENVATTING
EN
ALGEMENE DISCUSSIE**

Introductie

Het doel van deze studie betrof de relatie van haemodynamiek en morfologie te onderzoeken bij de normale en abnormale hartontwikkeling. Om de ontwikkeling van het abnormale hart te bestuderen is het van essentieel belang diermodellen te hebben met specifieke en reproduceerbare hartafwijkingen. Het spontaan optreden van hartafwijkingen geeft niet die reproduceerbaarheid van afwijkingen in opeenvolgende stadia die noodzakelijk is voor haemodynamische studies. In het kippe-embryo zijn twee interventie modellen ontwikkeld (hoofdstuk 2). Het retinoic acid model en het veneuze clip model. Beide modellen leiden tot hetzelfde morfologische spectrum van aangeboren hartafwijkingen, in het bijzonder: "double outlet right ventricle". Hoewel deze twee modellen éénzelfde spectrum van hartmalformaties genereren, is het effect op de hartfunctie mogelijk verschillend.

Mechanismen van morfogenetische processen

Een hypothese werd geopperd dat retinoic acid toediening zowel een direct als ook een indirect effect heeft op de myocardfunctie. Het indirect effect is het gevolg van een abnormale parasympatische innervatie van het hart die veroorzaakt wordt door een verstoring van de migratie van neurale lijstcellen. Het is beschreven dat neurale lijstcellen een bijdrage leveren aan de cardiale ganglia (Kirby and Stewart 1983; Kirby 1993). Uit het in dit proefschrift beschreven onderzoek blijkt dat het parasympatisch innervatie patroon van het hart via de cardiale ganglia wordt aangetast na behandeling met retinoic acid. Het effect van all-trans retinoic acid op de neurale lijst is beschreven als cytotoxisch (Jelinek and Kistler 1981) of kan het gevolg zijn van veranderingen in regio-specifieke signalen die nodig zijn voor het innestelen van neurale lijstcellen of voor hun differentiatie (Hart et al. 1990). Het werkingsmechanisme van retinoic acid op cellulair niveau is verbonden met het feit dat neurale lijstcellen een bepaalde expressie vertonen van het retinoic acid bindings eiwit (CRABP) (Maden et al. 1991). Retinoic acid receptoren (RARs) en CRABPs hebben een belangrijke rol in het mechanisme van de gen expressie (Gudas 1992; Morris-Kay 1992; Ross 1993). Echter, de specifieke spatiotemporale patronen van expressie zijn zeer complex (Morris-Kay 1992; Ross 1993). De studie van Lohmes et al. (1994) en de begeleidende studie van Mendelsohn et al. (1994) van RAR dubbel gemuteerde muis foetussen, hebben aangetoond dat RARs betrokken zijn in de ontogenese van veel organen, en dat de hartafwijkingen in deze gemuteerde muizen vergelijkbaar zijn met hartafwijkingen die ontstaan na ablatie van de cardiale neurale lijst in kippe-embryos (Kirby and Waldo 1990). Bovendien wordt in-vitro migratie van mesenchymale cellen afgeremd door retinoiden (Thorogood et al. 1982; Smith-Thomas 1987). Onderdrukte parasympatische innervatie als gevolg van een verstoring van de migratie van neurale lijstcellen leidt tot een verandering in de tonus van de cardiale myocyten.

Retinoic acid beïnvloedt de cardiale myocyten direkt, namelijk door verstoring van het krommingsproces van het hart. De kromming van het hart is gerelateerd aan de ontwikkeling van de myofibrillen zelf en aan de structuur van de myofibrillen (Manasek et al. 1986; Itasaki et al. 1991; Shirashi et al. 1992). Het is beschreven dat retinoic acid multipale effekten heeft op de groei en differentiatie van cardiale myocyten, inclusief een inhibitie van cel proliferatie, ontwikkeling van hartcontracties, en een vertraagde synthese van α -actine (Wiens et al. 1992). Bovendien, is aangetoond dat een overmaat aan retinoic acid de integrine expressie in het embryonaal hart kan veranderen, en uiteindelijk kan leiden tot aangeboren hartafwijkingen (Hierck 1996). Integrines hebben belangrijke functies in de cel-cel en cel-matrix adhesie processen maar ook in de signaal transductie (Hierck 1996). Pexieder et al. (1995) heeft aangetoond dat all-trans retinoic acid in staat is de contractiliteit van het hart te veranderen. In rat foetussen, waarvan de moeder tijdens haar zwangerschap was behandeld met all-trans retinoic acid, werd een hogere sensitiviteit voor variaties in extracellulair calcium ionen gevonden. Dit is een indicatie voor een toegenomen permeabiliteit van het sarcolemma en/of een vertraagde ontwikkeling van het sarcoplasmatisch reticulum (Pexieder et al. 1995). Bovendien werd aangetoond dat na behandeling met all-trans retinoic acid het totale hoeveelheid eiwit significant was verminderd in morfologische normale muis harten en harten met een "double outlet right ventricle". In deze morfologische normale en abnormale harten was de concentratie van sarcoplasmatische eiwitten significant toegenomen en de concentratie van de contractiele eiwitten afgenomen. Een interactie van retinoic acid en contractiele eiwitten veroorzaakt een stoornis in de myofibrillogenese of rangschikking van de myofibrillen en leidt tot een myocardiale dysfunctie gepaard gaande met een abnormale kromming van het hart.

Het werkingsmechanisme van de abnormale hartontwikkeling na veneuze clip is mogelijk verschillend van het retinoic acid model. Veneuze clip interventie induceert specifieke cardiovasculaire malformaties zoals subaortale ventrikel septum defekten, naar rechts verplaatsing van de aorta, afwijkingen aan de semilunair en atrioventriculair kleppen, en kieuwboogarterie afwijkingen zoals interruptie van de aortaboog. De invloed die de bloedstroom heeft op de ontwikkeling van aortaboog, is beschreven bij de mens (Moulaert et al. 1975). Er werd verondersteld dat een afgenomen hoeveelheid bloed per tijdseenheid die door de embryonale aorta stroomt, mogelijk verantwoordelijk is voor de verschillende aortaboog afwijkingen. Daar er geen manipulatie plaatsvindt van de embryo zelf, zijn de intracardiale en kieuwboogarterie malformaties na veneuze clip interventie het gevolg van veranderde intracardiale bloeddorstomingspatronen. Het veneuze clip model is ontwikkeld om het effect van de bloeddorstoming op langere termijn te kunnen onderzoeken, zonder verstoring van de neurale lijst. Het myocard na veneuze clip interventie is niet veranderd zoals in het retinoic acid model, de parasympatische innervatie van het hart is normaal.

Haemodynamische evaluatie

In eerste instantie is de haemodynamiek gedurende de snelle cardiale morfogenese op een reproduceerbare manier gedefinieerd in de dorsale aorta van stadium 20 to 35 kippe-embryos. Er werd gebruikt gemaakt van een 20 MHz Doppler snelheidsmeter (hoofdstuk 3). Een opvallende toename werd gezien van gemiddelde bloedstroomsnelheid en oppervlakte van de dorsale aorta. Dit resulteerde in een 17-voudige toename van gemiddelde bloedvolume. Er was een 2-voudige toename van de hartfrequentie en een 9-voudige toename van het slagvolume. Bovendien was er een stadium afhankelijke toename van de piek acceleratie die een toename van de cardiale contractiekracht suggereerde.

Met behulp van het retinoic acid model en het veneuze clip model was het mogelijk haemodynamische parameters te verkrijgen in embryos met congenitale hartafwijkingen. De evaluatie van vorm en functie in stadium 24 embryos verschaftte informatie omtrent de hartfunctie in een jong stadium van de abnormale cardiogenese wanneer er nog geen innervatie van het hart is. In stadium 34 was het mogelijk embryos met een hartafwijking eenvoudig te diagnostiseren, waardoor een gedetailleerde correlatie kon plaatsvinden tussen haemodynamiek en morfologie.

Stadium 24 embryos vertoonden na behandeling met retinoic acid een significante afname van de hartfrequentie zonder een compensatoire toename van het slagvolume. Dit suggereert pacemaker en dysfunctie van het contractiele apparaat (hoofdstuk 4). Hoewel het hart nog niet geïnnerveerd is, zijn er variaties per hartcyclus beschreven van de dorsale aorta en vasculaire impedantie. Deze cyclische variaties suggereren een haemodynamisch controle mechanisme (Kempski et al. 1993). Dit controle mechanisme is een indicatie voor een terugkoppeling tussen ventriculaire functie en het vaatbed (Kempski 1995). Dit controle mechanisme is verstoord na behandeling met all-trans retinoic acid en leidt tot de afname van de hartfrequentie. De dysfunctie van het contractiele apparaat kan verklaard worden door het direct effect van retinoic acid op de cardiale myocyten leidend tot een verstoring in de myofibrillogenese of aantasting van de structuur van de myofibrillen.

Op stadium 34 was er een dramatische afname van alle haemodynamische parameters die waren afgeleid van de bloedstroomsnelheidscurve. Deze observatie suggereert een primaire funktiestoornis van het myocard (hoofdstuk 5). Naast het direct effect van retinoic acid op de cardiale myocyten, is er tevens een indirect effect op het myocard, dat gerelateerd is aan de neurale lijst. Neuronale populaties van cellen van het autonome zenuwstelsel stammen af van de neurale lijst. De parasympatische innervatie van het hart was abnormaal na behandeling met retinoic acid en leidt tot een funktiestoornis van het myocard. Onze hypothese werd bevestigd na het toepassen van immunohistochemische technieken waarbij gebruik werd gemaakt van markers die specifiek zijn voor het aantonen van de neuronale differentiatie (hoofdstuk 6).

Een abnormale parasympatische innervatie werd geconstateerd in embryos die behandeld waren met retinoic acid. Deze embryos vertoonden eveneens een afname van de haemodynamische parameters.

Na veneuze clip interventie lieten stadium 24 embryos slechts een afname zien in piek acceleratie. De hartfrequentie was verlaagd in stadium 34 embryos na veneuze clip. Een toename van haemodynamische parameters wezen op een compensatie mechanisme waarbij er geen sprake was van een funktiestoornis van het myocard (hoofdstuk 7).

Toekomstig onderzoek

In dit proefschrift hebben we geconstateerd dat kippe-embryos die aan het morfogen en teratogen retinoic acid of aan veneuze clip waren blootgesteld, éénzelfde morfologisch spectrum van congenitale hartafwijkingen vertonen. Echter, het haemodynamische profiel is verschillend. Retinoic acid behandelde embryos vertonen een primaire funktiestoornis van het myocard. Een compensatie mechanisme is aanwezig bij veneuze clip embryos. Deze observaties zijn gebaseerd op bloedstroomsnelheid en druk metingen in perifere vaten, dat wil zeggen er is geen directe informatie over de hartspierfunctie beschikbaar. In hoofdstuk 4 is de techniek van druk-volume relaties geïntroduceerd als een methode om hartfunctie direct te kunnen meten. Hoewel hartfunctie parameters direct gemeten kunnen worden, zullen een aantal parameters onderworpen moeten worden aan wiskundige modellen. Met behulp van deze modellen zal het mogelijk zijn verschillen in wandspanning, die informatie geeft over de myocardiale groei, te verkrijgen. Het is mogelijk onze hypothese omtrent myocardiale groei en functie te toetsen in gemanipuleerde embryos.

Curriculum Vitae

De auteur van dit proefschrift werd op 21 november 1957 geboren te Haarlem en groeide op in Californië, U.S.A. Na terugkeer in Nederland werd van 1970 tot 1977 de middelbare school bezocht, het Tweede Vrijzinnig Christelijk Lyceum te Den Haag, alwaar het eindexamen Atheneum-B in 1977 werd behaald. Door de numerus fixus werd in 1977 met de studie Scheikunde aangevangen aan de Rijksuniversiteit Leiden. Het propaedeuse werd behaald in 1978. In hetzelfde jaar kon na inloting, de studie Geneeskunde worden gevolgd, eveneens aan de Rijksuniversiteit Leiden. Tijdens de studie Geneeskunde werd in het kader van het keuzeonderwijs een retrospectief onderzoek verricht van de "Rastelli procedure". Supervisor van dit onderzoek was Prof. Dr. J. Rohmer die toen werkzaam was op de afdeling Kindercardiologie, Academisch Ziekenhuis Leiden. De medische studie werd afgesloten met het verkrijgen van het doctoraal diploma in 1985 en het artsexamen in 1986 aan de Rijksuniversiteit Leiden.

Na het artsexamen heeft zij foetaal cardiovasculair onderzoek verricht met betrekking tot de ontwikkeling van het atrium septum vanaf de foetale tot de neonatale periode onder begeleiding van Prof. Dr. A. C. Gittenberger-de Groot, van de afdeling Anatomie en Embryologie van de Rijksuniversiteit Leiden. In 1987 is zij als arts-assistent-niet-in-opleiding werkzaam geweest op de afdeling Interne Geneeskunde van het Academisch Ziekenhuis te Leiden. Na dit klinisch jaar werd zij aangesteld in 1988 als arts-onderzoeker van de afdeling Obstetrie/Gynaecologie, aan de Erasmus Universiteit en Academisch Ziekenhuis Rotterdam. In het kader van de prenatale diagnostiek werd een aanvang gemaakt met het opzetten van embryonaal cardiovasculair onderzoek in het kippe-embryo. In samenwerking met de afdeling Anatomie en Embryologie van de Rijksuniversiteit in Leiden werd in 1991 aangevangen met een uniek opgezet cardiovasculair onderzoek, waarvan dit proefschrift deel uit maakt (Jubileumsubsidie van de NHS, en NWO). Vanaf mei 1996 is zij wederom werkzaam als arts-onderzoeker op de afdeling Obstetrie/Gynaecologie aan de Erasmus Universiteit en Academisch Ziekenhuis te Rotterdam.

LIST OF PUBLICATIONS

Regular publications:

Broekhuizen MLA, Wladimiroff JW, Tibboel D, Poelmann RE, Wenink ACG, Gittenberger-de Groot AC. Induction of cardiac anomalies with all-trans retinoic acid in the chick embryo.

Cardiology in the Young 1992; 2:311-317

Broekhuizen MLA, Mast F, Struijk PC, van der Bie W, Mulder PGH, Gittenberger de Groot AC, Wladimiroff JW. Hemodynamic parameters of stage 20 to stage 35 chick embryo.

Pediatric Research 1993; 34:44-46

Broekhuizen MLA, Bouman HGA, Mast F, Mulder PGH, Gittenberger-de Groot AC, Wladimiroff JW. Hemodynamic changes in HH stage 34 chick embryos after treatment with all-trans retinoic acid.

Pediatric Research 1995; 38:342-348

Bouman HGA, Broekhuizen MLA, Baasten MJ, Gittenberger-de Groot AC, Wenink ACG. Spectrum of looping disturbances in stage 34 chicken hearts after retinoic acid treatment.

The Anatomical Record 1995; 243:101-108

Broekhuizen MLA, Hogers B, Bouman HGA, Poelmann RE, Gittenberger-de Groot AC, Wladimiroff JW. Haemodynamische veranderingen in het kippe-embryo na behandeling met all-trans retinoic acid.

Ultrasonoor bulletin 1996; 1:1-4

Regular publications in press

Bouman HGA, Broekhuizen MLA, Baasten MJ, Gittenberger-de Groot AC, Wenink ACG. A stereological study of stage 34 chicken hearts with looping disturbances after retinoic acid treatment: disturbed growth of myocardium and atrioventricular cushion tissue.

The Anatomical Record, in press

Regular publications in preparation:

Broekhuizen MLA, Gittenberger-de Groot AC, Baasten MJ, Wladimiroff JW, Poelmann RE. Impaired neural crest derived parasympathetic innervation of embryonic chick hearts in the presence of altered hemodynamics after treatment with all-trans retinoic acid.

Anatomy and Embryology, submitted

Broekhuizen MLA, Hogers B, DeRuiter MC, Poelmann RE, Gittenberger-de Groot AC, Wladimiroff JW. Altered hemodynamics in chick embryos after clipping the vitelline vein. In preparation for *Circulation Research*

Abstracts

Broekhuizen MLA, Mast F, Gittenberger-de Groot AC, Wladimiroff JW. Hemodynamic changes in stage 34 chick embryos after treatment with all-trans retinoic acid.

Cardiology in the Young 1993; Supplement to volume 3, nr 1: abstract nr 126, p 42

Broekhuizen MLA, Hogers B, Bouman HGA, Poelmann RE, Gittenberger-de Groot AC, Wladimiroff JW. Altered hemodynamics in chick embryos after treatment with all-trans retinoic acid and after clipping the vitelline vein.

European Journal of Physiology 1995; Supplement to volume 430, nr. 4: R 119 (abstractnr: 436)

Books in press:

Broekhuizen MLA, Wladimiroff JW, Gittenberger-de Groot AC. Experimentally altered hemodynamics in the chick embryo.

In: Wladimiroff JW, Pilu G (eds) *Ultrasound and the fetal heart, Parthenon Publishing, UK, in press*

Grants/Awards:

grant: Van Walree Fonds 1995 for experimental research in the chick embryo, the retinoic acid model, in Rochester, New York.

award: The 1995 Akzo-Organon Award for ultrasound research in the chick embryo, the retinoic acid model ("Organon Echoscopieprijs").



DANKWOORD

Tot slot zou ik stil willen staan bij het feit dat, hoewel ik de auteur ben van dit boekje, zonder anderen het niet gelukt was. Allereerst wil ik mijn twee promotores bedanken. Beste Prof. Wladimiroff en Adri, jullie enthousiasme en positieve uitstraling heeft op mij een stimulerende werking gehad, zodat ik telkens opnieuw iets verder dan mijn uiterste grens kon gaan. Beste Rob, als co-promotor was je voor mij, een enorme steun in de rug. Vaak de uitdrukking "je moet roeien met de riemen die je hebt, en het roer in de goede richting sturen" kon telkens een glimlach uitlokken op momenten dat ik het nodig had.

De Anatomie heeft een belangrijke plaats ingenomen in mijn leven. Alle medewerkers zou ik willen bedanken voor hun toegewijde medewerking en belangstelling. Bianca en Hannie bedankt voor jullie prettige en intensieve samenwerking. Margot, jij was altijd de steun voor mij waarop ik kon vertrouwen. Ik heb altijd genoten van de discussies met Marco, die mij weer een zet gaven in de goede richting. Monica, Mieke en Daniëlle hebben voor mij het meeste snij en kleur werk verricht, hiervoor zal jullie eeuwige roem ten deel vallen. Jan, op jouw fotografie en kennis hiervan kon ik altijd rekenen, zelfs als het ging om "last minute" opdrachten.

Ik dank mijn collega's van Dijkzigt en de Erasmus Universiteit. Het eerste contact met kippembryo's heb ik opgedaan op de afdeling Celbiologie in samenwerking met de afdeling Kinderheekkunde onder leiding van Prof. Dr. J.C. Molenaar, van de Erasmus Universiteit. Wim van der Bie is mijn technische steun en toeverlaat geweest in goede en slechte tijden. Collega's van de prenatale diagnostiek bedankt voor jullie belangstelling en medeleven. Waardevolle en aan het denken zettende discussies heb ik altijd gevoerd met Paula, Jacqueline en Nicolette. Sylvia bedankt voor de secretariële back-up. Wanneer het nodig was om in te springen stond Babek altijd voor mij klaar. Bij Steef kon ik altijd terecht, met name als het om financieel advies ging.

I would like to thank my colleagues and friends at the Department of Pediatric Cardiology, Rochester, New York. Ed, thank you for making it possible to learn everything about the "chicken intensive care unit" and more. Norman, thanks to your patience and guidance I was able to create a "chicken intensive care unit" in Rotterdam. I look forward to further collaboration with Brad, to whom I am grateful for all the discussions and brain-storm sessions. Maria, Megan, Masaaki, and Joe thank you for being there for me.

Mijn paranimfen Henrike en Paula, jullie ben ik dankbaar voor het doorzetten daar waar ik het even niet meer op een rijtje had. Ik denk met veel plezier terug aan die tijd toen Henrike als analiste werkzaam was op de Anatomie. Meerdere malen hadden wij felle discussies die uiteindelijk resulteerden in nieuwe wetenschappelijke experimenten. Henrike en Paula jullie steun als collega en vriendin, en paranimf wordt ontzettend gewaardeerd en nooit vergeten.

Mijn moeder wil ik bedanken voor de nimmer aflatende steun en medeleven. Zij heeft mij altijd de gelegenheid en ruimte gegeven mijn eigen weg te zoeken en te vinden. Last but not least Evert. Jij bent voor mij een lot uit de loterij. Jij zorgde voor rust in deze hectische periode van mijn leven. Daar waar nodig haalde jij de hete kolen uit het vuur zodat ik weer kon opladen. Ontzettend bedankt voor de buitenkant maar ook voor het steunen van de binnenkant. Bindelijk is het zover, het is afl!!